University of
South-Eastern Norway

www.usn.no

FMH606 Master's Thesis 2024
Electrical Power Engineering

Emergency-SIME for real-time assessment and evaluation of transient stability

Sigurd Hansen

Faculty of Technology, Natural Sciences and Maritime Sciences
Campus Porsgrunn

University of South-Eastern Norway

www.usn.no

Course: FMH606 Master's Thesis 2024

Title: *Emergency-SIME for real-time assessment and evaluation of transient stability*

Pages: *126*

Keywords: *E-SIME, Transient Stability, PowerFactory*

Student: *Sigurd Hansen*

Supervisor: *Gunne John Hegglid and Manjula Edirisinghe*

External partner: *Skagerak Kraft*

Summary:
The primary objective of this thesis is to evaluate the potential of the method Emergency-Single machine equivalent (E-SIME) to be used as a tool for assessing transient stability. To do this E-SIME was applied to a 9 bus system and also to a model of the New England grid. This was done utilizing the software PowerFactory for simulation of the transient event, then subsequent calculations using Excel and Python.

The results show that E-SIME successfully identified stable and unstable scenarios, where in the latter case corrective measures were taken for it to remain stable. Results indicate that E-SIME will tend to perform unnecessary corrective measures, if the fault location is closer to the center of the power grid. Conversely, in cases where the fault occurs on the outer limits of the grid, and the clearing time (CT) is close enough to the critical clearing time (CCT), it may falsely classify an unstable case as stable.

In conclusion, the E-SIME method has demonstrated its potential as a viable tool for assessing transient stability on different transmission systems of varying sizes. Moreover, the method seems to be within reach of today's technology if necessary Phasor Measurement Units (PMUs) are installed in the system. Further, it shows the potential to both increase transmission capabilities and enhance grid security. Therefore, the method could become a valuable resource for the Nordic power system.

Preface

The thesis is authored by a Master's student specializing in Electrical Power Engineering at the South-Eastern Norway University's Porsgrunn campus, and was written in collaboration with Skagerak Kraft.

Writing on the subject of transient stability has been a humbling process. The short time frame in which transient instabilities can occur presents constant time pressure in assessment and implementing controls. This journey of writing a thesis about this, while demanding at times, has also been very rewarding.

I would like to extend my deepest gratitude to my supervisors, Gunne John Hegglid and Manjula Edirisinghe, for providing valuable feedback and consistently encouraging me to delve deeper into the subject. I am also grateful to my friends and family for their continuous support and encouragement, which has been a cornerstone of this thesis.

In this project, these tools have been used:

- DigiSilent PowerFactory
- Python 3.1.1
- Overleaf, Online LaTex Editor
- Microsoft Visio
- Microsoft Project
- Microsoft Teams

Porsgrunn, 15th May 2024

Sigurd Hansen

Contents

List of Figures

List of Tables

Nomenclature

Abbreviation	Explanation
AVR	Automatic Voltage Regulators
CM	Critical Machine
CCT	Critical Clearing Time
CSV	Comma-Separated Values
CT	Clearing Time
DAE	Differential Algebraic Equation
DigiSILENT	Digital Simulation of Electrical Networks
EAC	Equal Area Criterion
EEAC	Extended Equal Area Criterion
E-SIME	Emergency Single Machine Equivalent
firel	Rotor angle referred to the reference machine rotor angle
firot	External rotor angle
LS	Least Squares Method
NM	Non-Critical Machine
OMIB	One Machine Infinite Bus
PMU	Phasor Measurement Unit
PSS	Power System Stabilizer
q-axis	Quadrate Axis
RMS	Root Mean Square
SIME	Single Machine Equivalent
TD	Time Domain
TDS	Time Domain Solution
WLS	Weighted Least Squares Method

1 Introduction

The introduction includes a background and motivation section, followed by a discussion of the goals and methodology. Additionally, the scope of the thesis is outlined, and an overview of the project report is provided.

1.1 Background and Motivation

A challenge with the power grid today is that it is increasingly being operated closer to its transmission limits. In some cases, transient stability will limit the maximum transmission capacity of the system [1]. In such cases, enhancing the method that is employed to handle a transient event, could allow for an increase in the transmission limit [2]. However, one challenge with this is that the modern power grid has an increased susceptibility to transient instabilities [3]. Even though the occurrence of transient instability is rare, it tends to have disastrous consequences when it does [4]. One such possible consequence of transient instability is power outages, which can inflict significant costs and lead to widespread loss of electricity supply [5]. To address both these challenges a possible solution is using a real-time method. This method can measure the stability margin or index, and then take emergency control to prevent the system from becoming unstable. A challenge with the implementation of a real-time method is the fast development of transient instabilities. Before instability has occurred, the method needs to have assessed and also implemented Emergency control [4].

This Master's thesis is part of research initiated by the University of South-Eastern Norway (USN) and is in collaboration with the company Skagerak Kraft, where it is wanted to find such a real-time method to both possibly increase transmission capabilities and also enhance grid security. This was done by first finding a real-time transient stability method, and also finding suitable test cases. After researching different cases the New England grid was chosen, which is shown in Figure 1.1. Given this, a literature review was performed to investigate which methods could fit this, which is included in Appendix D. Initially, it was tried to use neural networks, but this was dropped due to issues faced with making it understand the underlying dynamics. Rather, it was decided to use the Emergency Single Machine Equivalent (E-SIME) methodology.

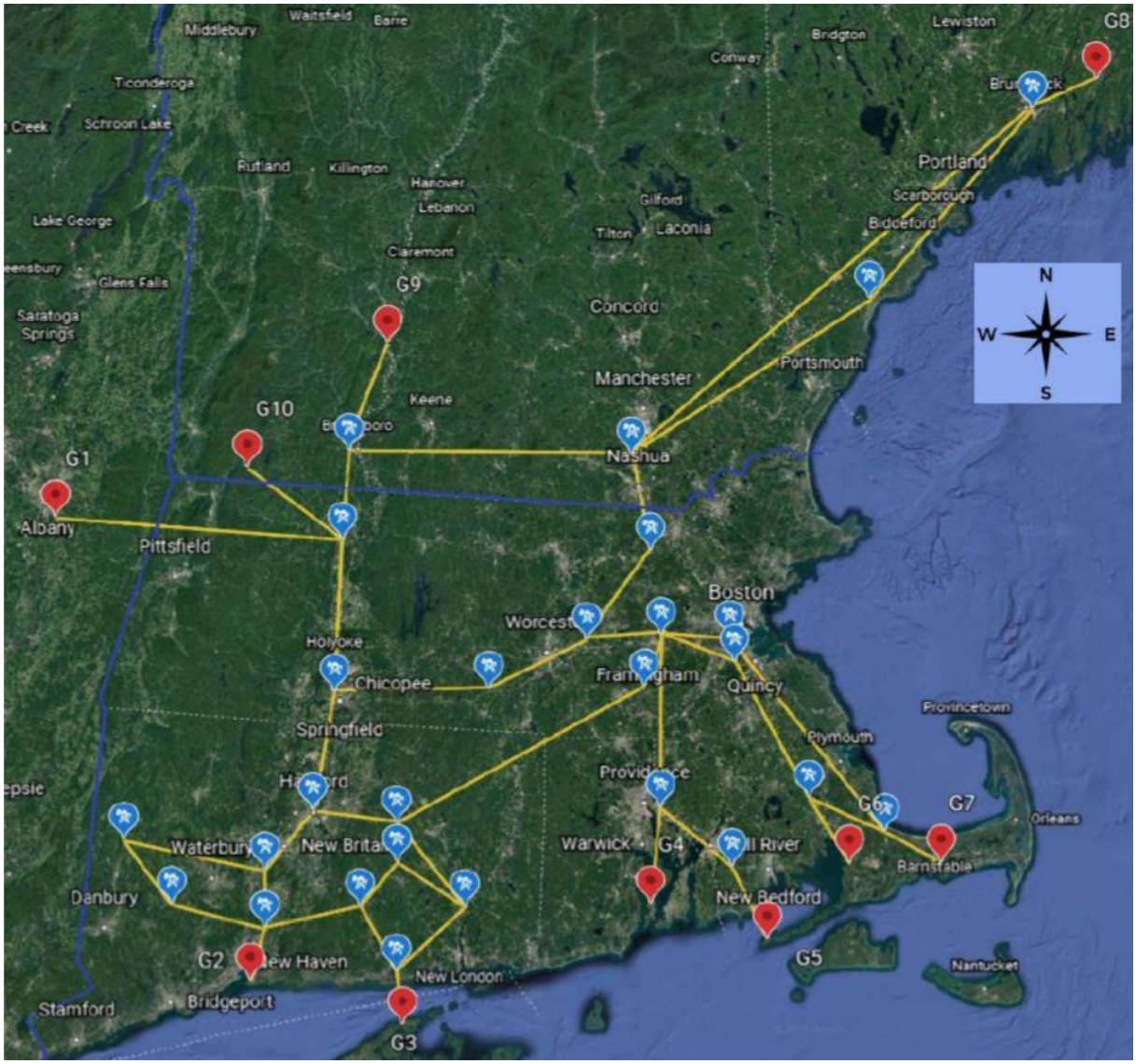

Figure 1.1: The 39 Bus New England power system showed geographically with lines marked with yellow, load marked with blue and generator units marked with red [6].

The method stems from the Preventive SIME that introduced the stability margin (η). This method utilizes Time Domain (TD) programs for calculating η under potential contingencies, where using this it can take preventive actions so the system will remain stable if a contingency occurs. However, these actions inherently increase operating costs. In contrast, E-SIME reacts to contingencies from real-time measurements, promptly estimating if it is necessary to do corrective actions for the system to remain stable, which it does using an estimation of the η [1].The hardware requirements for using the E-SIME method are Phasor Measurement Units (PMUs), which need to be placed at the main power plant stations and need communication systems to transmit the information. Nowadays, these

requirements seem to be within reach of today's technology [4]. In this thesis to test the E-SIME method it is employed on the 39 bus system model, which includes 10 generators, and dynamic models for Automatic Voltage Regulators (AVRs), Power System Stabilizers (PSSs), and governors [7]. This model is a pre-made example included inside of PowerFactory based on the IEEE-39 bus system, where the obtained results through the complete Time Domain Solution (TDS) will be compared to the E-SIME results. To start with a more simple example it was decided to first use the E-SIME on the 9 bus system, which has 3 generators and does not have dynamic models for AVR, PSS, and governor [8].

1.2 Goals

The primary goal of this thesis is to evaluate the potential of the E-SIME to be used as a tool for assessing transient stability, as well as to determine if it can increase the transmission capability of the system and enhance grid security.

Sub-goals:

1. Conduct a literature review on real-time transient stability methods, focusing on the E-SIME method.
2. Select two models for use in PowerFactory: a basic model with few generators and a more complex system equipped with dynamic components such as AVR, PSS, and governors.
3. Analyze full TDS results using the SIME methodology and implement E-SIME in PowerFactory to predict stability margin η and identify Critical Machines (CMs).
4. Compare E-SIME calculations with TDS results to evaluate the reliability and accuracy of the E-SIME methodology.
5. Use the results to determine the potential of E-SIME as a real-time tool for transient stability assessment. Also, see if results suggest that E-SIME can be used to increase transmission capabilities and enhance grid security.

1.3 Method

This study commenced with a literature review to comprehend developments in the field of real-time transient stability assessment and to gain an understanding of E-SIME. Insights gathered from the literature guided the employment of two core methodologies:

- **Experimental Method:** This method was utilized to obtain results from the model and test the E-SIME methodology, particularly to verify if it can accurately predict unstable cases before instability occurs. It was also used to derive results from the complete TDS to ascertain the actual η and to measure time to instability (t_u).
- **Analytical Method:** This method is employed to compare the results from the TDS and to analyze these results in-depth.

1.4 Scope of thesis

The only renewable energy source in this thesis is hydropower. The focus is placed on handling the inclusion of many generators with AVR, PSS, and governors, with also possibly detailed generator modeling.

No automatic process is created for the initiation of corrective measures. Also, there are only two different corrective measures that are employed in this thesis, which is either disconnection of CMs or splitting the grid.

The focus is on transient stability assessment. Therefore, small signal instability, voltage, and frequency stability are not directly addressed in the results.

1.5 Project report overview

Chapter 2: Theoretical Background
This chapter delves into the theoretical foundations necessary for understanding the SIME methodology. It begins by introducing and defining transient stability. The Equal Area Criterion (EAC) is then introduced for later use in the SIME methodology. The chapter continues by describing how transient events are modeled and how the TDS can be derived using PowerFactory.

Chapter 3: Theoretical background on Single Machine Equivalent (SIME) Metholodogy
This chapter provides an introduction to the SIME methodology, and also how to distinguish between CMs and Non-Critical Machines (NMs) using the complete TDS. It then

explores the One Machine Infinite Bus (OMIB) equivalent, calculation of η, and how the η can be utilized for sensitivity analysis concerning any given parameter (p).

Chapter 4: Introduction for Emergency SIME and methodology
The chapter begins with an introduction to E-SIME, followed by an overview of how the methodology operates. It elaborates on the use of Taylor expansion for identifying potential critical machines and the formation of the OMIB. The techniques used for estimation of η and t_u are discussed. It also covers how test data created from PowerFactory was managed for use in this analysis.

Chapter 5: E-SIME applied on 9 and 39 bus system
This chapter applies the methodology discussed in the previous chapter to the 9 and 39 bus systems. It presents the technical data from the PowerFactory models, planned disturbances, identification of CMs, and the formation of the OMIB equivalent. Lastly, it presents and compares results from using the TDS and the E-SIME, as well as between the 9 and 39 bus system outcomes.

The Python code that was developed and used, is listed below:

- Appendix A.1: Weighted Least Squares method to estimate δ_u
- Appendix A.2: Optimization of weights for least squares method.
- Appendix A.3: Integral of $P_a(\delta)$ and calculation of η_u.
- Appendix A.4: Estimation of time to instability t_u.
- Appendix A.5: Unwrapping angles for δ.
- Appendix A.6: 9 bus system δ prediction and identification of CMs.
- Appendix A.7: Calculating OMIB variables and plot for 9 bus system
- Appendix A.8: 9 bus system case check of kinetic energy change against integral of P_a and δ for a single time-step.
- Appendix A.9: 39 bus system case check of kinetic energy change against integral of P_a and δ for a single time-step.
- Appendix A.10: Calculating OMIB variables and plot for the 39 bus system.

2 Theoretical background on transient stability

This chapter presents the essential theoretical background for transient stability in power systems, where this knowledge is needed for later understanding of the SIME methodology. First, the chapter introduces transient stability and its definition. Furthermore, it explores the use of the EAC, then how the TDS can be obtained through using the PowerFactory software.

2.1 Introduction to Transient stability and definition

Transient stability is a sub-category of power system stability, where power system stability can be broadly defined as the system's ability to remain in an acceptable state of equilibrium following a disturbance [9]. The categories for power system stability are illustrated in Figure 2.1, which were categorized in 2004 by the Task Force of the IEEE Power System Dynamic Performance Committee alongside CIGRE Study Committee 38 [10]. In 2020, the classification of power system stability was expanded to include new categories such as Converter-driven stability and resonance stability. This is due to the effects that High-voltage direct current (HVDC), photovoltaic, and Flexible AC Transmission Systems (FACTS) devices have on the grid [11]. The emphasis of this thesis is placed on transient stability.

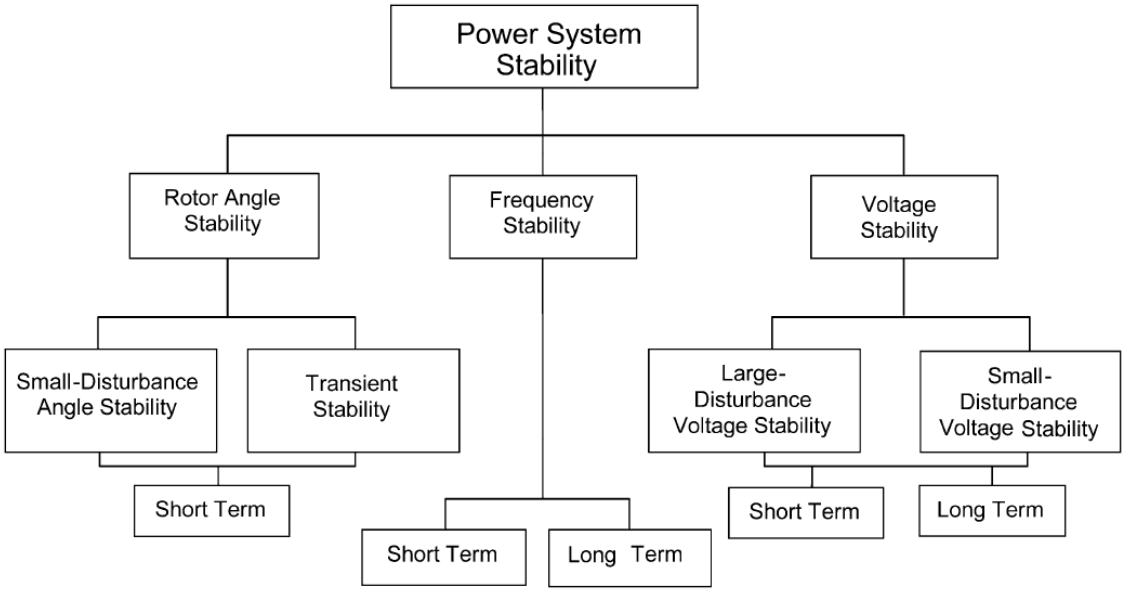

Figure 2.1: Classification of power system stability developed in 2004 [10].

The transient stability is placed inside the Short-term category, where the study time can be from 3-5 seconds, but if the system is very large with dominant inter-area swings it could be extended to 10-15 s [10]. Here rotor angle ($\boldsymbol{\delta}$) stability means that the generators in a power system will retain synchronism with each other following a disturbance. Transient stability, which is a sub-category of rotor angle stability, is for the case that these disturbances are severe [9]. Some examples of severe disturbances are listed [12]:

- Short circuits in the system.
- Fault on transmission facilities.
- Loss of generation power.
- Loss or variation of a large load.

However often it will be evident that it will remain stable within 2 to 3 seconds of the initial disturbance [9]. The most relevant information in transient stability is found in the relative $\boldsymbol{\delta}$ evolution over time, which means studying its oscillation curves [12]. Three different responses of $\boldsymbol{\delta}$ following a transient disturbance are shown in Figure 2.2, which shows different kinds of oscillation curves that can occur. A explanation of the three different cases is listed below [9], [12]:

- **Case 1:** The stable case, in which the rotor angle, after several damped oscillations, reaches a constant post-disturbance steady-state value.

- **Case 2:** The unstable case, also called first-swing instability, in which the rotor angle increases continuously until loss of synchronism occurs.
- **Case 3:** The case in which the generator in the first swing is stable, but during the subsequent oscillations as they start to grow in magnitude until stability is lost; this form of instability generally occurs when the post-disturbance state does not fulfill small-signal stability conditions.

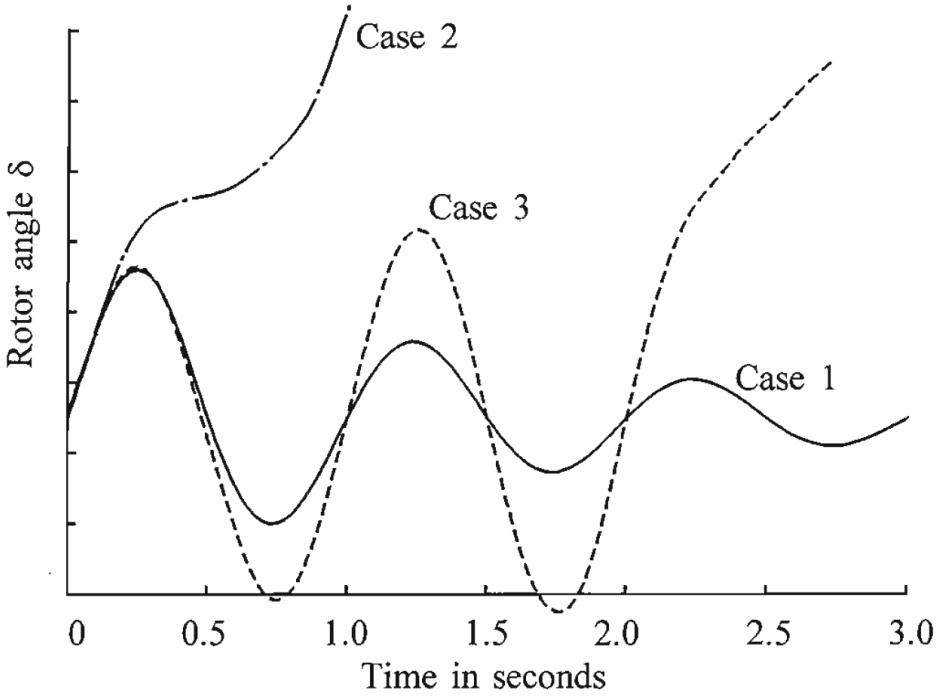

Figure 2.2: Transient event response for δ, three cases are presented: Case 1 is stable, Case 2 is unstable and exhibits first-swing instability, and Case 3 is unstable with increasing subsequent oscillations [9].

The important factor for determining if the system is synchronous is the angular distance (δ) between the rotating machines, where δ is shown for a two-machine example in Figure 2.3. There are two synchronous machines connected with a line in between, as shown in (a). Machine one is working as a generation unit, while machine number two is a motor unit. An equivalent diagram is shown in (b), where the resistance and capacitance are negligible and the machines are represented by two voltage sources E_G and E_M. X_G and X_M are the internal reactance of their respective machines, while X_L represents the line. The resulting phasor diagram of the system and the angle δ are shown in (c). The electrical power output of the generator (P_e) is a function of the angular separation δ between the two rotors, and in the simplified case it is given as in (2.1) [9].

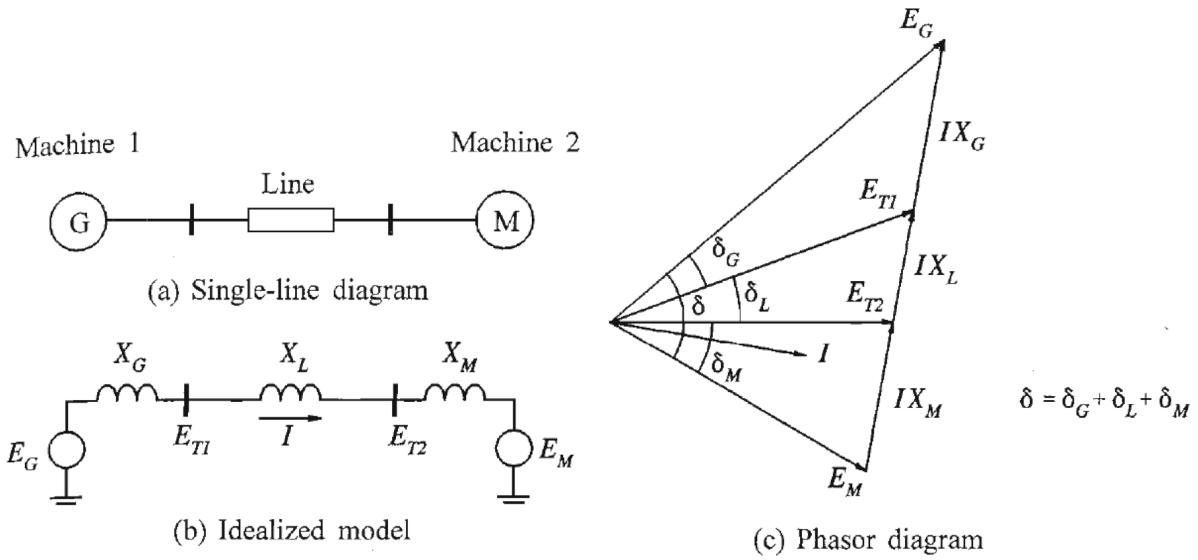

Figure 2.3: Picture showing (a)single line diagram, (b) idealized model and (c) resulting δ from the system, adapted from [9].

$$P_e = \frac{E_G E_M}{X_T} \sin\delta \ ; \ X_T = X_G + X_L + X_M \tag{2.1}$$

The governing equation that relates the change in δ with the difference between the mechanical power of the rotor (P_m) and the P_e is known as the swing equation. The difference between P_m and P_e is commonly denoted as P_a. If the units of P are [p.u.] the inertia constant H is used as shown in (2.2), where the (ω_0) is the initial angular velocity given in units $[rad/s]$ [9].

$$\frac{2H}{\omega_0}\frac{d^2\delta}{dt^2} = P_m - P_e = P_a \ [p.u.] \ ; \ H = \frac{\frac{1}{2}J\omega_{mec}^2}{S_n} \ [s] \tag{2.2}$$

Rather if the units are $[MW]$ the inertia constant M can be used as displayed in (2.3) [12], [13]. In regards to the units of the rotor angle (δ) it is given in electrical radians or degrees, and the difference between the electrical or mechanical angle is given in (2.4), and they are related by the number of pole pairs (P_p) of the synchronous machine [9].

$$M\frac{d^2\delta}{dt^2} = P_a \ [MW] \ ; \ M = \frac{2H}{\omega_{mech}} S_{gn} \ \left[MW \cdot s^2/rad\right] \tag{2.3}$$

$$\theta = P_p \theta_m \tag{2.4}$$

Following a transient disturbance, there will be a mismatch between P_m and P_e that changes the initial rotor angle δ_0. In a stable case, δ will decreasingly oscillate around a new equilibrium point (δ_1), approaching it more with time [9]. The EAC is explained in subsequent Chapter 2.2 to introduce more of the dynamics related to this.

2.2 Equal area criterion

To introduce some of the dynamics related to the swing equation and since some of the same concepts are used later in the SIME methodology, a basic introduction to the EAC is presented. The EAC is shown in (2.5) and it states that for an amount of accelerating area (A1), there has to be an equal amount of decelerating area (A2) for the system to remain stable [9], [12]. It is a method that is used to evaluate transient stability. That can be used to find the critical clearing angle (δ_c) and critical clearing time (CCT). If the angle is increased by any value more than δ_c it would become unstable, due to not enough decelerating area being available (A_{dec}) in regards to the accelerating area (A_{acc}) [12].

$$\textbf{Equal Area Criterion: } A1 = A2 \tag{2.5}$$

In Figure 2.4 an example of a stable case is shown in (a) and an unstable case in (b). In the stable case, the $\delta_{c1} > \delta_c$ and therefore the accelerating area is balanced by having an equal amount of decelerating area, Where what is the maximum angle that is created by the disturbance is defined as (δ_m). In the unstable case the $\delta_{c2} < \delta_c$, which means the accelerating area is bigger than the decelerating area. [9].

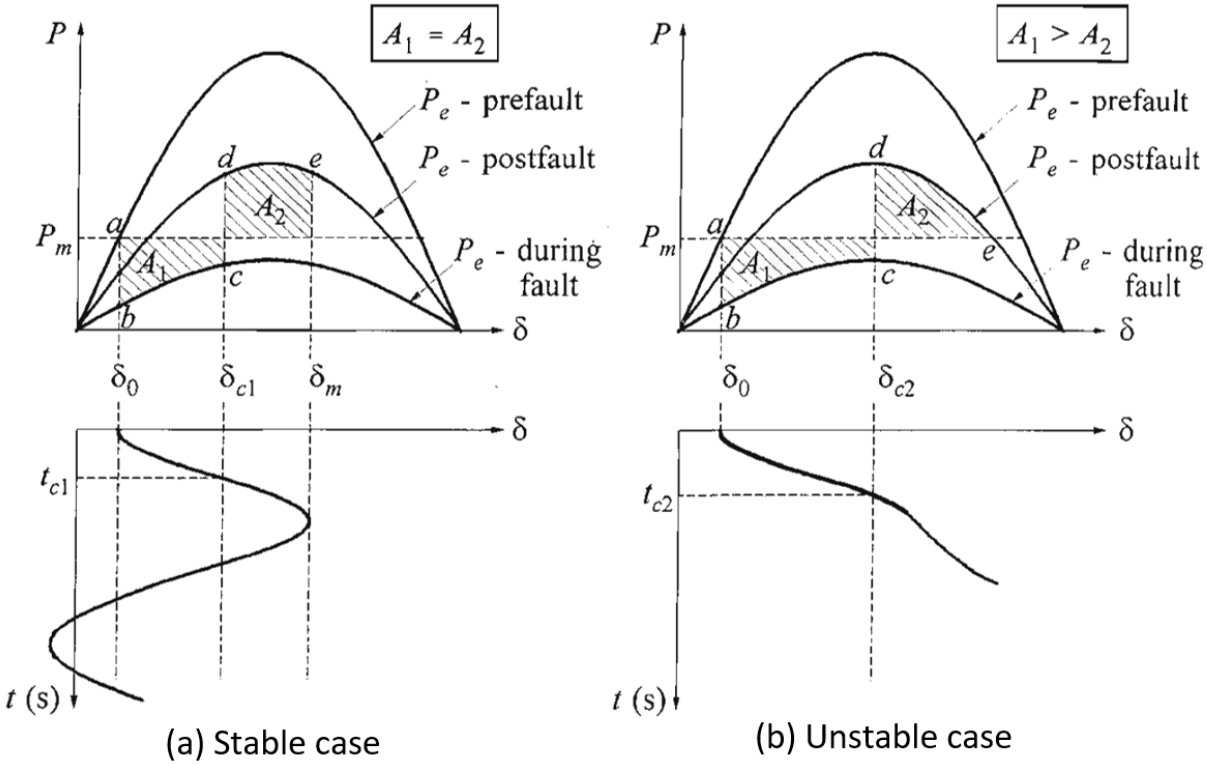

Figure 2.4: A plot showing stable case (a), where A1 = A2 and $\delta_{c1} < \delta_c$. It also presents a plot for an unstable case (b), where A1 exceeds A2 and $\delta_{c2} > \delta_c$. The plot is adapted from [9].

The EAC is a classical method in electrical power engineering, which is nearly a hundred years old [14]. It remains a prevalent topic that is presented in electrical engineering books to understand transient stability, such as Kundur [9] and PM Anderson [13],The application areas of the EAC are listed below [12]:

- **Case one**: Single synchronous machine connected to an infinite bus through a passive network.
- **Case two**: Two synchronous machines of that are connected through a passive network.
- **Case three**: Multimachine system, where all generators are aggregated into two equivalent synchronous machines, which is called the Extended Equal Area Criterion (EEAC).

As mentioned the criterion can be extended to multi-machine systems when all generators are aggregated into two equivalent synchronous machines, an approach known as the EEAC. The limitations of EAC prompted the development of the EEAC during the 1980s and 1990s. The EEAC was proposed as a solution to address the constraints posed by computation time for a TDS, thus offering a more practical option for real-time stability

assessments in power systems [15]. There are certain simplifications when EAC and EEAC methods are used [1]:

- Synchronous machines are represented by a constant voltage source behind the transient reactance.
- Synchronous machines have constant mechanical power and negligible damping.
- Loads have constant impedance characteristics.

More detailed modeling can be done by obtaining the TDS, where the general outline of this is in the subsequent Chapter 2.3.

2.3 Time domain solution and the inclusion of more detailed model

To get the TDS it is necessary to model all the connected elements inside the grid, which includes generators, motors, and loads. To model the generators more detailed can mean to include dynamic models for the AVR, PSS and governor. The TDS is found by piece-wise integration with sufficiently low enough step value (Δt), where the solving time generally is too long for it to be implemented in real-time assessment of transient stability [16]. The formulation of the transient event is articulated through a Hybrid Differential Algebraic Equation (DAE) as in (2.6). Here g encapsulates algebraic equations, while f is the differential equations. The vector $\mathbf{x}$ signifies inertial state variables, including variables like δ and ω. Electrical metrics such as voltage and current, constrained by network dynamics, are represented by $\mathbf{y}$. The vector $\mathbf{p}$ is the system parameters, prone to discrete modifications that can shift the system's topology. These abrupt discrete transitions are the classification of this as a hybrid model [1], [12].

$$\begin{aligned} \dot{x} &= f(x, y, p) \\ 0 &= g(x, y, p) \end{aligned} \tag{2.6}$$

In modeling a transient event, there are three distinct phases to consider. The phases are the pre-fault, the fault, and the post-fault [12]. The number of state variables in the model is dependent on the size of the system, and also how detailed components are modeled [1]. For example in the 39 bus model used in this thesis, there are 166 state variables in the model [7]. In terms of including more details in the model and how these can affect the transient stability, some points of interest are listed below:

- **Resistance:** Dual impact on system damping. It enhances system stability by dissipating energy after disturbances. However, generating transient energy can destabilize the system by amplifying oscillations [17].

- **AVRs:** Enhance transient stability but may compromise oscillation stability due to their high-gain, fast-response nature [18].
- **PSSs:** Improve oscillation stability by complementing AVRs, but could negatively impact transient stability by modifying the voltage signal to the exciter [18].
- **Renewable Energy Sources:** The absence of synchronous generators reduces system inertia, potentially impacting transient stability [19]

One software that can provide the TDS results from a transient event is PowerFactory, which is employed in this thesis and discussed in subsequent Chapter 2.4.

2.4 Time domain solution using PowerFactory

PowerFactory, developed by DIgital SImuLation of Electrical NeTworks (DigiSILENT), is a software used in the electrical power industry for grid simulation and analysis. It assists industry professionals in sizing and validating grid configurations to ensure expected functionality under various operational scenarios [20]. To assess transient stability using PowerFactory, electromechanical simulation is performed, which uses a steady-state root mean square (RMS) network model. If the fault is unsymmetrical then use RMS unbalanced 3-phase and if it is symmetrical RMS balanced, where the latter is the option used consistently in this thesis. A typical value for step size (Δt) for solving this is 0.01 s. Various events that can be included for RMS-Balanced simulation are listed [21]:

- Change of any system parameter (p).
- Symmetrical short-circuit events.
- Load-shedding.
- Start-up and/or loss of generators or motors.
- Variations of controller setpoint.
- Line and transformer switching/tripping.

Generators inside PowerFactory have the possibility of including dynamic models for AVR, PSS, or governor. It also can include components such as motors, renewable energy sources, and more. Post-simulation, various variables can be plotted to analyze the system's response. Additionally, PowerFactory offers the functionality to export simulation results in formats such as CSV (Comma-separated values) [21].

In a multi-generator system such as the 39 bus system, δ can be represented by the two variables, the rotor angle referred to the reference machine rotor angle (firot) or the external rotor angle (firel). One advantage of these variables is that both have a common

reference which all the δ angles are referenced to. An illustration of firot and firel is shown in Figure 2.5. Here it is shown that firel is the angular distance between the rotor of the machine in regards to the reference machine's rotor, while firot is the angular distance between the rotors of the machine to the angle of the reference machine's terminal voltage. These two means that the system is referred to a common reference point [22]. Here it is worth noting that PowerFactory uses the quadrate axis (q-axis), where the induced internal voltage (EMF E) inside the generator is primarily along the q axis and δ can be represented by how much the q-axis leads the stator terminal voltage [9], [13].

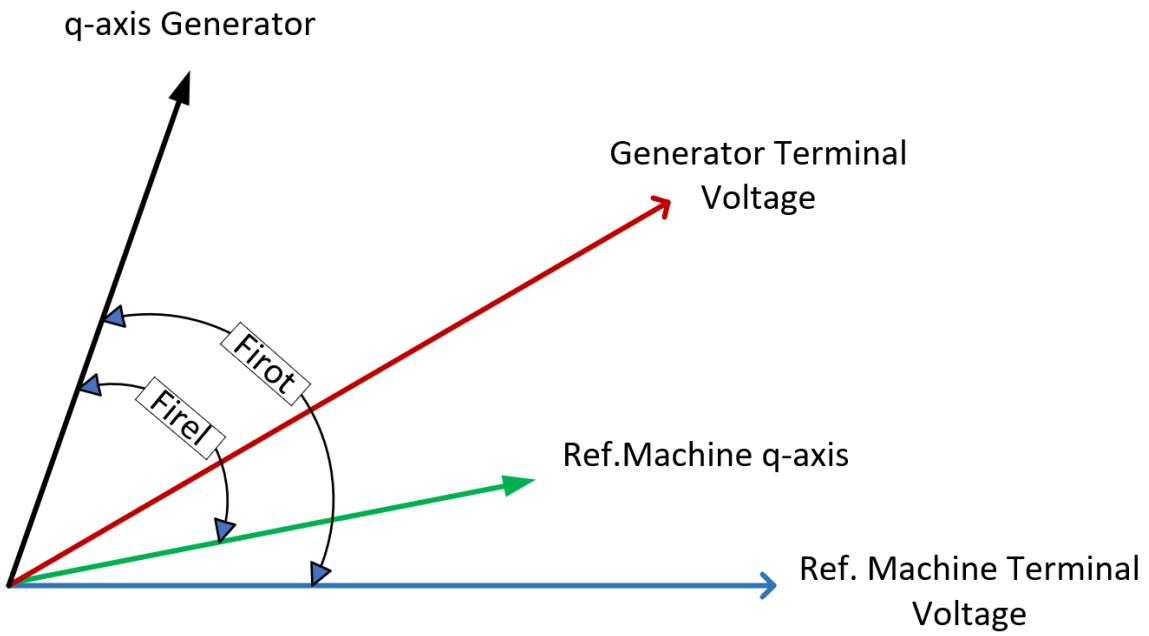

Figure 2.5: Diagram of how δ is calculated using firot or firel, adapted from [22]

An example following a contingency on the New England 39 bus system is displayed in Figure 2.6, where both the variables firot and firel are shown. This contingency is stable, where CT was 0.18 s, and is taken from the later Chapter 5.2.2.

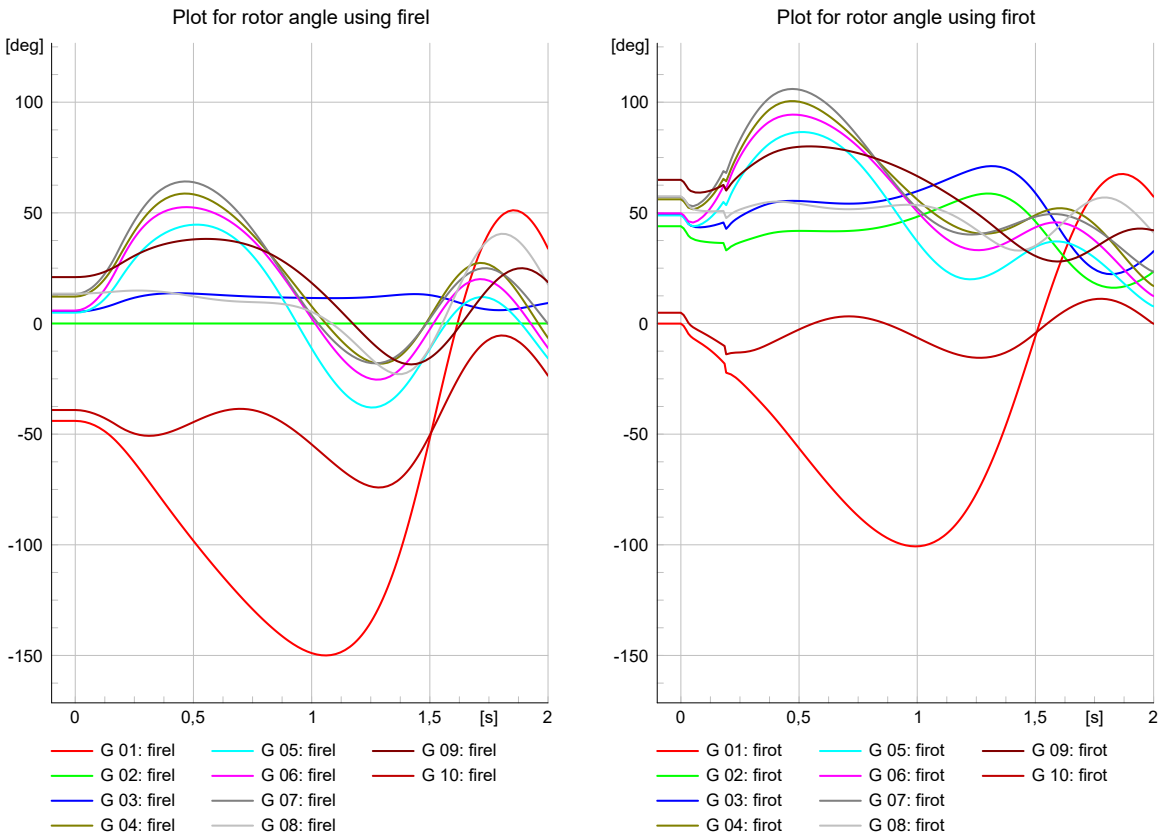

Figure 2.6: Plot of δ for 10 generators taken from simulation contingency Fault bus 16 Stable, with CT = 0.18 s, where generator nr.2 is reference machine.

There is a warning that a generator has pole slipped that is called out-of-step detection. Here it means that either the generator is 360 degrees away from its initial position or that it is 360 degrees away from the reference machines. This is measured using the variable firel and is a clear indication that the generator is not synchronous to the rest of the generation units. The value is default set to 360 degrees [22].

3 Theoretical background on Single machine equivalent (SIME) Methodology

This section provides some necessary theoretical background on the SIME methodology. It first contrasts the Preventive-SIME and E-SIME and introduces the stability margin (η), which tells how stable or unstable the system is in its post-fault trajectory. It is also introduced to its capability to perform sensitivity analysis using the found values of η.

3.1 Introduction to SIME and stability margin

SIME initially started by using concepts from EEAC and trying to relax it from its associated constraints, where these constraints are already explained in Chapter 2.2. This gradually led to the development of "dynamic" and "hybridized" versions of the EEAC that eventually resulted in the SIME method, which still uses concepts from the EEAC. The method used software to find the TDS solution, which was then used as input data. This version is now referred to as the Preventive SIME, which is used to see how the preventive state can be optimized. This means taking preventive actions to minimize the effects that contingencies have on the system stability and also minimize the operating costs. It is worth noting that these actions that place it in a more optimized preventive state inherently increase operating costs. At a later time, the E-SIME was created, which in contrast to the Preventive SIME uses real-time measurements as input. These measurements are analyzed to predict if the system will remain stable and consequently decides if corrective measures are necessary. More on the E-SIME method and how it is employed in this thesis is presented later in Chapter 4. The two methods and some of their differences are summarized in Table 3.1 [1].

Table 3.1: Comparison of Preventive-SIME and E-SIME [1].

Method	**Data Acquisition**	**Possible course of action**
Preventive-SIME	TDS	Change operation region to minimize cost and risk if the contingency occurs.
E-SIME	Real-time measurement	Do real-time corrective measures to keep stability.

One feat that is accomplished by either receiving input data from the TDS or real-time measurement is a time-variant model as described in (3.1), where even though it is time-variant the EAC still holds [1]. The stability margin η that is proposed in the SIME methodology uses this fact, where η is the difference between the A_{dec} and the A_{acc}, which is shown in (3.2) [1].

$$M\frac{d^2\delta}{dt^2} = P_m(t) - P_e(t) = P_a(t)\ [MW] \tag{3.1}$$

$$\eta = A_{dec} - A_{acc}\ [MW \cdot rad] \tag{3.2}$$

To normalize the values for the stability margin it can be divided by the inertia constant M, which is shown in (3.3) [4]. In this thesis the first version shown in (3.2) without dividing by M is used consistently.

$$\frac{\eta}{M} = \frac{A_{dec} - A_{acc}}{M}\ [(rad/s)^2] \tag{3.3}$$

Both SIME methods focus on analyzing post-fault conditions, establishing a η for the resultant trajectory. It accomplishes this by creating the OMIB, which encapsulates the dynamics of the entire multi-generator system. In SIME two propositions lay the foundation of the method [1].

Proposition 1: The process of losing synchronism in a power system occurs because the generators split into two distinct groups. The first being the CMs, which is responsible for the loss of synchronism, and the second is NMs. Consequently, the transient stability of the entire system can be evaluated through the OMIB that is created using the two mentioned groups [1].

Proposition 2 The stability properties of an OMIB can be deduced from the EAC created for that OMIB. Here the data that is used is either sourced from TDS as in Preventive

SIME, or from live measurements that capture the system's behavior during an actual contingency as in E-SIME. In both contexts, SIME derives an OMIB that compresses the data from the multi-machine system, so that the EAC can be applied and the margin η can be calculated. Were in doing this the SIME method will also provide information about any CMs [1].

Using proposition one on a three-generator system the OMIB-δ can be found and is shown as an example in Figure 3.1 (a). Here it can be seen that the δ dampens over time and this case is stable, where δ for the first time starts to decrease following the transient event is known as the return time (t_r). Then using proposition 2 the EAC can be constructed for this OMIB as shown in Figure 3.1 (b). The P_m and P_e is plotted against the δ. The electrical power during the fault is denoted P_{eD}, and post fault is P_{eP}. The angle at which $P_{eP} > P_m$ is marked as $\delta_c h$. This can be used for further analysis and then to calculate η the stability properties of the multi-machine temporal data [1].

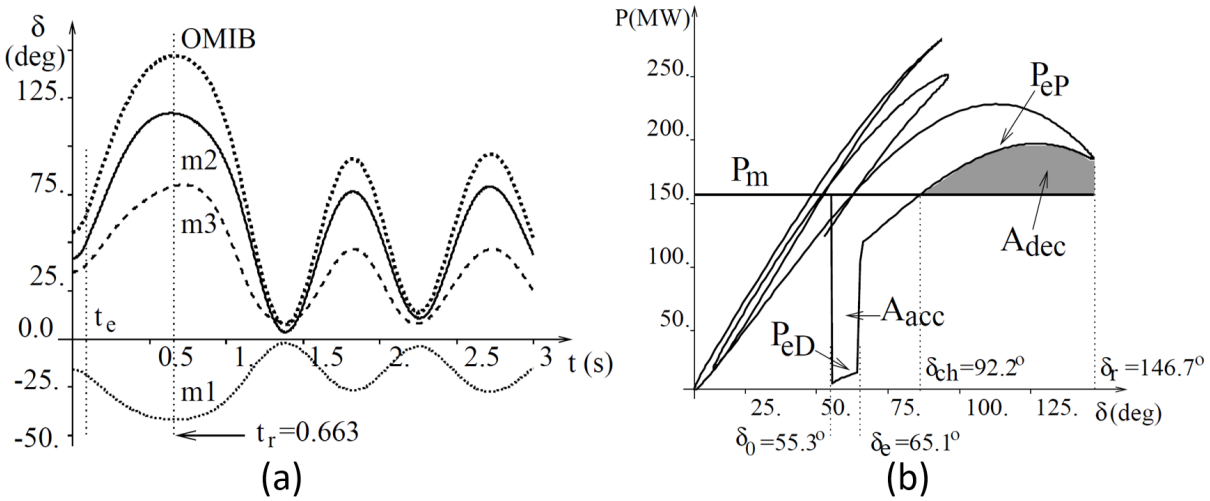

Figure 3.1: (a) Picture of the δ of three generators and the corresponding OMIB δ. (b) Shows the OMIB $P_m(\delta)$ and $P_e(\delta)$ plotted against δ [1].

Here the available decelerating area (A_{dec}) is bigger than the accelerating area (A_{acc}), which means that η has a positive value. However, the A_{dec} shown in the picture lacks some available area that needs to be estimated. This is due to it actually never reaching the unstable state, where consequently the amount of available decelerating area that is left is unknown. Later it will be explained how this remaining area can be estimated and subsequently how η can be calculated. In the plot, the δ_0 is the initial rotor angle at fault inception, δ_e is when the fault is cleared and δ_r is the return angle. Here in the stable case, the speed at the return angle (ω_r) is equal to zero and $P_a(t_r) < 0$. These two facts can be used to check if the system has reached stability, which can done using the criterion shown in (3.4) [1].

$$\textbf{Stability Criterion :}\ P_a(t_r) < 0, \omega_r = \frac{d\delta_r}{dt} = 0 \tag{3.4}$$

However in contrast the instability criterion is given in (3.5). Here the time when instability occurs is denoted as t_u and the angle is at this point δ_u. At this point the $P_a(\delta_u) = 0$ but the rotor will still have energy due to $A_{acc} > A_{dec}$, which means that $\omega_u > 0$. Now if both sides of the swing equation (3.1) are multiplied with $d\delta/dt$ and using that $\omega_0 = 0$, then it can be shown that the unstable margin (η_u) can be calculated using (3.6). This gives a measure of how much kinetic energy is still left in the rotor at the point of δ_u [1].

$$\textbf{Instability Criterion :}\ P_a(t_u) = 0, \dot{P}_a(t_u) = \left.\frac{dP_a}{dt}\right|_{t=t_u} > 0 \tag{3.5}$$

$$\textbf{Unstable Margin :}\ \eta_u = -\int_{\delta_0}^{\delta_u} P_a \, d\delta = -\frac{1}{2} M \omega_u^2 \tag{3.6}$$

To calculate the stable margin (η_{st}) the trajectory of the post-fault curve of the electrical power P_{eP} is projected to where it would have crossed $P_a = 0$ again. This as in the unstable case is denoted as δ_u, but here it needs to be approximated since the system actually never reaches this angle [1]. One method that can be used to approximate it is the weighted least squares method (WLS), where the preventive SIME is stated to put all weights equal to the same value, which means it uses the least squares method (LS) [1]. Another method that can be used is the triangle approximation, The margin will then be the estimation of the area from δ_r to δ_u. This is expressed in (3.7) [1].

$$\textbf{Stable Margin :}\ \eta_{st} = -\int_{\delta_r}^{\delta_u} P_a \, d\delta. \tag{3.7}$$

The calculation of η_{st} using triangle approximation is depicted in the Figure 3.2 (b), with subsequent Figure 3.2 (a) for showing the unstable case and marking the point at which it loses stability δ_u and that ω_r at this point is used to calculate η_u [23].

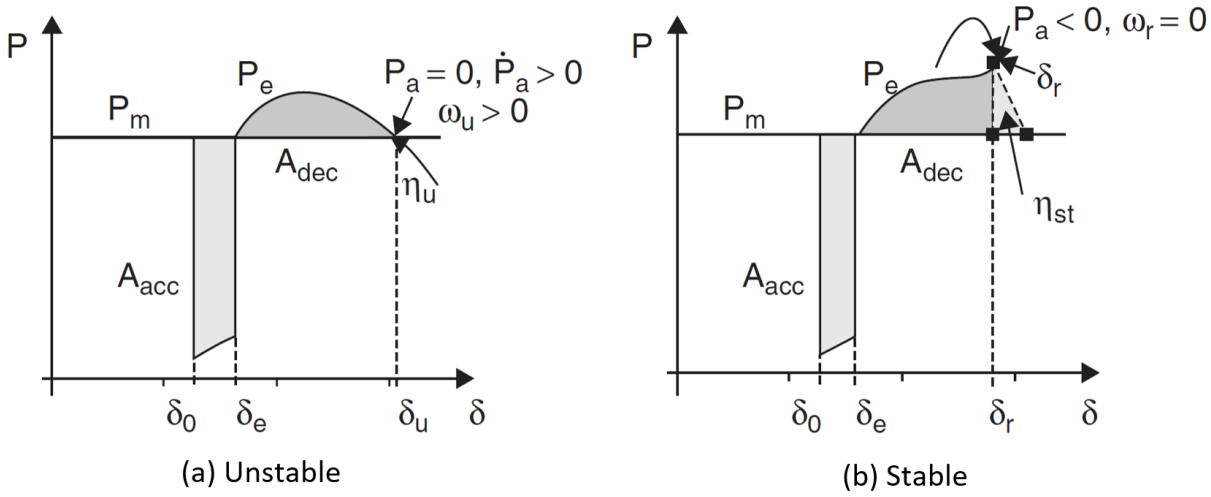

Figure 3.2: (a) OMIB P_e, P_m and δ for unstable case, where η_u can be calculated using ω_u.(b) OMIB P_e, P_m and δ for Stable case and estimation of η_{st} using triangle approximation [23].

The steps to apply the SIME method using TD software, which is applied in the post-fault phase, are listed below [1]:

1. For all generator units measure the δ, P_m, P_e and ω
2. Arrange the δ values for the generators in descending order.
3. Measure the difference between adjacent generators and find the biggest one.
4. The ones that are on the higher end of the adjacent difference is candidate CMs and the rest are candidate NMs.
5. Calculate the candidate OMIB: δ, P_m, P_e and ω. The equations for calculating this is presented in subsequent Chapter 3.2.
6. See if it has reached the stable criterion (3.4) or unstable criterion (3.5), and if either is reached the correct OMIB is found. If not, then take one time step forward and repeat from step 1.
7. Calculate the margin η, using the formula for η_{st} (3.7) if the case is stable, or the formula for η_u (3.6) if unstable.

3.2 Formulas for OMIB-equivalent

The OMIB equivalent is created by dividing the generators into two groups, where one contains the CMs, where k will take on every value for the generator inside that group. Similarly, another group contains the NMs, where j will take on every value. The first

calculation that needs to be done is the calculation of the M for CMs (M_C) and for NMs (M_N), which is shown in (3.8), where these values can be used to calculate the inertia constant of the system denoted as M using (3.9) [1]

$$M_C = \sum_{k \in C} M_k \ ; \ M_N = \sum_{j \in N} M_j \tag{3.8}$$

$$M = \frac{M_C M_N}{M_C + M_N}. \tag{3.9}$$

The δ for each of the groups can be calculated using (3.10), and the OMIB δ is calculated as the difference between these, as is shown in (3.11). In similar fashion to the OMIB δ the ω_C and ω_N can be calculated using (3.12) and the equivalent OMIB ω is found through (3.13) [1].

$$\delta_C(t) = M_C^{-1} \sum_{k \in C} M_k \delta_k(t) \ ; \ \delta_N(t) = M_N^{-1} \sum_{j \in N} M_j \delta_j(t) \tag{3.10}$$

$$\delta(t) = \delta_C(t) - \delta_N(t) \tag{3.11}$$

$$\omega_N(t) = M_N^{-1} \sum_{j \in N} M_j \omega_j(t) \ ; \ \omega_C(t) = M_C^{-1} \sum_{k \in C} M_k \omega_k(t) \tag{3.12}$$

$$\omega(t) = \omega_C(t) - \omega_N(t) \tag{3.13}$$

The OMIB P_m is calculated using (3.14) and P_e is calculated using (3.15). This can be used to find OMIB P_a, which is the difference between calculated P_m and P_e, as shown in (3.16) [1].

$$P_m(t) = M \left(M_C^{-1} \sum_{k \in C} P_{mk}(t) - M_N^{-1} \sum_{j \in N} P_{mj}(t) \right) \tag{3.14}$$

$$P_e(t) = M \left(M_C^{-1} \sum_{k \in C} P_{ek}(t) - M_N^{-1} \sum_{j \in N} P_{ej}(t) \right) \tag{3.15}$$

$$P_a(t) = P_m(t) - P_e(t) \tag{3.16}$$

3.3 SIME for sensitivity analysis

Using found values of η sensitivity analysis for a given parameter (p) can be done, where an example of a p is the CT or P_m. This is formally written in (3.17), where the sensitivity S_p^m margin can be found. Here the $\eta(k)$ and $\eta(k-1)$ are two different margins found for two values of the $p(k)$ and $p(k-1)$. From this the critical value of the $p|_{\eta=0}$ can be estimated using (3.18), which makes the $Acc = Adec$ effectively making $\eta = 0$. This is shown in Figure 3.3 [1].

$$\textbf{Sensitivty Margin :}\ S_p^m = \frac{\Delta\eta}{\Delta p} = \frac{\eta(k) - \eta(k-1)}{p(k) - p(k-1)} \tag{3.17}$$

$$p|_{\eta=0} = p(k) - \frac{\eta(k)}{S_p^\eta} \tag{3.18}$$

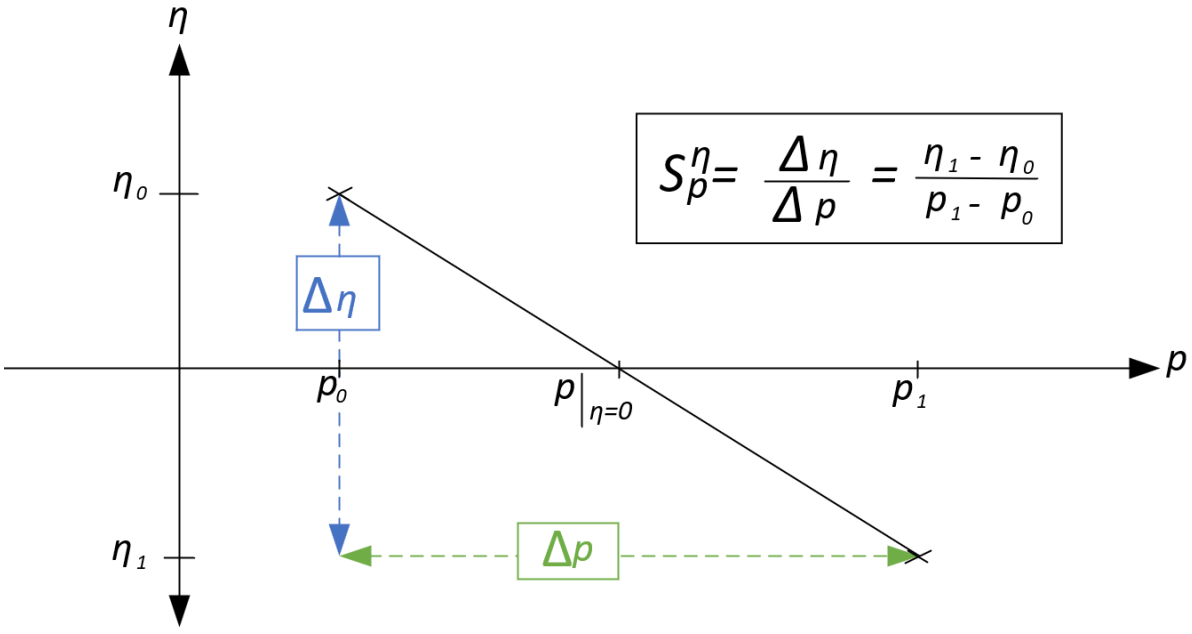

Figure 3.3: Illustration of estimation of $p|_{\eta=0}$ using (3.18), through two measured values η and p.

4 Introduction to Emergency SIME and methodology

The section serves as an introduction to how E-SIME is employed in this thesis and lays out the steps involved. This includes the identification of any CMs, then how the OMIB is formulated, and how it can be tested by checking the area against the kinetic energy. After this, it goes into how the WLS method is used to predict the P_a δ curve, which also shows how the weights for the method was found. All culminating in the calculation of the unstable margin η_u and time to instability t_u, then how corrective measures are implemented following an unstable case. The section concludes with how the data from PowerFactory was gathered and used.

4.1 Introduction to Emergency SIME and overview of methodology

The method E-SIME is designed to in real-time correct emergency states, and also provide a real-time assessment of system stability. This is done using the stability margin η. If this is found to be negative, then the time to instability t_u is also calculated. Here using the estimated t_u will indicate if there is more time to perform more measurements, or if corrective measures are needed. An overview of the steps involved with E-SIME is listed below [4]:

E-SIME Steps:

1. **Trajectory Prediction for finding candidate OMIB:** Predict δ for each generator by using Taylor expansion and rank them in descending order. Identify the largest adjacent angle between the ordered set of δ, to determine which are candidate CM and NM. More on how is implemented is covered in Chapter 4.2.
2. **Estimating δ_u:** Calculate the candidate OMIB P_a and δ. After this, use the WLS to search for a valid solution for δ_u, if it does it is a critical candidate OMIB. If no solution is found, resume measurements and restart the process. More on how this was implemented in Chapter 4.3.

3. **Estimate the η_u:** Use δ_u to calculate η_u. If this is negative, then also estimate the t_u. More on how this was implemented in Chapter 4.4.
4. **Decision on if corrective measures are needed:** Determine if corrective measures are needed using t_u or else continue monitoring. More on how this was implemented in Chapter 4.6.

4.2 Taylor expansion for rotor angle prediction and finding candidate critical machines

The first step in E-SIME is to use the Taylor series expansion to predict each one of the δ trajectories [4], where this prediction is done for a given time forward (t_p). An example of doing this on a 9 bus system that has 3 generator units is shown in Figure 4.1, where the 9 bus system is later presented in Chapter 5.1.1. The plot presents δ using firot, which exhibits a notable sudden shift at the moment the fault is cleared, potentially resulting in erratic estimations around this event. The use of firel, in contrast, would ensure a continuous change at this specific point. For technical details into the case used here, the short circuit fault occurs at line 7-8 and the clearing time (CT) is 0.15 s, with a 0.01 s step size.

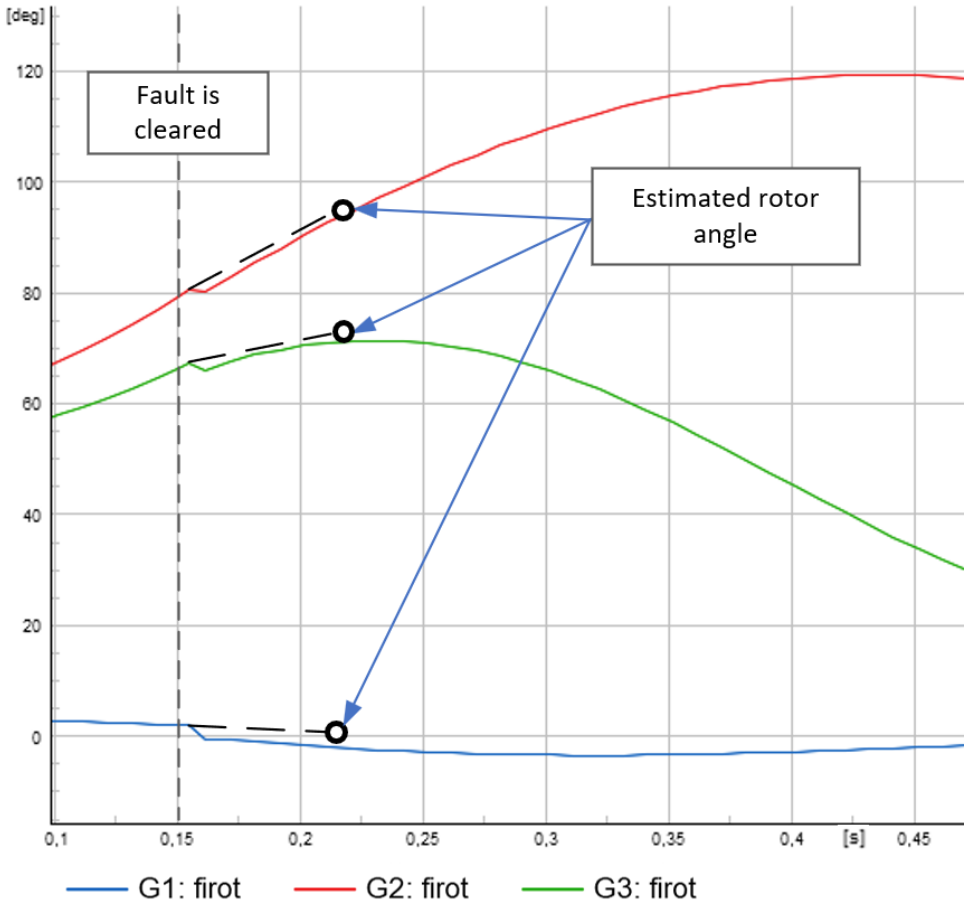

Figure 4.1: Prediction of δ for three different generators following a transient disturbance using Taylor expansion, where generator nr.1 is the reference machine.

The measured values used to estimate δ are done at the current processing time (t_i), and values measured at this time are denoted with the subscript $_i$. In this thesis two methods of predicting δ are going to be tried out, where both of these were made to try and accomplish the step. In the literature [4] there was not a detailed explanation of how the Taylor expansion is employed to predict the values for δ, and the two proposed methods in this thesis are two attempts to accomplish this step. The first uses the measured values of the ω_i and the angular acceleration (γ_i) as shown in (4.1). The second method uses only measured values for the rotor angle δ_i and δ_{i-1} calculated as in (4.2). Both methods use firot as a measurement for δ. Both these two proposed methods will be used and compared, to see which one gives the highest accuracy and has the closest values to the TDS.

$$\textbf{Method 1:}\ \ \delta_p \approx \delta_i + \omega_i \Delta t + \frac{\gamma_i}{2}\Delta t^2 \tag{4.1}$$

$$\textbf{Method 2: } \delta_p \approx \delta_i + \delta'(t_i)\Delta t \ ; \ \delta'(t_i) \approx \frac{\delta_i - \delta_{(i-1)}}{t_i - t_{i-1}} \tag{4.2}$$

The estimations are continually being updated as more measurements come in, and the predicated δ values are sorted in descending order. One example would be if the $\delta_{p3} > \delta_{p2} > \delta_{p1}$ then they would be sorted in the following vector: $[\delta_{p3}, \delta_{p2}, \delta_{p1}]$

The next step is to measure the adjacent distances between them and identify the biggest gap. Continuing with the same example then the adjacent angles would be $[\delta_{p3} - \delta_{p2}, \delta_{p2} - \delta_{p1}]$. The generator set on the high end of the gap is the candidate CMs, and the one on the lower end is the candidate NM. An example to show this is included in Figure 4.2, where this is continuing with the same example as shown in Figure 4.1.

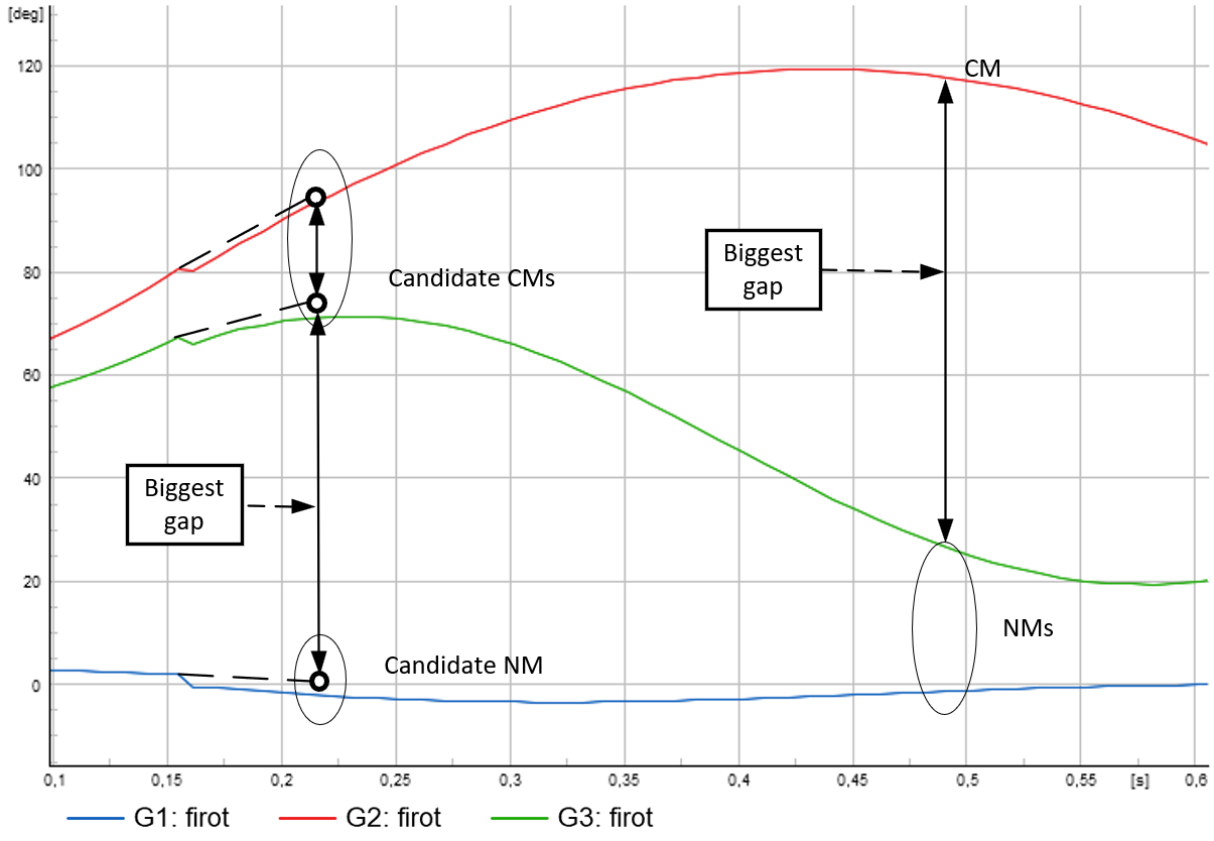

Figure 4.2: Example of determining which generators are candidate CM or NM, where the biggest adjacent gap changes as time progresses. Here generator nr.1 is the reference machine.

Here it is shown that as time progresses the biggest adjacent gap changes, and subsequently one of the candidate CM changes to become an NM. This is included to highlight the importance of having updated measurements come in, when looking for the

biggest adjacent gap. This is because the candidate is not necessarily correct as time progresses.

4.3 Forming OMIB, estimating δ_u and finding weights for weighted least squares method

This chapter goes into how the OMIB is formed from measurements and also how δ_u is estimated using the WLS method. Lastly, it goes into how the weights used in the WLS method were found in this thesis.

4.3.1 Forming OMIB and estimating δ_u

The OMIB equivalent is constructed using the candidate CM and NM, where the relevant equations to construct the OMIB are shown in (3.8) to (3.16). Now with the OMIB equivalent the trajectory of P_a and δ can be estimated past the point of t_i, which is done by solving (4.3) [4].

$$P_a(\delta_u) = a\delta_u^2 + b\delta_u + c = 0 \tag{4.3}$$

To solve the (4.3) there needs to be at least 3 measurements for P_a and δ [4]. A created illustration of 5 measurements after a disturbance, with a sampling time of 0.01 s, is shown in Figure 4.3.

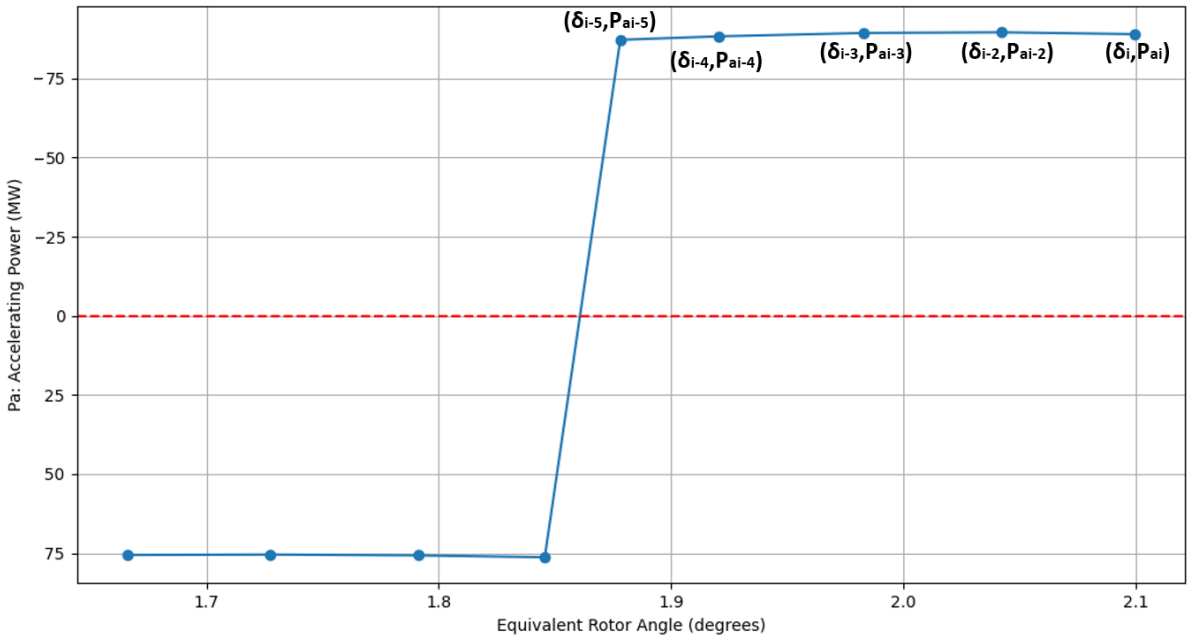

Figure 4.3: Plot showing Pa and δ, where 5 measurements are taken after the fault has cleared.

In Figure 4.4 it is shown that when more measurements are included, it makes the estimated $\boldsymbol{\delta_u}$ converge towards $\boldsymbol{\delta_u}$ [1]. The code that was developed and used for estimating $\boldsymbol{\delta_u}$ is shown in Appendix A.1. It is worth noting that the P_a $\boldsymbol{\delta}$ curve is plotted with the y-axis being $-P_a$. Moving forward in this thesis it will be the case that the y-axis is flipped to match this.

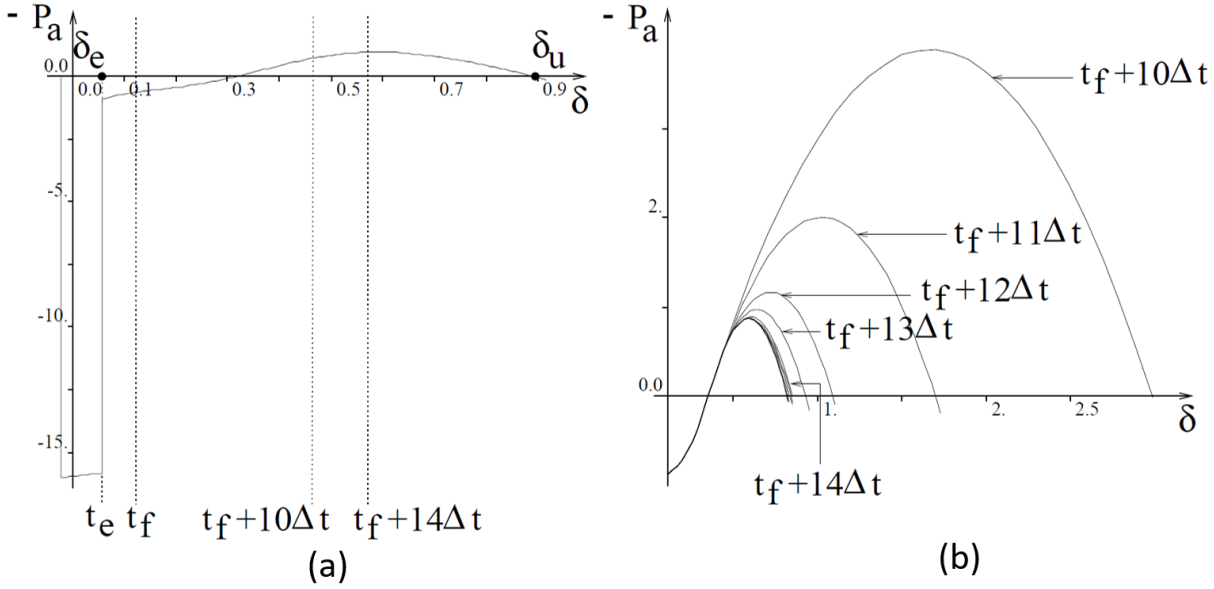

Figure 4.4: Plot (a) shows the trajectory of P_a and δ, while (b) shows estimation of δ_u converges as more measurements are included [1].

4.3.2 Finding values for weights used in weighted least squares method

The WLS method uses weights on each measurement given their significance and in E-SIME the latest measurements have a higher value for weights (w) [4]. However, beyond this specific information on values used for w was not found. Therefore, an optimization process to find the optimal set of w using the known value δ_u from the TDS is used to optimize the weights. The created methodology is listed in the steps below:

1. Find δ_u through complete TDS.
2. initialize the weights, where first all are equal to one.
3. Fit a second order polynomial line $\hat{P}_a(\delta)$ with the current set of weights and Pa_i, δ_i.
4. Compute the loss by using the known value for δ_u, meaning that $L(w) = \hat{P}_a(\delta_u)^2$ should be made as close to zero as possible.
5. Repeat with adjustments made to weights.

This was decided to only do once and was done using the unstable case for the 9 bus system, which is presented in a later Chapter 5.2.2. The code that was developed for finding the optimal weights is given in Appendix A.2. The results are shown in Figure 4.5 (a) and (b), where it also can be seen that the estimations of δ_u converge to the correct value when more measurements are included.

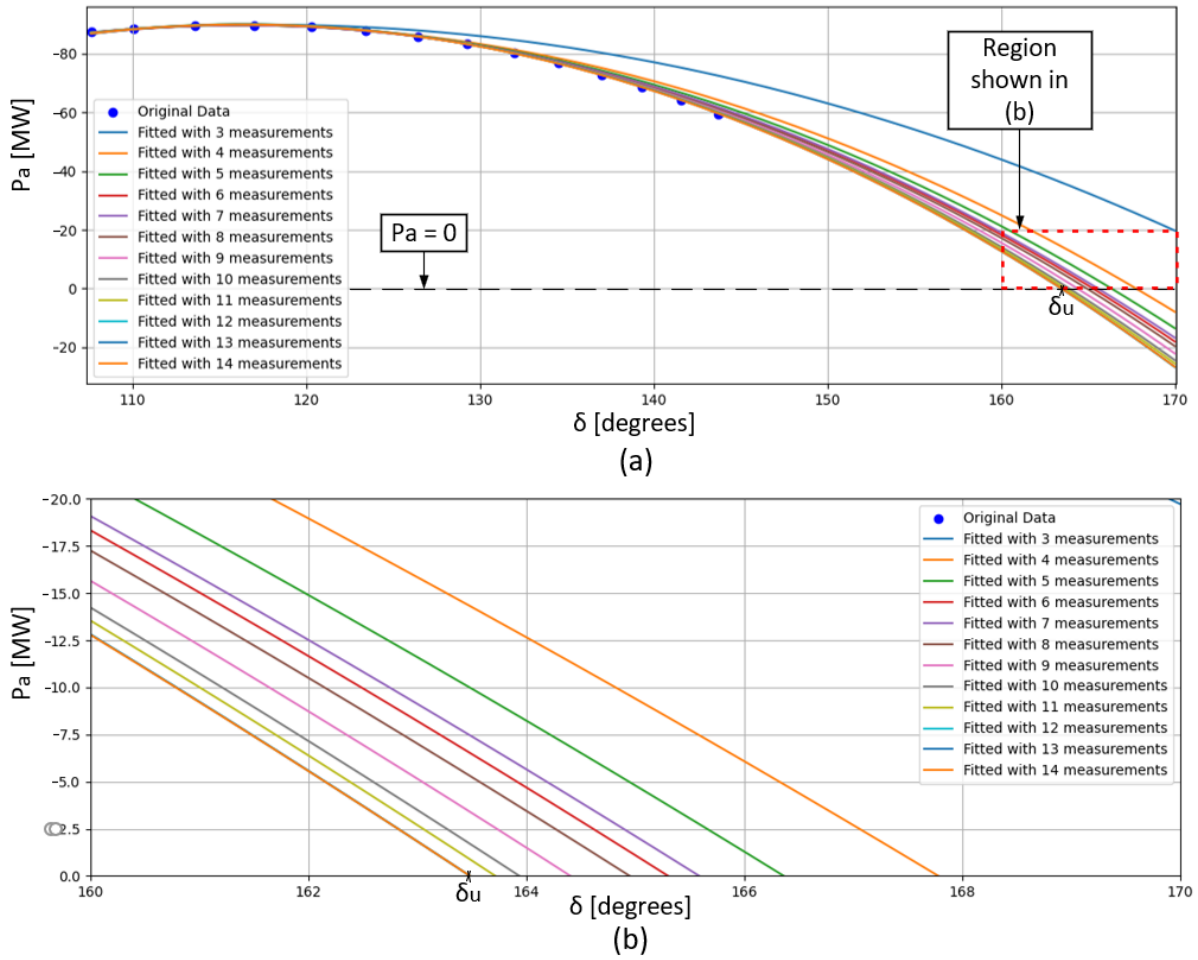

Figure 4.5: (a) Showing δ_u converges when more measurements are included. (b) Zoomed in area of red mark out.

After this, the found optimized weights are displayed in Table 4.1 with 3 decimal places. δ_u can only be estimated in an actual Emergency, meaning this set of weights would not be found. However, the results are used to find a set of weights that can be used. Here it can be seen that there is a tendency of higher value for the w for the last measurements compared to previous measurements. From this result, the following set of weights is chosen to be used $w = [0.1, 0.1.....0.1, 1, 1, 1]$. However, it is important to note that in the TDS the weight set used is filled only with ones. This is equivalent to using the LS method as previously discussed in Chapter 3.1.

Table 4.1: Optimized weights for each measurement with known δ_u, which is done including different number of measurements.

w_1	w_2	w_3	w_4	w_5	w_6	w_7	w_8	w_9	w_{10}	w_{11}	w_{12}	w_{13}	w_{14}	**Meas. Incl.**
1.000	1.000	1.000	-	-	-	-	-	-	-	-	-	-	-	3
0.000	0.000	1.000	1.000	-	-	-	-	-	-	-	-	-	-	4
0.000	0.000	1.000	1.000	1.000	-	-	-	-	-	-	-	-	-	5
0.000	0.000	0.000	1.000	1.000	1.000	-	-	-	-	-	-	-	-	6
0.000	0.629	0.000	0.000	1.000	0.000	1.000	-	-	-	-	-	-	-	7
0.000	1.000	0.000	0.000	0.000	1.000	0.000	1.000	-	-	-	-	-	-	8
0.000	0.548	0.000	0.000	0.000	0.000	1.000	0.000	1.000	-	-	-	-	-	9
0.000	0.857	0.000	0.000	0.000	0.000	0.000	1.000	0.000	1.000	-	-	-	-	1
0.000	0.982	0.000	0.000	0.000	0.000	0.000	0.000	1.000	0.000	1.000	-	-	-	11
0.000	0.625	0.093	0.000	0.000	0.000	0.329	0.957	1.000	0	0.470	0.999	-	-	12
0.000	0.999	0.802	0.034	0.002	0.739	0.997	0.999	0.968	0.894	0.575	0.999	0.936	-	13
0.745	0.998	0.991	0.913	0.892	0.936	0.999	0.999	1.000	1.000	0.971	0.957	0.999	0.997	14.0

The reason for choosing 0.1 for w for measurement values taken at $i-3$ is previous measurements are not ignored completely. This is done to have a set of weights that can cover the grounds for different scenarios, without overly optimizing it to the given situation. This process is only done for one case in this thesis but could be done for more. The set of w is used for the case of 14 measurements, where using this δ_u is estimated to be equal to 162.787 degrees and the actual value is 163.481 degrees. This means that in this case, the error is in the order of 1 degree, which has a minimal effect on the value of η_u.

4.4 Calculation of unstable margin and time to instability t_u

η_u formula in emergency case is (4.4) [4], where ω_i is the speed at the point of the last measurement performed. The term that has ω_i and M is used to estimate how much the system needs to be decelerated to remain stable. The other term is related to P_a and is the available decelerating area left after the point of the last measurement. The integral term can be solved by integrating the 2-order polynomial fit of P_a, as shown in (4.5). Calculation of this was performed by using the script in Appendix A.3

$$\eta_u = -\int_{\delta_i}^{\delta_u} P_a \, d\delta - \frac{1}{2} M \omega_i^2 \tag{4.4}$$

$$\int_{\delta_i}^{\delta_u} P_a \, d\delta = \frac{a}{3}(\delta_u^3 - \delta_i^3) + \frac{b}{2}(\delta_u^2 - \delta_i^2) + c(\delta_u - \delta_i) \tag{4.5}$$

If $\eta_u < 0$ or very close to zero it will result in a possible unstable case, where after this t_u can be calculated using (4.6) [4]. Furthermore more inserting that P_a is after δ_i is

given by a second order polynomial fit it can be calculated using (4.7). Now this was solved by numerical integration using Python, where the relevant code for this is shown in Appendix A.4. Following more measurements, then the values δ_u, η_u and t_u will need to be updated. Here it is chosen to denote the time in between the time to instability and measurement time is denoted (t_{ui}), which is expressed as shown in (4.8). This was done due to it being a useful quantity in the later Chapter 4.6, where it is used to determine if corrective measures are needed.

$$t_u = t_i + \int_{\delta i}^{\delta u} \frac{d\delta}{\sqrt{(2/M)\int_{\delta_i}^{\delta} -P_a d\delta + \omega_i^2}} \tag{4.6}$$

$$t_u = t_i + \int_{\delta_i}^{\delta_u} \frac{d\delta}{\sqrt{(2/M)(\frac{a}{3}(\delta_i^3 - \delta^3) + \frac{b}{2}(\delta_i^2 - \delta^2) + c(\delta_i - \delta)) + \omega_i^2}} \tag{4.7}$$

$$t_{ui} = t_u - t_i \tag{4.8}$$

4.5 Checking OMIB using integral of P_a against kinetic energy change

In this thesis, the following test was created for a single time as described in (4.9), where both sides of the equation have units of $[MW \cdot rad]$. The test checks that the integral of P_a approximately equals the kinetic energy change, where if there is a substantial numerical deviation, this would indicate an error in the OMIB calculations. This was formulated by using the way the unstable margin η_u is calculated in E-SIME [4], which was previously shown in (4.4). It was shown that η_u in E-SIME is calculated using two terms, where the term relating to M and ω_i gives a measure of how much kinetic energy is left in the rotor. The other term is the integral of P_a from δ_i to δ_u, which represents the available decelerating area that is left. From these two terms, it was seen that the kinetic energy change should be equal to the integral of P_a.

$$\textbf{Test for single time step: } \frac{1}{2}M(\omega_{w2}^2 - \omega_{w1}^2) \approx (\delta_2 - \delta_1)(\frac{P_{a1} + P_{a2}}{2}) \tag{4.9}$$

This was also expanded upon so it could be done for more time steps as shown in (4.10). Here the term for the integral of P_a with δ is simply referred to as "Integral of P_a", and the term relating to the ω as "Kinetic energy change". These two terms are used to calculate the percentage error, which was done using (4.11). If this error was a very high percentage

in the order of 10% it would be an indication that it was formulated wrong. This test was created to try and control if the OMIB formulation was correctly done.

$$\textbf{Test for multiple time steps: } \frac{1}{2}M(\omega_{wn}^2 - \omega_{w1}^2) \approx \sum_{i=1}^{n-1}(\delta_{i+1} - \delta_i)\left(\frac{P_{ai} + P_{a(i+1)}}{2}\right) \quad (4.10)$$

$$\textbf{Percentage Error: } = \left(\frac{\text{Integral of } P_a - \text{Kinetic energy change}}{\text{Kinetic energy change}}\right) \times 100\% \quad (4.11)$$

4.6 Corrective measures

The corrective measures can be either increasing the OMIB P_e, where this can be achieved through dynamic braking, HVDC links, and other FACTS devices. Another possibility is to decrease the OMIB P_m which can be done through generator tripping [24] [1] . The two corrective measures that are employed in this thesis are disconnecting generators or splitting the grid. Figure 4.6 is included to show the effect of reducing P_m through disconnecting CMs.

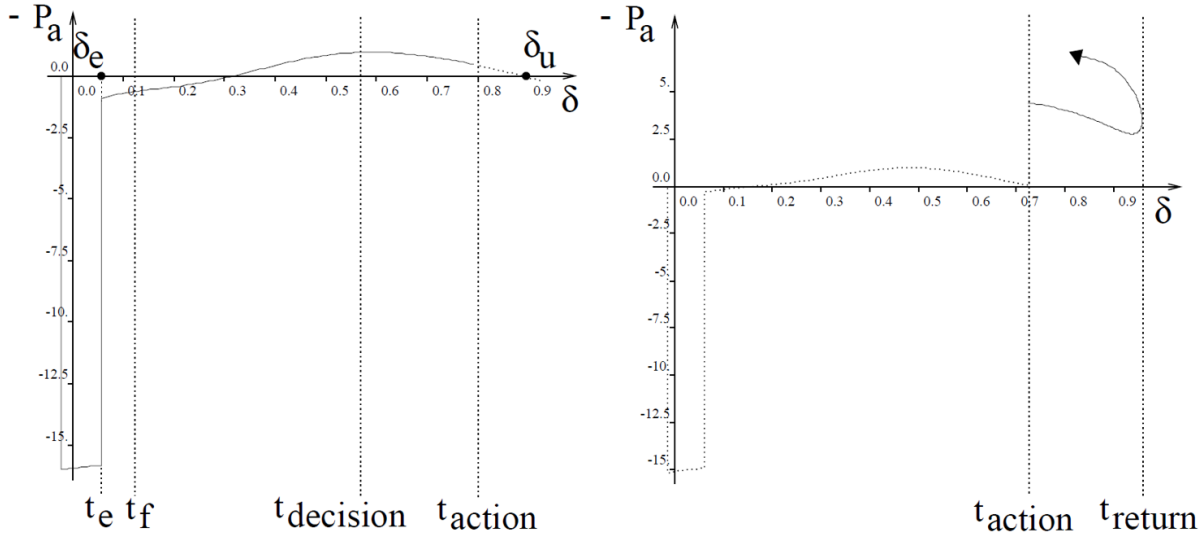

(a) Uncontrolled OMIB P - δ curve (b) Controlled OMIB P - δ curve

Figure 4.6: P δ curve for (a) Uncorrected case and (b) corrected case where corrective measures make the system remain stable [1].

The value t_u can be used to decide if corrective measures should be taken or to continue monitoring [4]. In this thesis, the time to cut a generator (t_d) is chosen to be 0.1 s, which in real-life applications could be slightly larger. Also, the sampling rate for taking measurements is 0.01 s. From this, a criterion for corrective measures is formulated and shown in (4.12), where if this is reached then CMs will be cut. Here it is possible to add terms for either tolerances or errors, where the inclusion of noise might affect the results.

$$\textbf{Corrective Measures Criterion: } t_{ui} \leq t_d + \Delta t \tag{4.12}$$

4.7 Generation of test data for E-SIME using PowerFactory

This chapter goes into which variables in PowerFactory are used, a discussion about the variable used to represent δ and subsequently how to unwrap the values for the δ. Later it discusses how the OMIB formulation data was created and exported.

4.7.1 Variables in PowerFactory used for E-SIME

Here the choice for representing δ stood between firot and firel, where this is because they both are measured using the reference machine [22]. This makes both choices valid for constructing the OMIB, due to the OMIB δ being defined as the difference between the δ_C and δ_N. An illustration is included in Figure 4.7 that shows that both firot (a) and firel (b) end up measuring the angular distances between the rotors. However, using firot for the prediction of δ values has the disadvantage that values can have abrupt discontinuous changes when for example a fault is cleared. The reason this happens is due to these events affect the terminal voltage abruptly. In turn, this can affect the δ prediction and cause erratic predictions, but this is more pronounced in the first measurement after a discrete event. After the first measurement after a discrete event the issue subsidies, due to it returning to having a continuous behavior.

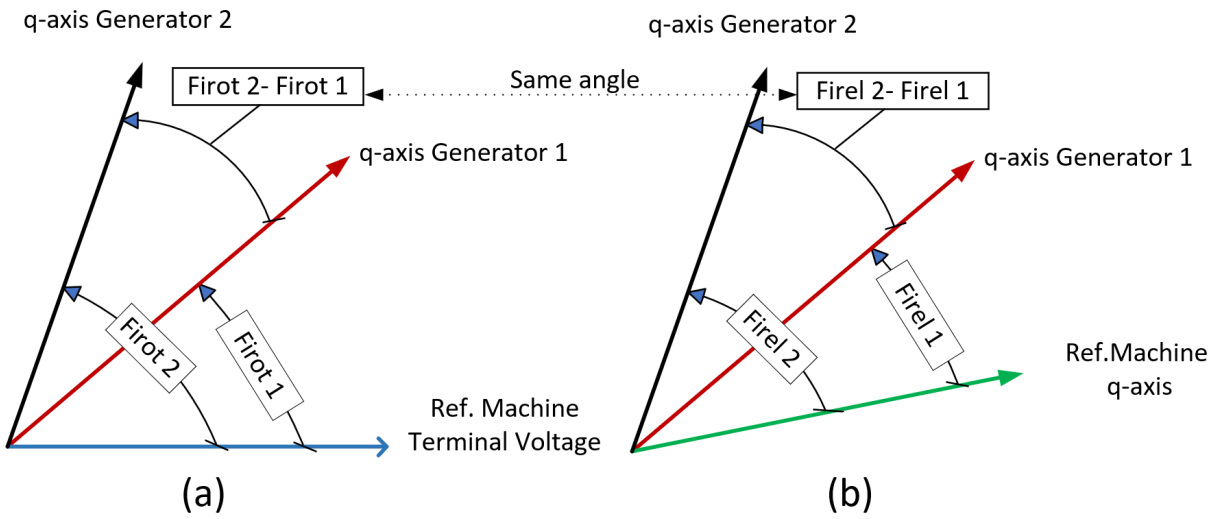

Figure 4.7: Diagram showing two generators represented using firot (a) and using firel (b), where taking the distance between the angles results in the same angle.

Values for the P_e the variable $s:pgt$ was used and P_m the $s:pt$. Both these variables are given in [p.u.] and are rated to the generation unit's rating (P_r) in PowerFactory. This was converted to [MW] using the formula (4.13). Also, the value for the speed deviation ω can be found using the rotor speed (ω_{rot}) variable s:x:speed, as shown in the formula (4.14).

$$P = P_{p.u.} P_{nr} \ [MW] \tag{4.13}$$

$$\omega = \omega_{rot} - \omega_s \ [p.u.] \tag{4.14}$$

The variables that are exported in CSV files from the simulation are displayed in Table 4.2 [22], where γ is only used in method nr.1 of the δ prediction as discussed in Chapter 4.2.

Table 4.2: PowerFactory variables used for E-SIME.

Variable	Name in PowerFactory	Description	Unit
P_{elec}	s:pgt	Electrical Power	p.u.
P_{mech}	s:pt	Turbine Power	p.u.
δ	firot	External rotor angle	degrees
ω_{rot}	s:x:speed	Speed of rotor	p.u.
γ	speed:dt	Speed, derivative	p.u./s

4.7.2 Unwrapping angles for δ

Both the firot and firel variables are wrapped, meaning that when 180 degrees angle is exceeded it will wrap to -180 degrees [22]. This needs to be a continuous value to plot either the P_a δ curve or the phase diagram past the point of one generator having wrapped around. The unwrapping of angles was achieved using a created Python code that is listed in Appendix A.5. The code adjusts the δ values after it has wrapped by adding 360 degrees, where this effectively so unwraps it. The threshold value was chosen to be -340 degrees to give some leeway, due to the sampling rate between measurements being around 0.01 s. A picture of this applied to an unstable case can be seen in Figure 4.8.

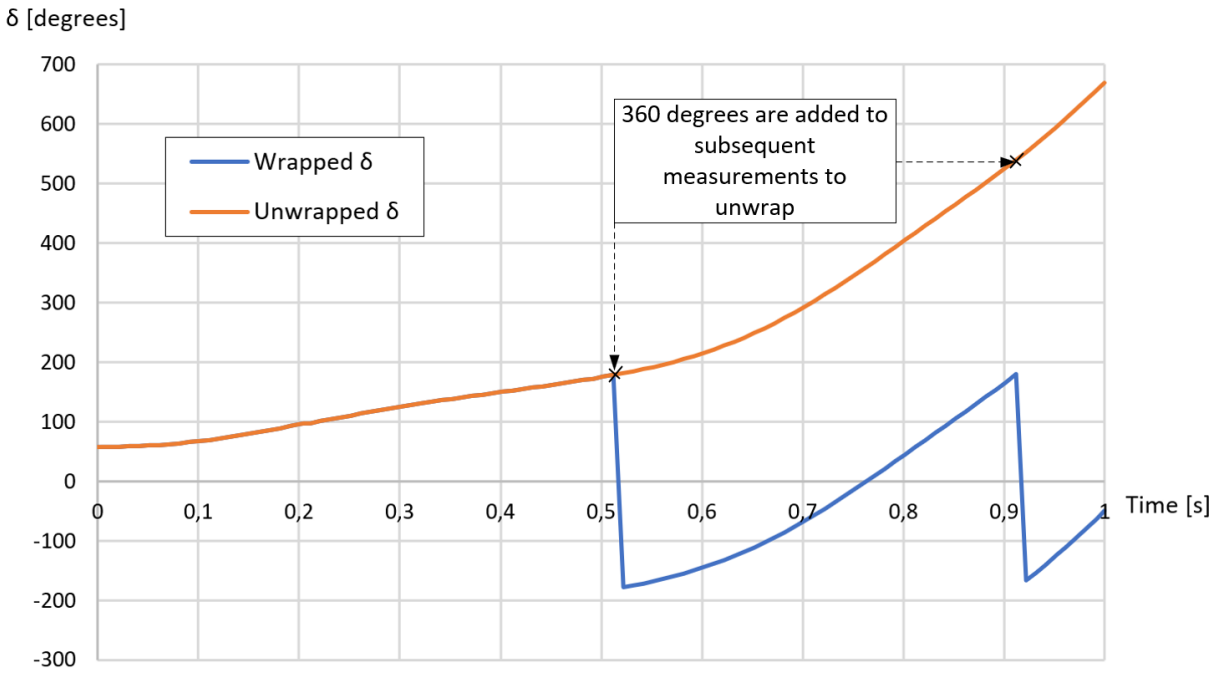

Figure 4.8: Unstable case showing the original wrapped for δ, and then by adding 360 degrees δ becomes unwrapped.

4.7.3 Exporting data for the creation of OMIB formulation or directly inside PowerFactory

In this thesis, the TDS generated using PowerFactory was exported as CSV files, where after this they were further analyzed using Python and Excel. However, the results for the the OMIB ω, P_a and δ for the 9 bus system were also calculated directly by using residual calculation inside PowerFactory. This was only employed on the 9 bus system, when the step size was 0.001 s, whereas E-SIME consistently only had a step size of 0.01 s. A result from using residual calculations is shown in Figure 4.9, where all the relevant OMIB values are plotted against time. Here this is a contingency on line 8-9 with CT 0.245 s, where more details about this is presented in Chapter 5.2.2. Similarly, this could also be done for the 39 bus system. However, due to the amount of variables in the 39 bus system, the residual calculation was not done for this one. In the 39 bus system, the step size was always 0.01 s, part of this choice was due to data management.

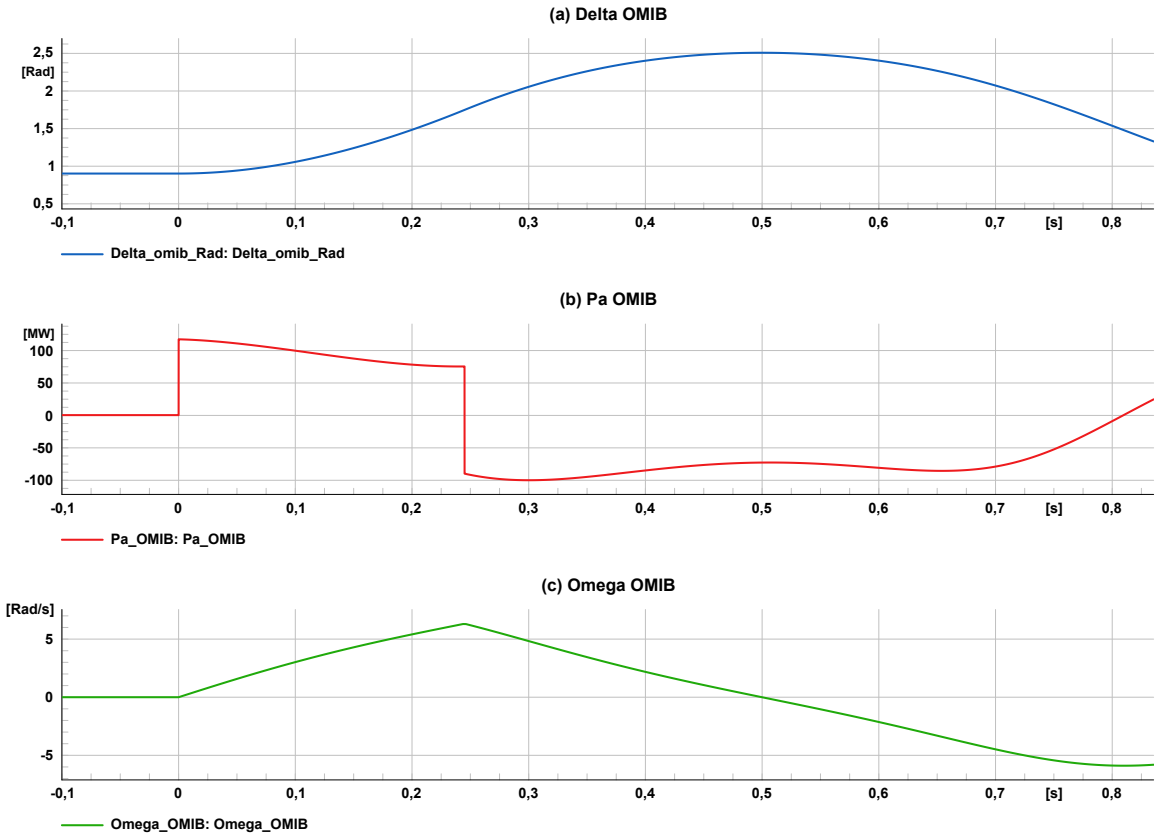

Figure 4.9: Plots of the OMIB parameters (a) δ, (b) P_a, and (c) ω plotted vs time in PowerFactory.

However, a weakness with residual calculations is that the angles are not unwrapped, meaning that if one generator has wrapped the results will not be accurate. The second disadvantage is it cannot be used to plot the P_a δ curve after one generator has been disconnected, as the OMIB then would change. However, the values from the cut generator would still be included and affect the results.

5 E-SIME applied on 9 and 39 bus system

In this chapter, the E-SIME methodology discussed in Chapter 4 is applied to the 9 bus and 39 bus system. Initially focusing on the 9 bus system, its technical specifications and PowerFactory model are introduced, followed by a presentation of the planned disturbances. Then the process of identifying CMs, forming the OMIB equivalent, and using E-SIME to obtain results for the contingencies. This sets the stage for a more complex investigation of the 39 bus system, where the same steps are applied.

5.1 SIME on 9 bus system

This section delves into the application of the E-SIME methodology on the 9 bus system. It covers the system's technical specifications, identifies CMs, and presents results obtained through the E-SIME approach. These findings are then compared with the TDS results.

5.1.1 Technical data on 9 bus system

The 9 bus system is shown in Figure 5.1. This system consists of 3 interconnected generators and 9 buses, where the nominal frequency of the system is 60 Hz. The task case is taken by the book [13].

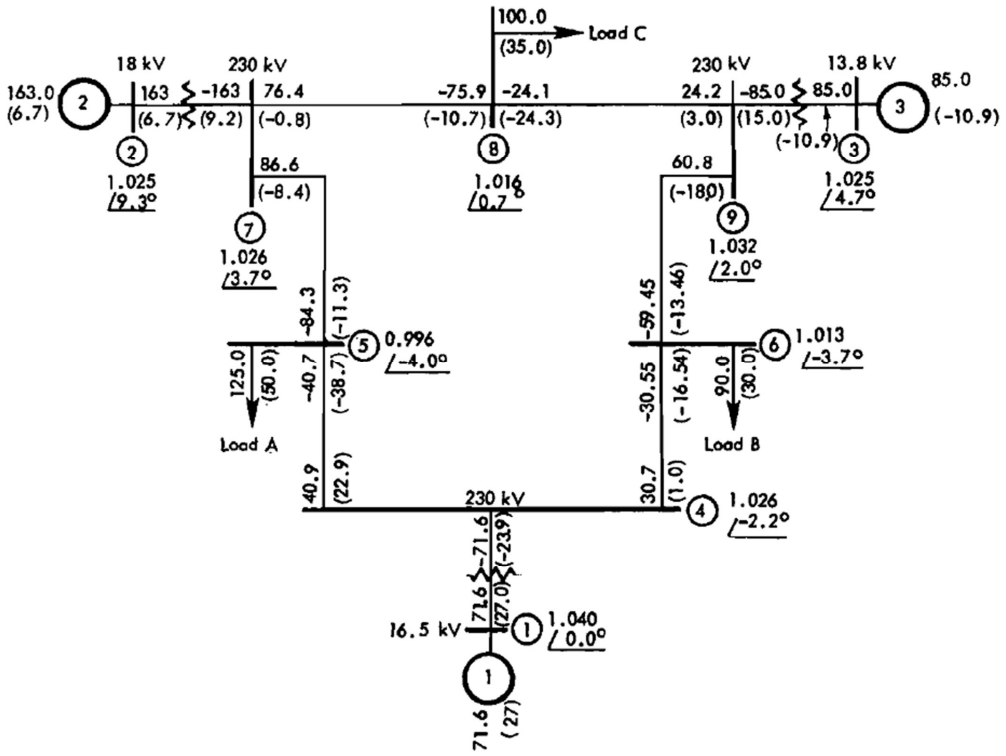

Figure 5.1: Picture of 9 bus, with load flow result [13].

The 9 bus system PowerFactory model is shown in Figure 5.2, where the different voltage levels are represented with color. This is taken from the example included inside PowerFactory, where more details about technical data can be found in [8]. Here the following is true of the program in PowerFactory:

- The generator is modeled with the standard model, where more details about this can be found in the technical reference to the synchronous machine in [22].
- Lines are modeled with R, X, and Susceptance (B), with lumped parameters.
- Loads have constant active and reactive power demand, they are not voltage-dependent.
- Generators are not equipped with Governor, AVR, and PSS.

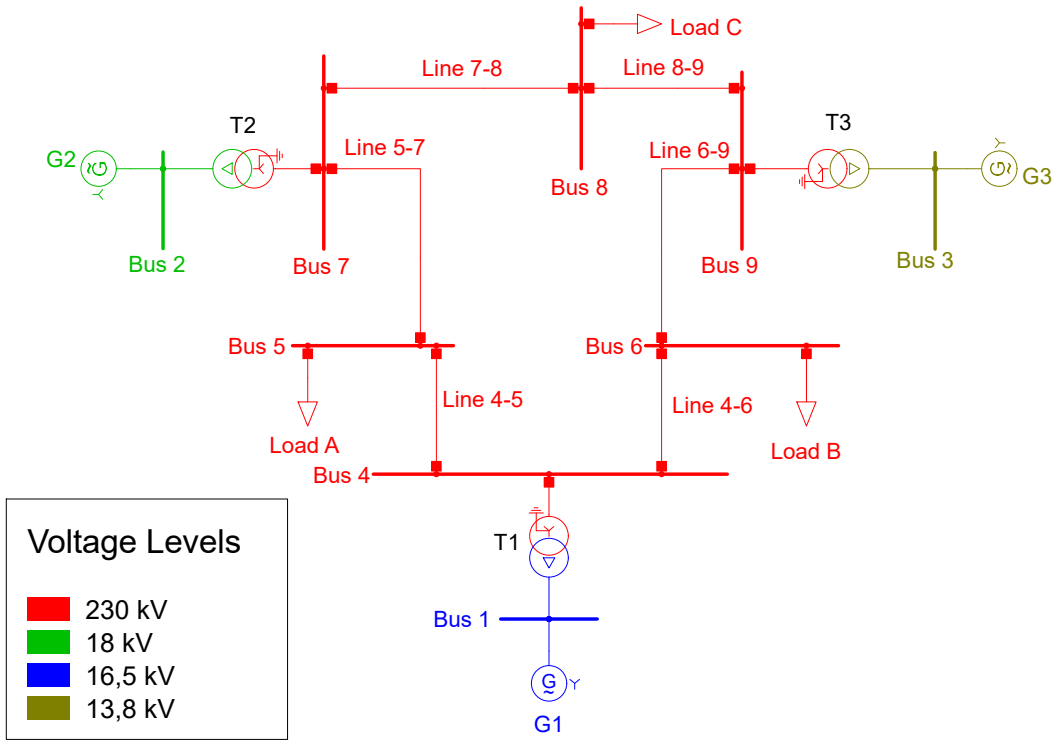

Figure 5.2: Scheme of the 9 bus system implemented in PowerFactory.

Here it is worth noting that generator units 2 and 3 had rpm 3600, which implies one pole pair. However, generator unit No.1 is said in technical reference to have an rpm of 180, meaning it would have 20 pole pairs [7]. This was checked for the generators using the variable t:polepairs inside the PowerFactory project. Here it was discovered it was defined with 1 pole pair for all generators, which means that the (5.1) is true for all generators. The reason this is important is it would introduce numerical errors to M if the number of pole pairs was wrong.

$$\omega_{mech} = \omega_s = 2\pi 60Hz \tag{5.1}$$

In the technical data, the ratings are given [8], and the value for M is calculated using the formula (2.3). The relevant data that was used to calculate the M for each generator is shown in Appendix B.1.

5.1.2 Planned disturbances

The planned disturbances are all a fault that occurs in the middle of the line 8-9, but there are four different CTs. One of them includes the CCT, which was found in 5 decimal precision to be 0.25150 s using PowerFactory. Details of all the planned disturbances are presented in Table 5.1.

Table 5.1: Overview of planned disturbances for the 9 bus system.

Fault Location and Distance	**Switching Time (s)**	**Stable?**
Line 8-9, 50%	0.2450	Yes
	0.2500	Yes
	0.2515	Yes
	0.2600	No

5.1.3 Finding Critical machines and OMIB-equivalent

Finding CMs was done using the approach laid out previously in Chapter 4.2, where the relevant code developed for $\boldsymbol{\delta}$ prediction and finding CMs is presented in Appendix A.6. This code was applied for the unstable case that had CT of 0.26 s, where firot was used to represent $\boldsymbol{\delta}$. The code was used to see if it could predict the values for 0.37 s forward in time. The two methods were employed and compared with the TDS results, and the error is calculated as the difference between the TDS and the predicted value. The results of this are presented in Table 5.2. Both methods could be used to find the correct CMs and NM because they both find that the biggest adjacent gap is between Generator 1 and 2. However, method nr.2 gave an overall better estimation for $\boldsymbol{\delta}$, and due to this method nr.2 was chosen to be used moving forward. One advantage of method nr.2 is that it would be simpler to implement in real-life applications, due to it only using $\boldsymbol{\delta}$ as input. However, method nr.1 would also need $\boldsymbol{\omega}$ and $\boldsymbol{\gamma}$

Table 5.2: Comparison of TDS Results with those from Method nr.1 and nr.2.

Values from simulation		**Method nr.1**		**Method nr.2**	
		Measured	**Error**	**Measured**	**Error**
δ_1	-5.250	0.377	-5.627	-0.365	-4.885
δ_2	127.086	104.069	23.017	119.541	7.545
δ_3	148.992	117.113	31.879	139.329	9.663

To further test the accuracy of method nr 2, another test was also performed. In this test, values were predicted until one of the generators hit approximately 180 degrees, and then this was compared with the TDS result. The results of this test are included in Figure 5.3. Here the difference between the prediction and the actual value of when Generator unit nr.3 hits 180 degrees, is measured to be 0.025 s. Both methods would detect the CMs and NM, but due to easier implementation and overall better accuracy method nr.2 shows more promise. Both methods would have found the CMs and NM that are shown in (5.2).

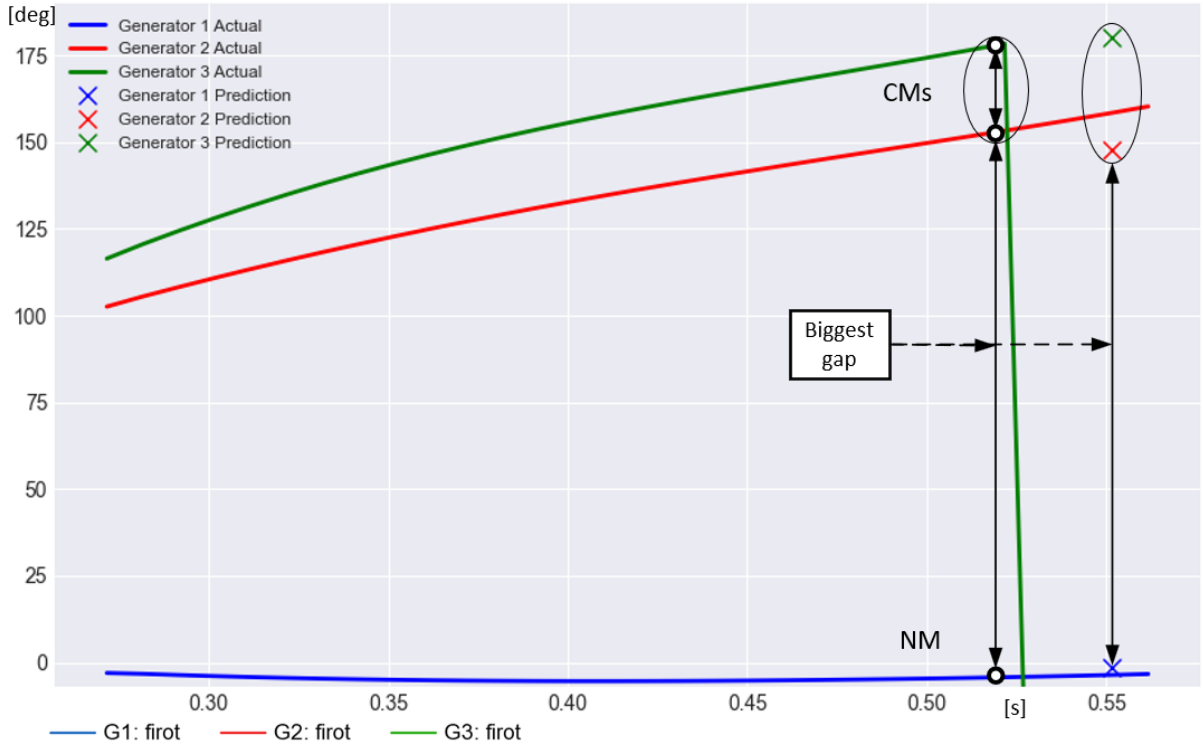

Figure 5.3: TDS compared with predicted δ value, were method nr.1 was used. Here generator nr.1 is the reference machine.

$$\mathbf{CMs} = [G2,\ G3]\ \mathbf{;}\ \mathbf{NM} = [G1] \tag{5.2}$$

Knowing the CMs and NM, then the inertia constants M, MC, and MN values are found. The result of this and the M for each generator are shown in Table 5.3. Then subsequently the OMIB δ (5.3), ω (5.4) and P_a (5.5) are calculated, where all the relevant equations for this is already presented in Chapter 3.2. There was also developed code to handle a CSV file containing all the necessary variables from each generator and calculate the values for the OMIB, this code is shown in Appendix A.7. This code was used to get the E-SIME results and other results that also had a step size of 0.01 s. However, to get results that had 0.001 s step size the residual calculation function inside PowerFactory was used, where more about this can be read in Chapter 4.7.3.

Table 5.3: Values of the different inertia constants M for 9 bus system.

Name	M	MC	$(MN = M1)$	$M2$	$M3$
Value	3.5708	4.9922	12.5414	3.3953	1.5969

$$\delta(t) = \frac{(3.3953\delta_2(t) + 1.5969\delta_3(t))}{4.9922} - \delta_1(t) \tag{5.3}$$

$$\omega(t) = \frac{d\delta(t)}{dt} = \frac{(3.3953\omega_2(t) + 1.5969\omega_3(t))}{4.9922} - \omega_1(t) \tag{5.4}$$

$$P_a(t) = 3.5708\left(\frac{1}{4.9922}\left[3.3953 \cdot P_{a2}(t) + 1.5969 \cdot P_{a3}(t)\right] - \frac{P_{a1}(t)}{12.5414}\right) \tag{5.5}$$

5.1.4 Checking integral of P_a against kinetic energy change

A general test was first done to confirm that the whole area of A_{acc}, which is shown in Figure 5.4, is approximately equal to the kinetic energy change before the Pa changes sign. This was done using the test for multiple time steps (4.10). Here the time-step was chosen to be 0.001s. A more detailed discussion of why the kinetic energy change and area of P_a can be related and the outlines of this approach is already mentioned in Chapter 4.5.

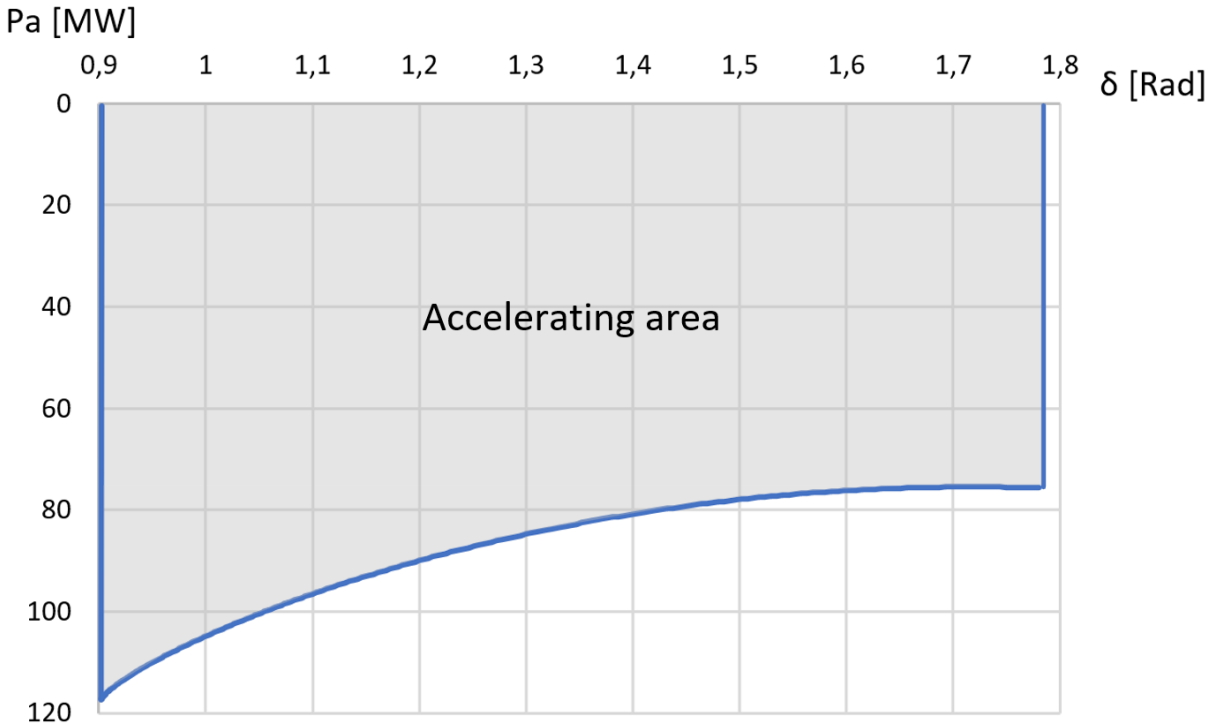

Figure 5.4: A_{acc} for 0.25 s CCT for 9 bus system, with 0.001 s time-step.

The same is also done for a single time-step during the decelerating phase. This was done using the single time step test (4.9), and more details on the calculation are included in Appendix A.8. The step size for the single-time step was 0.01 s. Here the results are summarized and shown in Table 5.4, where it is that there is a low percentage error in the single time step test. That the error is low indicates that the OMIB is defined with correct values.

Table 5.4: Result of testing Integral of P_a against Kinetic energy change.

	Whole of A_{acc}	**Single time step taken from A_{dec}**
Integral of P_a	76.36	-3.7303
Kinetic energy change	73.67	-3.7307
Difference	2.69	0.0004
Percentage Error (%)	3.65	-0.0107

5.1.5 Results from complete TDS

The P_a δ curve for the different CTs is included in Figure 5.5, where the step size for the solver was 0.001s. It is also worth noting that in the CCT case it should reach $P_a = 0$, however in the curve it can be seen that it does not reach $P_a = 0$. This might be because CCT is found with 5 decimal precision or possibly numerical errors in the OMIB. The phase plane of the different cases is shown in Figure 5.6. A created 3D plot of the cases CT 0.245 s and 0.260 s, is included in Appendix B.2, which shows the variables P_a, δ, and ω. This shows that these three variables are connected, where having a positive P_a will increase ω, which in turn will increase δ.

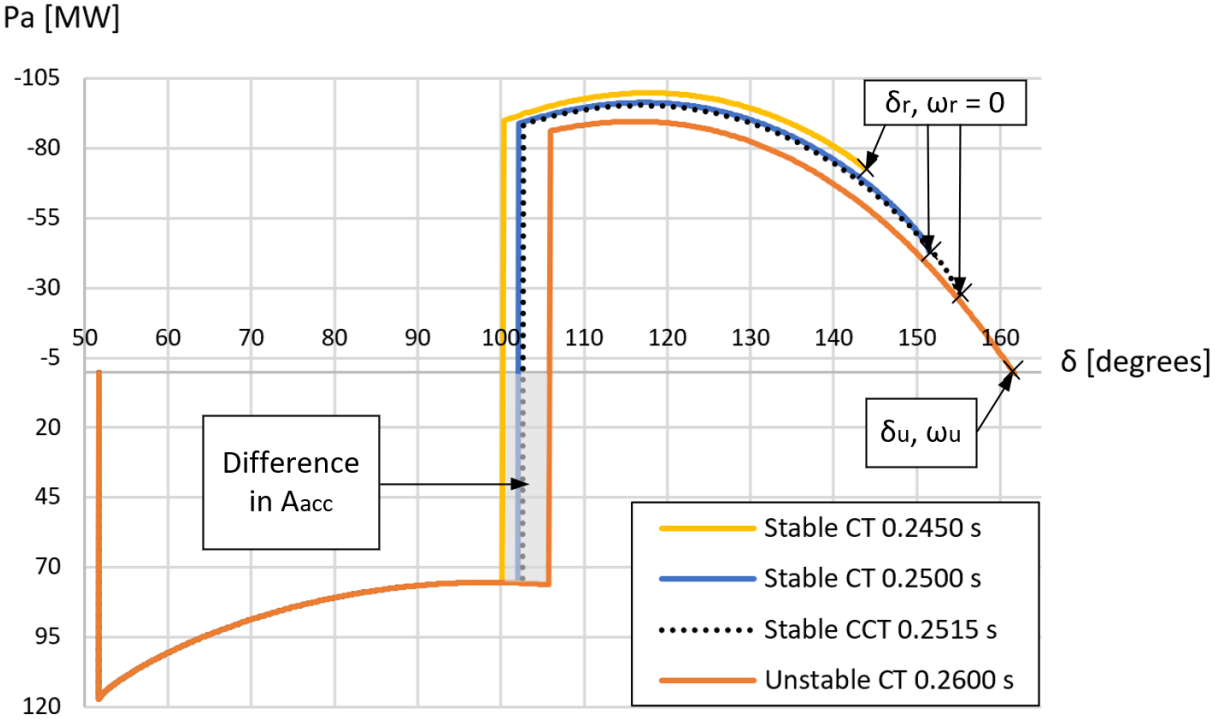

Figure 5.5: P_a and δ curves for the 9 bus system.

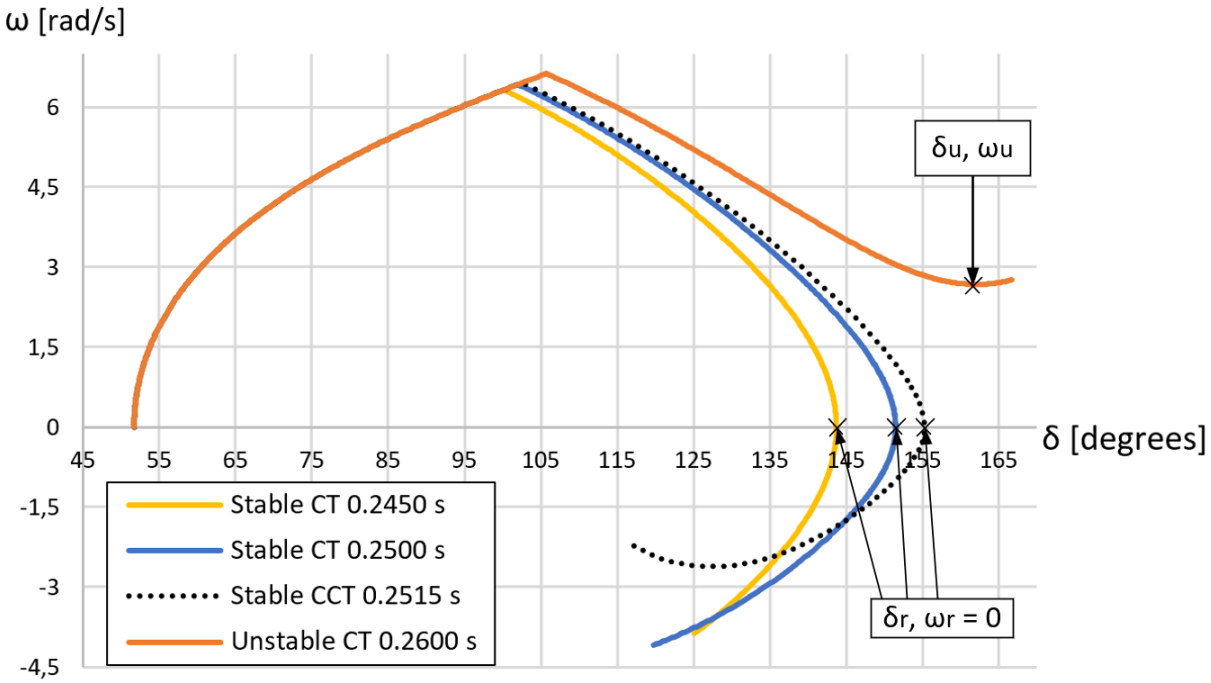

Figure 5.6: Phase plane of δ and ω for the 9 bus system.

Calculations of δ_u, t_u and η for TDS are done using the method that is previously discussed in Chapter 3.1. The results are summarized and presented in Table 5.5. Notably, the CCT has a calculated value for η_{st} equal to 1.974. This discrepancy is likely attributable to numerical inaccuracies, as evidenced by the graphical representation in Figure 5.5, demonstrating that it never actually hits the point of $P_a = 0$ line and there is a measurable gap.

Table 5.5: TDS results for 9 bus system for the various CTs.

CT (s)	δ_u **(degrees)**	η	t_u **(s)**
0.2515 CCT	162.658	1.974	-
0.2500 s CT	164.061	5.292	-
0.2450 s CT	168.235	12.644	-
0.2600	162.018	-12.776	0.498

a sensitivity analysis is displayed in Figure 5.7, which was done using the η for CCT 2.515 and CT 0.26s, where p = CT. The distance between the CCT that was found in

PowerFactory and the one that is estimated using sensitivity analysis is 0.011 s. The sensitivity analysis was done based on the information laid out in Chapter 3.3

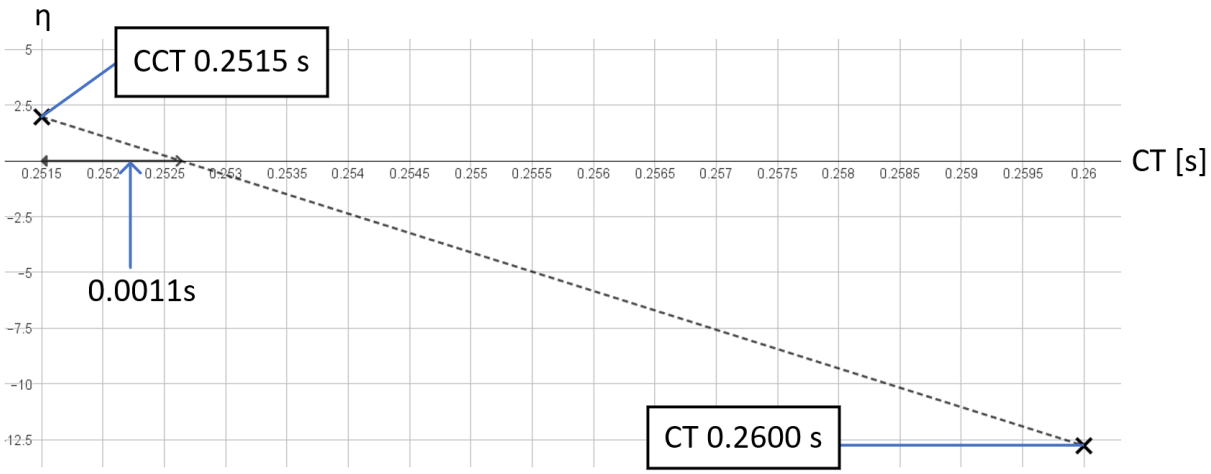

Figure 5.7: Plot for η given CCT 0.2515 s and CT 0.2600 s, showing error to be 0.011 s.

5.1.6 E-SIME Results and comparison with Full TDS results

To estimate δ_u the procedure in Chapter 4.3.1 was used. The approach presented in Chapter 4.4 was used to calculate the η, t_u and t_{ui}. Further, the criterion for corrective measures was used. This criterion states that corrective measures are needed if t_{ui} goes below 0.11 s, and this criterion is discussed in Chapter 4.6 was used. Results from running E-SIME calculations are shown in Table 5.6, where these were done for 3, 5 and 14 measurements that have a sampling rate of 0.01 s. The TDS results are also shown in the table. Here it was shown as time progresses the values converge and become more accurate. The only case to have η_u<0 at measurements, is the unstable one. Already at 5 measurements in unstable case the criterion for for corrective measures (4.12) is reached. However, 14 measurements are included and it is seen here that then the estimations for η and t_u are closer to the TDS result, and it can be seen that 5 measurements miss the t_u by approximately 1 s. Here in all cases, it is seen that as more measurements are included δ_u decreases in value.

Table 5.6: E-SIME results for 9 bus system for various CT cases, with comparison of TDS results.

CT Case (s)	**Measurements used**	δ_u **(degrees)**	η	t_u **(s)**	t_{u_i} **(s)**
0.2450	3	190.591	47.919	-	-
	5	175.253	25.674	-	-
	14	169.451	18.639	-	-
	Full TDS	168.236	12.644	-	-
0.2500	3	185.555	31.154	-	
	5	172.312	13.437	-	
	14	166.735	7.340	-	-
	Full TDS	164.061	5.292	-	-
0.2515	3	184.155	26.480	-	-
	5	172.312	13.437	-	-
	14	166.034	4.171	-	-
	Full TDS	162.658	1.974	-	-
0.2600	3	176.917	2.114	-	-
	5	167.179	-8.893	0.406	0.105
	14 measurements	162.787	-12.637	0.502	0.112
	Full TDS	162.018	-12.776	0.498	-

In the unstable case, corrective measures are taken to save it from losing synchronism, where at measurement 5 it is determined that it was needed. Following this, there is a 0.1s delay in implementing the corrective measures, which in this case is to cut the CMs. The results of cutting the CMs are displayed in Figure 5.8, where it is seen that the system remains stable.

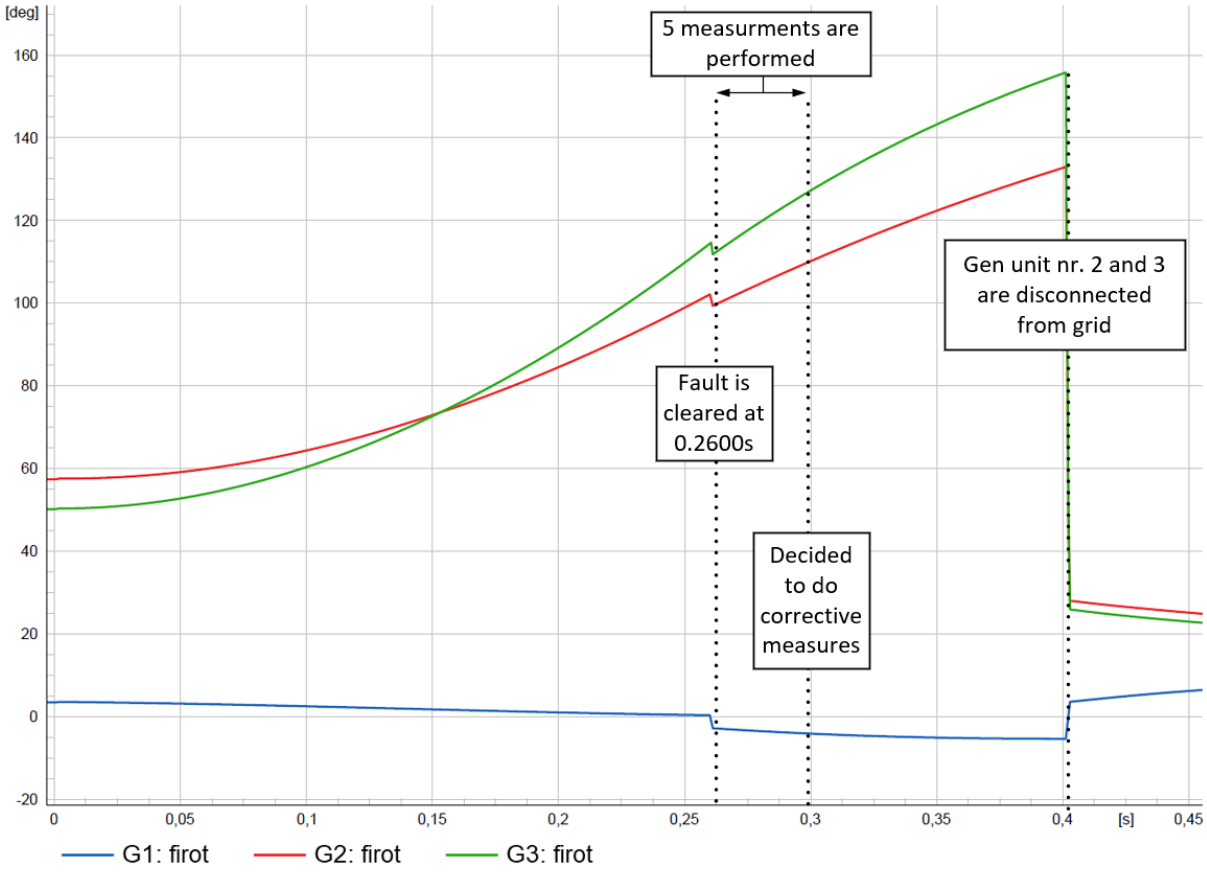

Figure 5.8: Corrected unstable case for 9 bus system, where generator nr.1 is the reference machine.

5.2 E-SIME on 39 Bus system

This section delves into the application of the E-SIME methodology on the 39 bus system. It covers the system's technical specifications, identifies critical machines, and presents results obtained through the E-SIME approach. These findings are then compared with the complete time-domain simulation (TDS).

5.2.1 Technical data on 39 bus system

A scheme of the 39 bus system inside PowerFactory is shown in Figure 5.9. Here the different voltage levels are represented with the colour and the generator unit No.1 represents connection to the rest of the grid. This is taken from the examples included inside PowerFactory, which is how it was created. The technical data for it is included in [7].

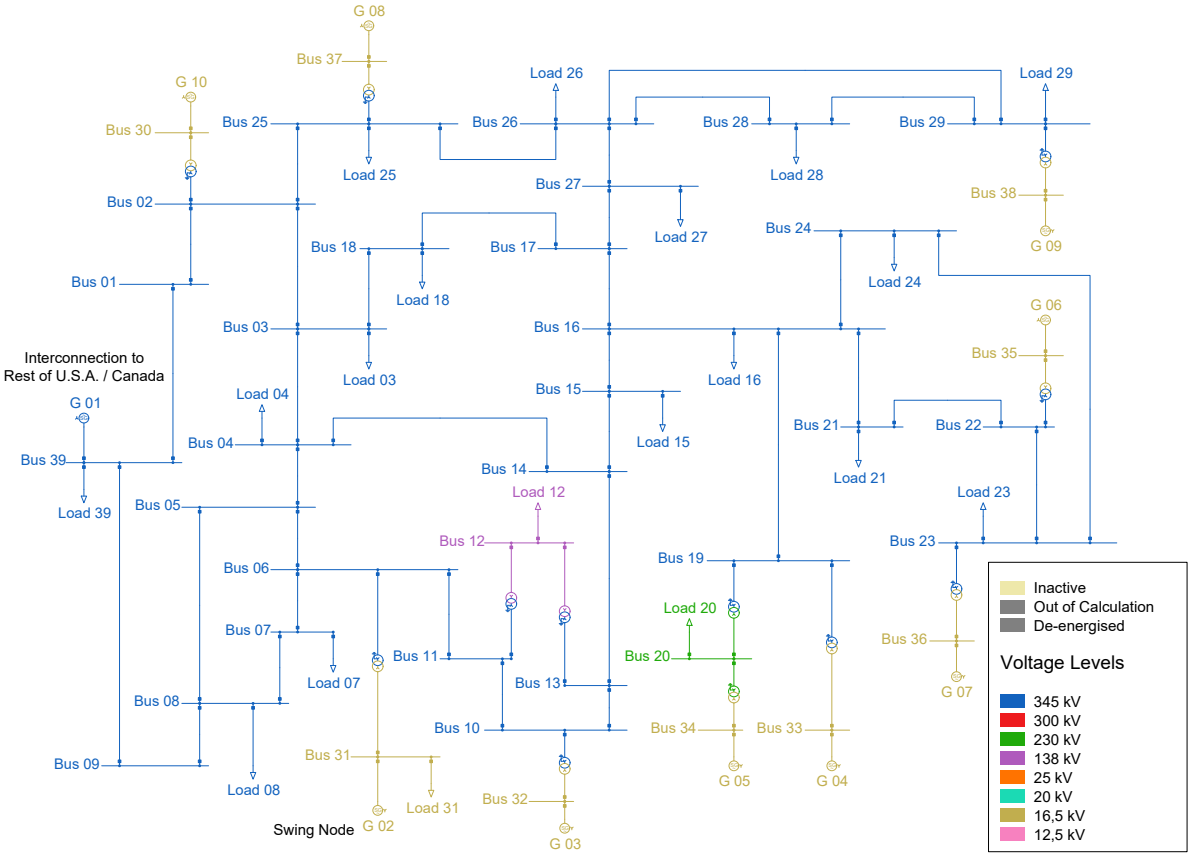

Figure 5.9: 39 bus system PowerFactory model.

In [7] technical data is given for the ratings, where it is worth noting that generator unit No.5 was defined with 2 parallel machines. The same check was done as in the 9 bus system to see the variable t:polepairs inside of the PowerFactory model. It is seen that it was defined with 1 pole pair for all generators. The value for M and the data that was used to calculate it is presented in Appendix C.1. A list that includes more details about the model is included below [7]:

- Governor, AVR, and PSS are included for all generation units except nr.1.
- The generator is modeled with the standard model, where more details about this can be found in the technical reference to the synchronous machine in [22].
- Lines are modeled with R, X, and Susceptance (B), with distributed parameters and frequency dependency.
- Loads are considered to have a voltage dependency, which means that the power demand of the load is proportional to the voltage at the load.

5.2.2 Planned disturbances

The planned disturbances on the 39 bus system are shown in Table 5.7, where both included one case for stable and another for unstable. These cases are taken directly from the example in the technical reference for the system [7]. The CCT was found using PowerFactory and was found to be 0,1843 s in 4 decimal precision.

Table 5.7: Overview of planned disturbances for the 39 bus system.

Fault Location and Impedance	**Fault Clearing Time (s)**	**Stable?**
Bus nr.16, 0.001 p.u.	0.18	Yes
	0.20	No

5.2.3 Critical machines and OMIB-equivalent

Finding the CMs was done by looking at the TDS and looking for the biggest gap as as displayed in Figure 5.10. From this, it is seen that the CMs and NM are made up of the groups shown in (5.6). Here the method for finding the candidate CMs is skipped and this simplified approach was done instead. However, looking at the slopes just after the fault is cleared, would probably identify the correct biggest gap given some measurements following the clearing of the fault. Given this, it was skipped due to it would repeat a lot of the steps already done for the 9 bus system, and rather was decided to place more focus on the OMIB calculations and estimations of η and t_{ui}. However, it would follow the principles laid out in Chapter 4.2 and be done similar fashion to what was done for the 9 bus system, which was shown in Chapter 5.1.3.

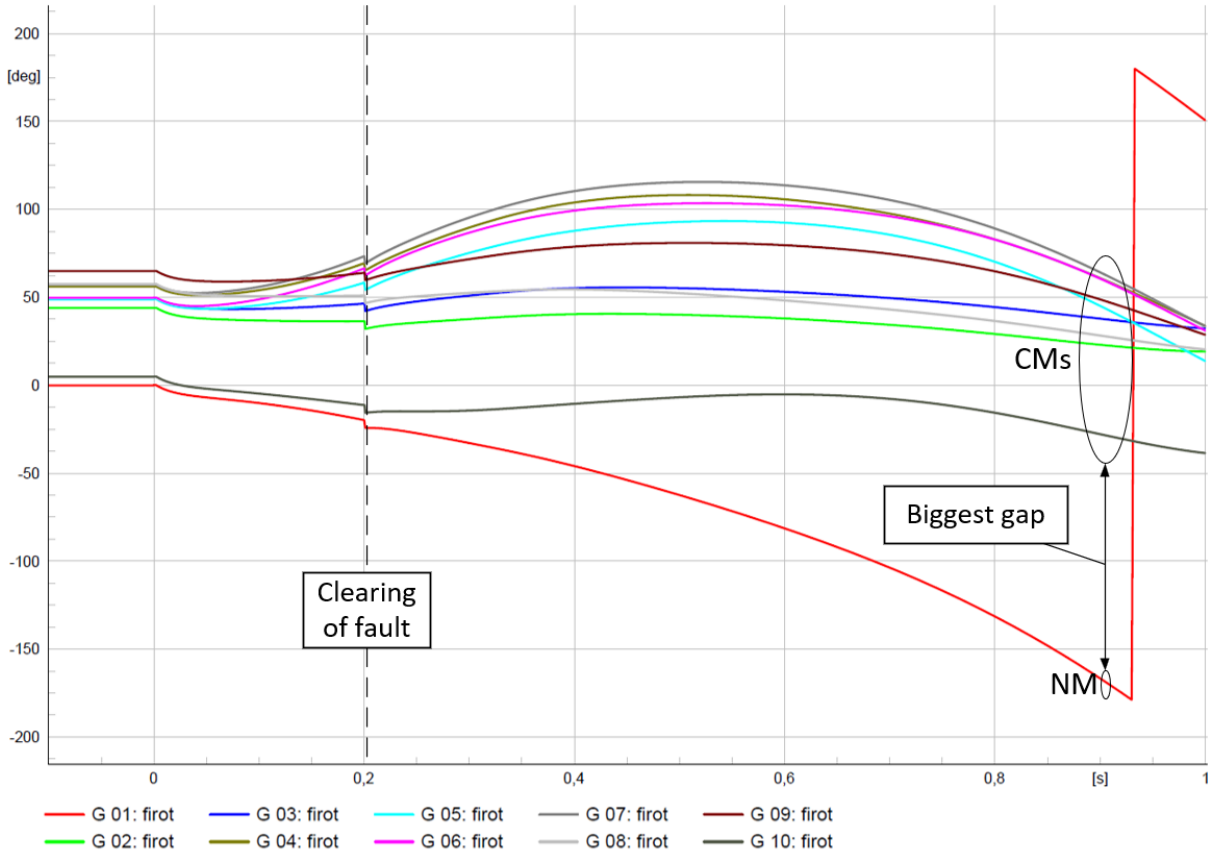

Figure 5.10: CMs and NM for 39 bus system, where generator nr.2 is reference machine.

$$\mathbf{CMs} = [G2,\ G3, ..., \ G9,\ G10]\ ;\ \mathbf{NM} = [G1] \tag{5.6}$$

The found CMs and NM were used to formulate the OMIB, where this is done using the equations in Chapter 3.2. The inertia constants M, MC, and MN values are displayed in Table 5.8. The actual calculations of the OMIB - P_a, δ, and ω were done in Excel, and the calculated values for the stable case are shown in Appendix C.2, and the unstable case in Appendix C.3. Further, to be able to handle the data, the code presented in Appendix A.10 was developed.

Table 5.8: Inertia constants M for OMIB formulation found for 39 bus system.

Name	M	MC	MN
Value	101.254	163.767	265.258

5.2.4 Checking integral of P_a against kinetic energy change

A general test was first done to confirm that the whole area of A_{acc}, which is shown in Figure 5.11, is approximately equal to the kinetic energy change before the Pa changes sign. Here it was decided to use a step size of 0.01 s, where the test for multiple time steps (4.10) was used to calculate this. In contrast, when the same test was performed on the 9 bus system the step size was 0.001 s, as discussed in Chapter 5.1.4. Therefore it was expected to have a larger error in this test, in comparison to the results for the 9 bus system. A more detailed discussion of why the kinetic energy change and area of P_a can be related and the outlines of this approach is already mentioned in Chapter 4.5.

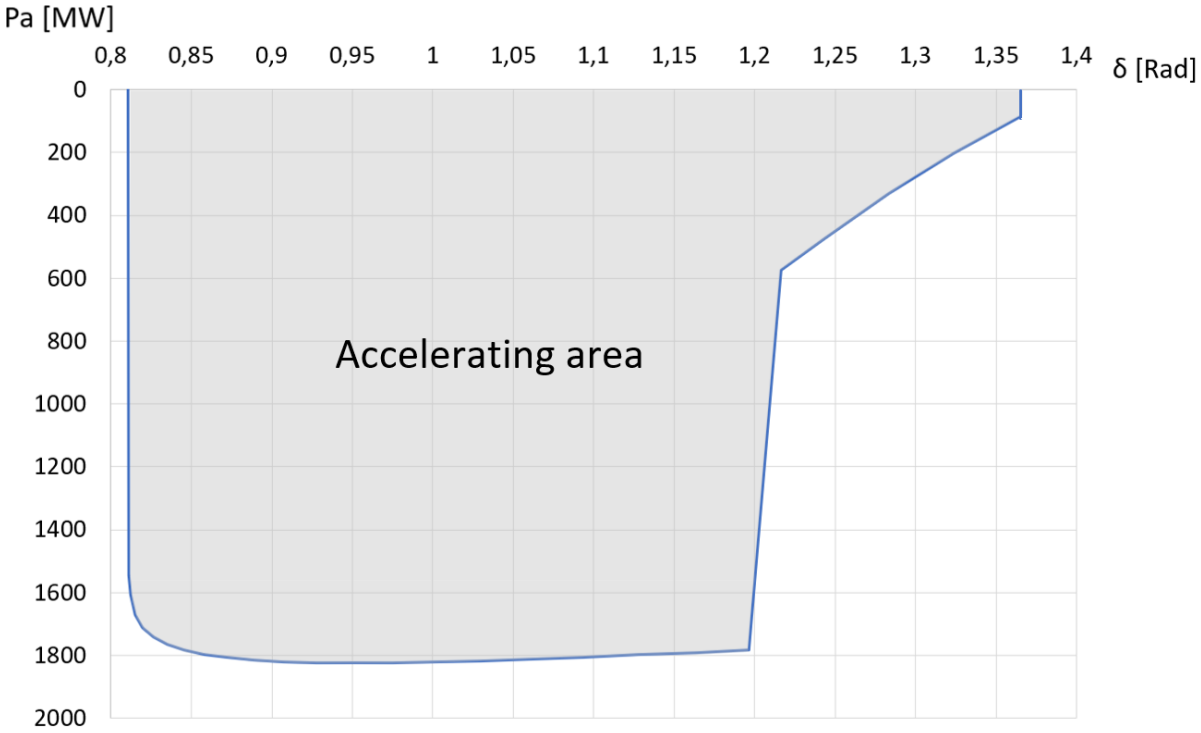

Figure 5.11: A_{acc} for 0.18 s CCT for 39 bus system, with 0.01 s time-step.

Another test was done for a single time step, where the time step was taken from the decelerating phase. This was calculated using the test for the single time step (4.9), and more details on the calculation is included in Appendix A.9. Here the results are summarized and shown in Table 5.9. No further tests were done, because the results indicated that the OMIB formulation is correct, but the error in the case of whole of A_{acc} is larger than in the 9 bus system. The reason for this is possibly that the step size was 0.01 s, and a larger error is expected. Further, also there are more errors in the single time step, where a probable reason is that there is more change in value for P_a than in the 9 bus system.

Table 5.9: Result of testing Integral of P_a against Kinetic energy change.

	Whole of A_{acc}	**Single timestep taken from A_{dec}**
Integral of P_a	765.02	-3.45
Kinetic energy change	842.71	-3.52
Difference	-77.68	0.08
Percentage error (%)	-9.22	-2.13

5.2.5 Results from complete TDS

The P_a δ curve for the two CTs is included in Figure 5.12, and the phase plane of the unstable and stable case is shown in Figure 5.13. To make these the complete TDS solution was used, and the solver step size was 0.01 s. The governor has shown little effect on P_a δ curve, which from δ_0 to δ_u changed to 99.9 percent of its original value, the plot of the P_m can be seen in Appendix C.4.

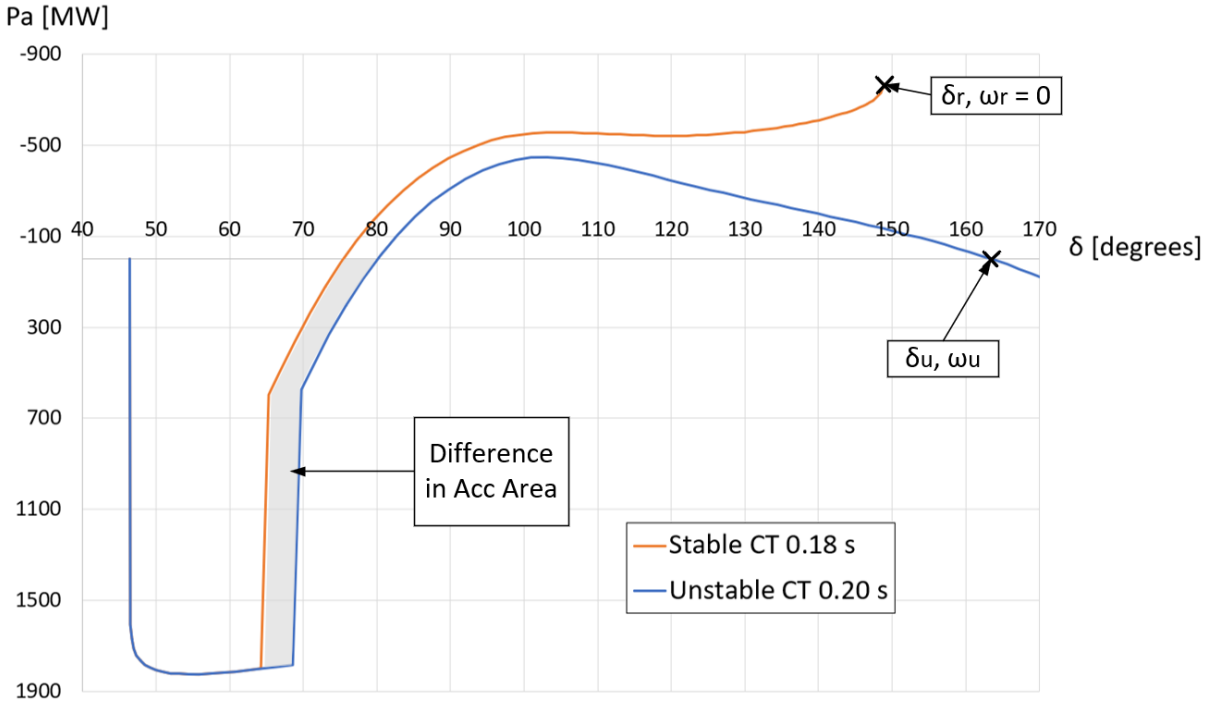

Figure 5.12: P_a and δ curves for the 39 bus system.

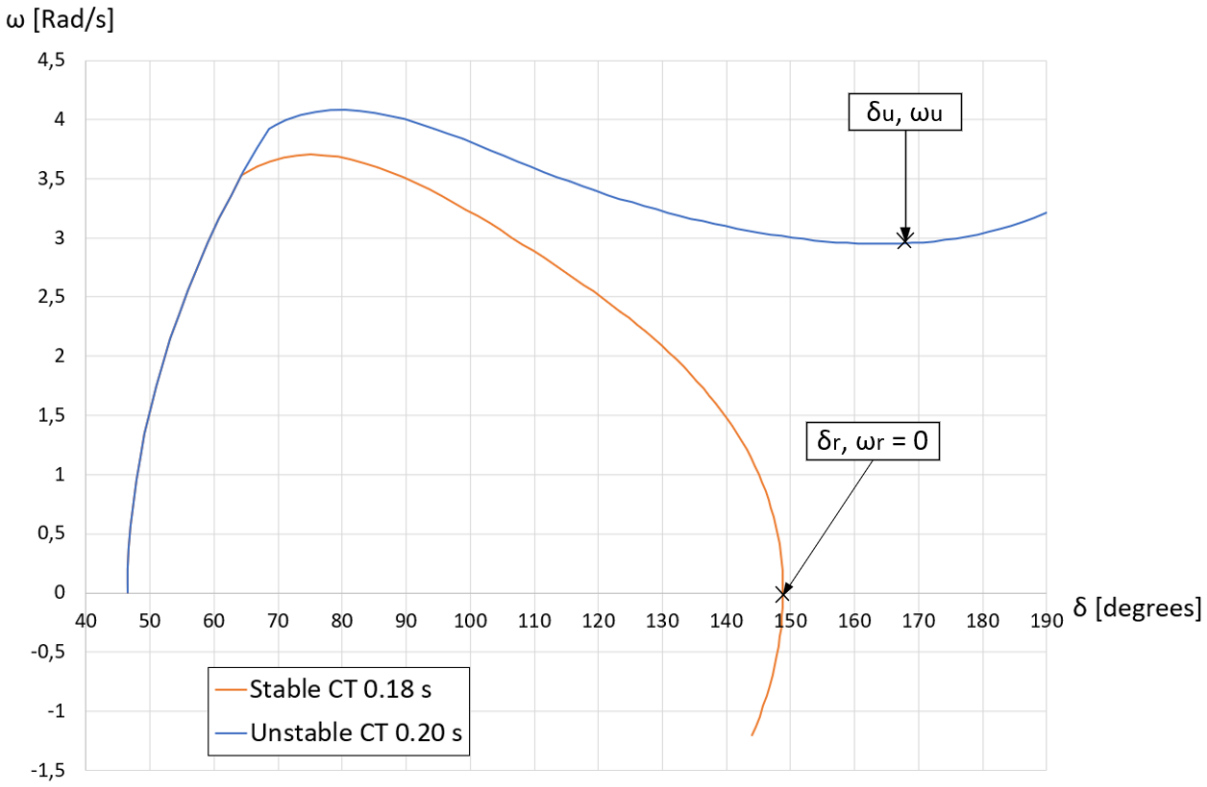

Figure 5.13: Phase plane of δ and ω for 39 bus system.

The calculation of the δ_u, t_u and η for TDS are done using the method that was discussed in Chapter 3.1. The results are summarized and presented in Table 5.10. It is shown that the unstable case has a negative η, while the stable has a positive value η. Here also the values for η are seen to be bigger than in the 9 bus system, where the reason here is that the 39 bus system is a larger system with more power.

Table 5.10: TDS results for 39 bus system for CT 0.18 s and 0.20 s.

CT (s)	δ_u **(degrees)**	η	t_u **(s)**
0.18	190.232	268.064	-
0.20	163.907	-440.188	0.682

Sensitivity analysis of the CT was performed using the found values for η and the results of this are plotted in Figure 5.14. Here the fact that the CCT has a η equal to zero is used and it is marked on the graph. The estimated CCT is compared to the CCT that

was found using PowerFactory, and the error between them is 0.0033s. The sensitivty analysis was done using the approach described in Chapter 3.3.

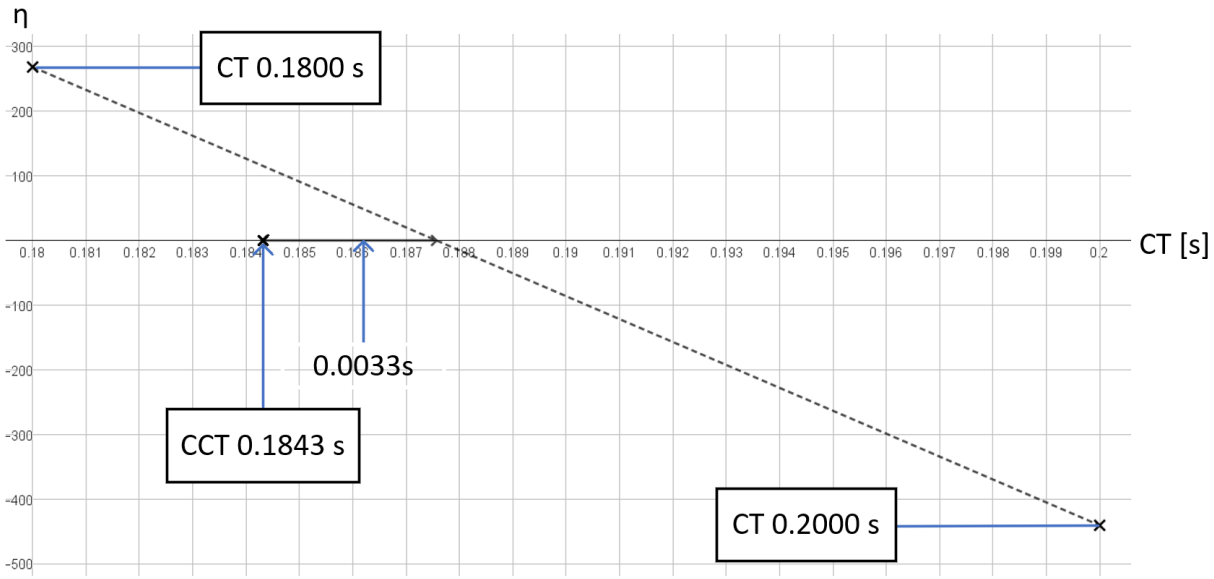

Figure 5.14: Plot of CT and η for 10 generator case.

5.2.6 E-SIME Results and comparison with Full TDS results

Here the method presented in Chapter 4.3.1 is used to estimate δ_u. The method presented in Chapter 4.4, was used to estimate η, t_u and t_{ui}. Further, the decision that corrective measures are needed is made using the criterion presented in Chapter 4.6, which states that corrective measures are needed if $t_{ui} < 0.11$ s. Using the found results Figure 5.15 was created. This plot displays the P_a δ curve, for both the stable case that has a CT equal to 0.18 s and the unstable one that has a CT equal to 0.2 s. These curves are also marked with measurement points, and when the unstable case reaches the corrective measure criterion.

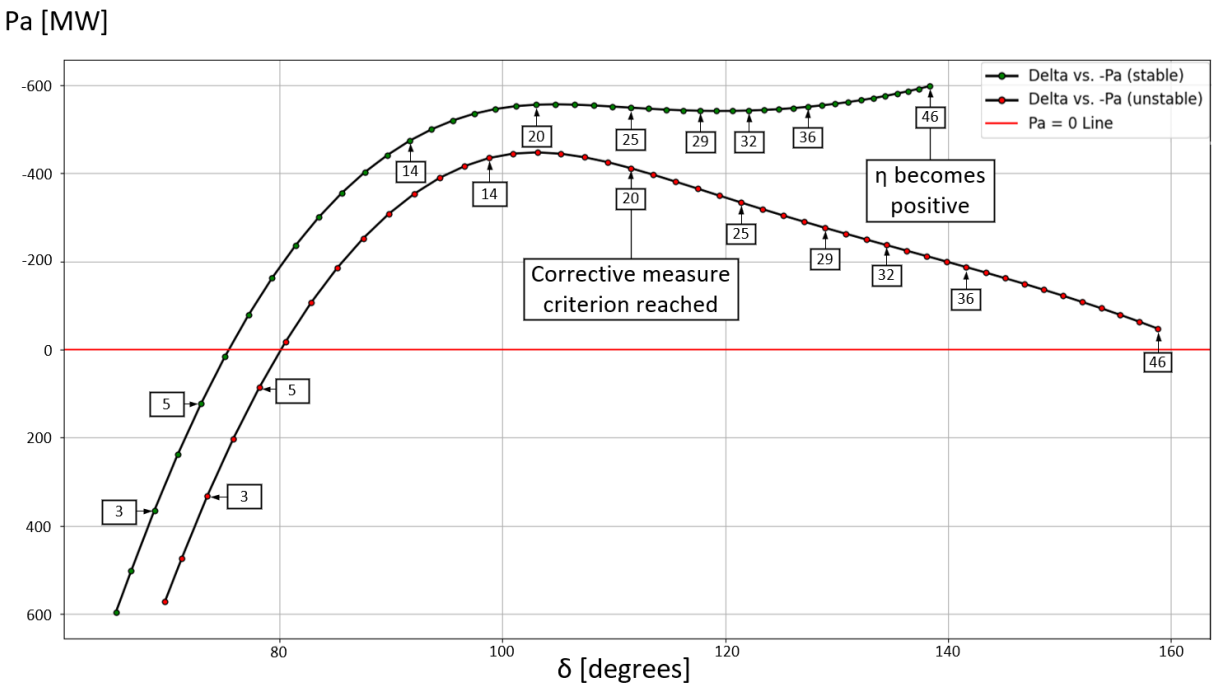

Figure 5.15: P_a δ curve drawn from measurements, with indications of where the case is deemed stable or unstable.

In Table 5.11 more detailed results from the E-SIME calculations are shown. It is shown here that as more measurements are included, the estimations δ_u and t_u become more refined. Initially, the stable case has a positive η and the unstable has a negative η. However, as additional measurements are taken, η decreases. Eventually, in the unstable case corrective measure criterion is reached at measurement number 20, it is reached due to t_{ui} becoming below the set criterion (0.11 s). The stable case is indicated to be stable at measurement number 46 because then η becomes positive again. This iterative process benefits from using t_{ui} to know if a decision on corrective measures is required, or if more measurements can be included to assess the transient event more thoroughly. However, it is shown that the estimations for t_u are not so close until measurement number 46.

Table 5.11: E-SIME and TDS results for both unstable case CT 0.2 s and stable case CT 0.18 s.

Meas. Incl.	**Stable Case**				**Unstable Case**			
	δ_u **(deg)**	η	t_{u_i} **(s)**	t_u **(s)**	δ_u **(deg)**	η	t_{u_i} **(s)**	t_u **(s)**
3	160.566	519.396	-	-	142.282	-266.414	0.376	0.598
5	112.196	-512.652	0.198	0.420	113.563	-707.540	0.158	0.399
14	120.703	-414.072	0.164	0.475	122.726	-615.045	0.115	0.447
20	127.066	-343.471	0.150	0.522	127.698	-573.222	0.082	0.474
25	133.106	-283.587	0.148	0.570	133.808	-534.950	0.067	0.507
29	138.879	-229.314	0.160	0.622	139.180	-507.334	0.056	0.537
32	143.675	-185.086	0.180	0.671	143.358	-489.079	0.050	0.561
36	150.586	-121.956	0.227	0.759	148.862	-469.139	0.041	0.593
46	169.668	56.0223	-	-	160.357	-442.274	0.009	0.661
Full TDS	190.232	268.064	-	-	163.907	-440.188	-	0.682

A plot for the t_{ui} against the number of measurements included, is shown in Figure 5.16. At first the t_{ui} decreases in both cases, but eventually for the stable case this turns around when 29 measurements are performed. In the stable case when t_{ui} increases with more measurements, this is an indication that the system could be approaching stability. Eventually at measurement number 46 for the stable case η is positive, and the t_{ui} can not be calculated. It is also seen that at measurement 20 for the unstable case is below the point of 0.11 s, which is the reason it was deemed that corrective measures are need to be initiated.

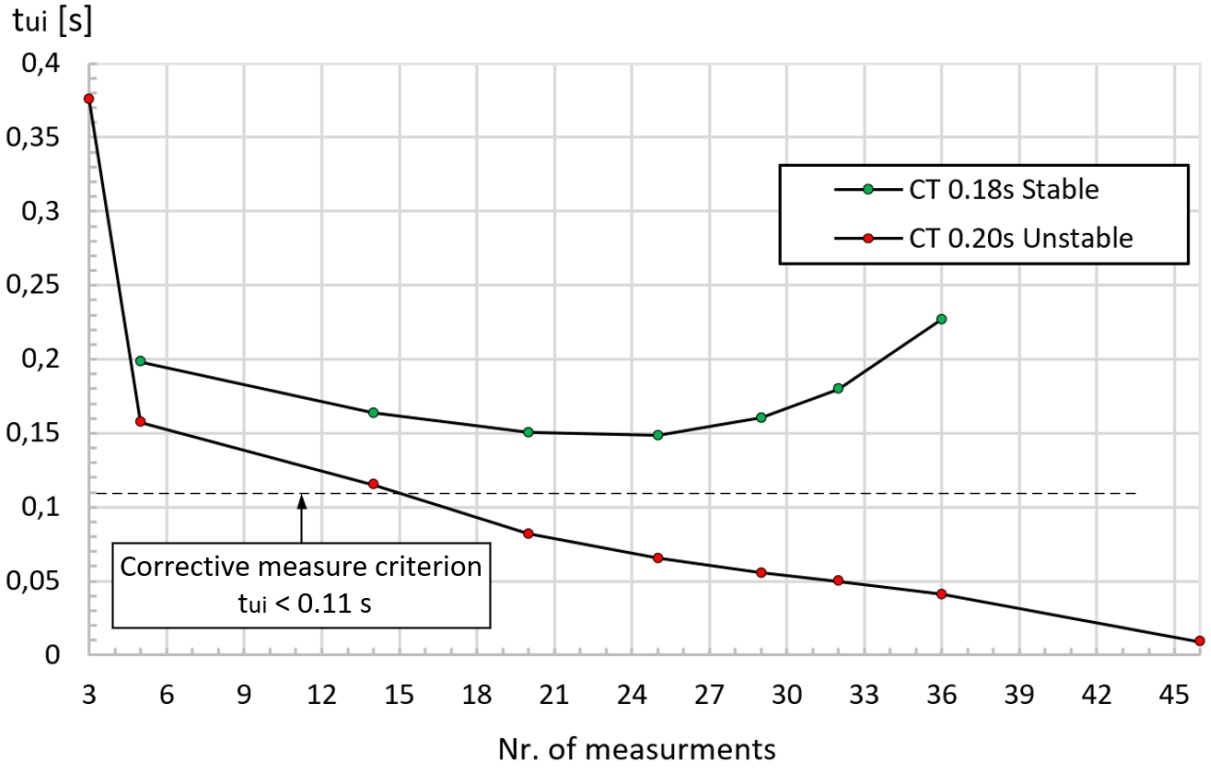

Figure 5.16: t_{ui} estimations for the unstable and stable case in the 10 generator system.

Corrective measures for the unstable case begin after the 20th measurement at 0.3917 s, as shown in Figure 5.17. A 0.1 s delay was applied, so critical generators were cut at 0.4917 s. Here due to the fault location being bus nr.16, which is in the center of the grid, this led to it being one of the most severe faults that could occur. This was because it caused so many generators to be accelerated away from generator nr.1. This means that every generator in New England‘s grid is accelerating away from the rest of the USA grid connection. Therefore, a lot of generators are cut, because the CM cluster is made up of all generator units inside the New England grid.

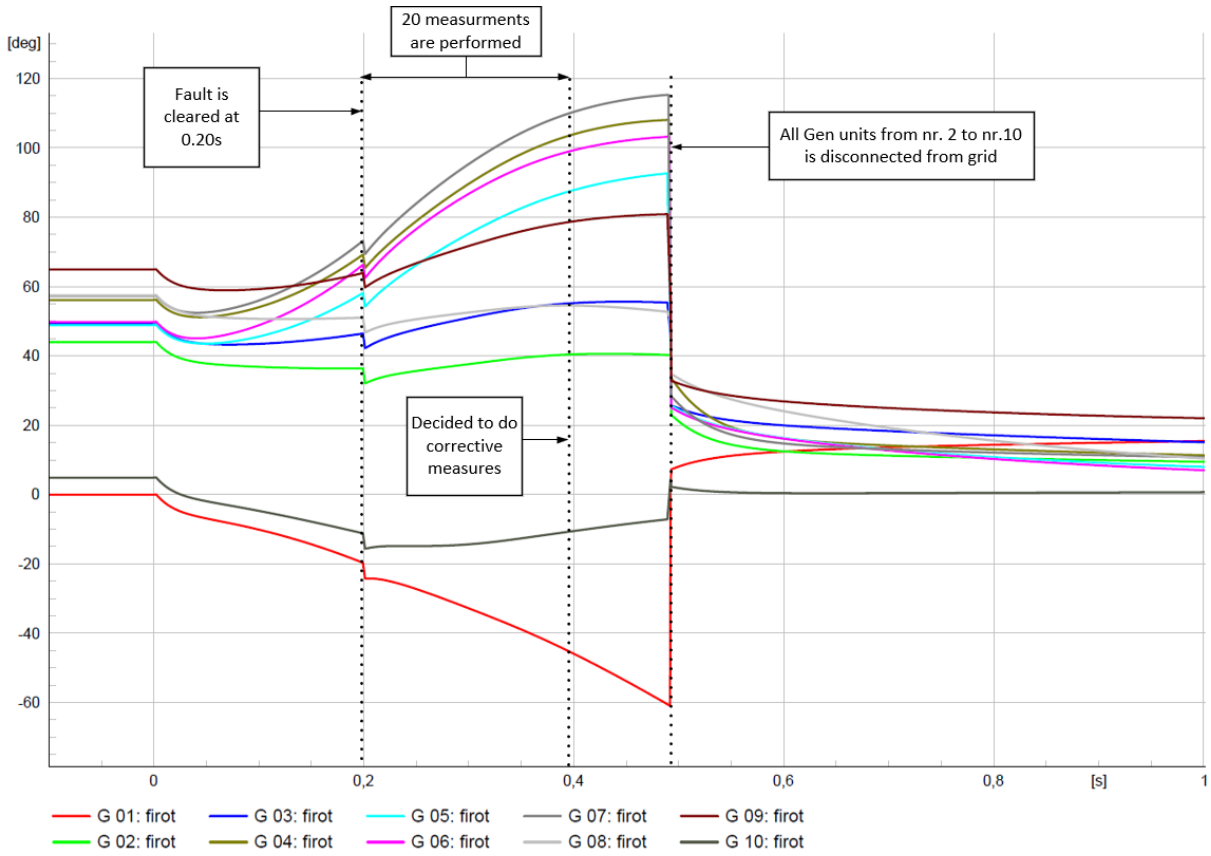

Figure 5.17: Plot of correction of unstable trajectory by cutting CMs, where generator nr.2 is reference machine.

Another corrective measure that is less drastic, is to disconnect the two lines that are connected to bus nr.39 at the same instance as corrective measures were done in the previous example, meaning at 0.4917 s. The results of doing this are shown in Figure 5.18, where at a later instance they can be connected. Part of the reason that the CMs get decelerated is that the OMIB formulation was changed, which happened since generator 1 was disconnected. This helped stabilize the other generators, where the system oscillations dampen over time and the system remains synchronous.

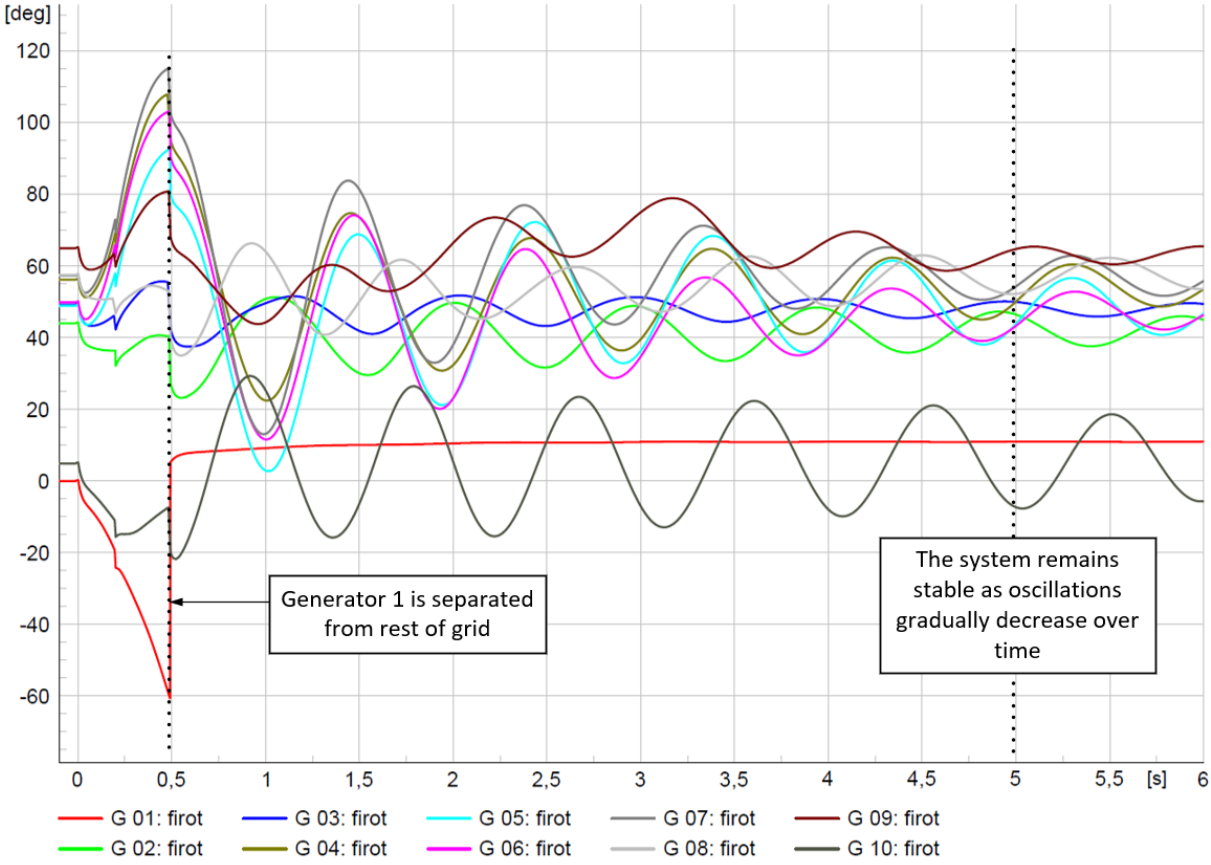

Figure 5.18: Plot of correction of unstable trajectory by splitting grid, where generator nr.2 is reference machine.

The rotor speed ω_{rot} is shown in Figure 5.19, as this might give a more intuitive view of how the generators were behaving. It shows that by doing a corrective measure the generator units that still are connected remain synchronous, and oscillations dampen over time. A comparison of with or without corrective measures is included in Appendix C.5, and this comparison is both done for firot and ω_{rot}. That clearly shows that there is a substantial improvement when the corrective measure is taken. However, in the results for ω_{rot} there is a decline of value for generator nr.1, which is because a governor is not included [7]. Governor was added and it changed the model. The technical data for the tuning is included in Appendix C.6. The result of including a governor in generator 1 this is shown in Figure 5.20, which shows that the speed of generator 1 stops declining at around 6 s.

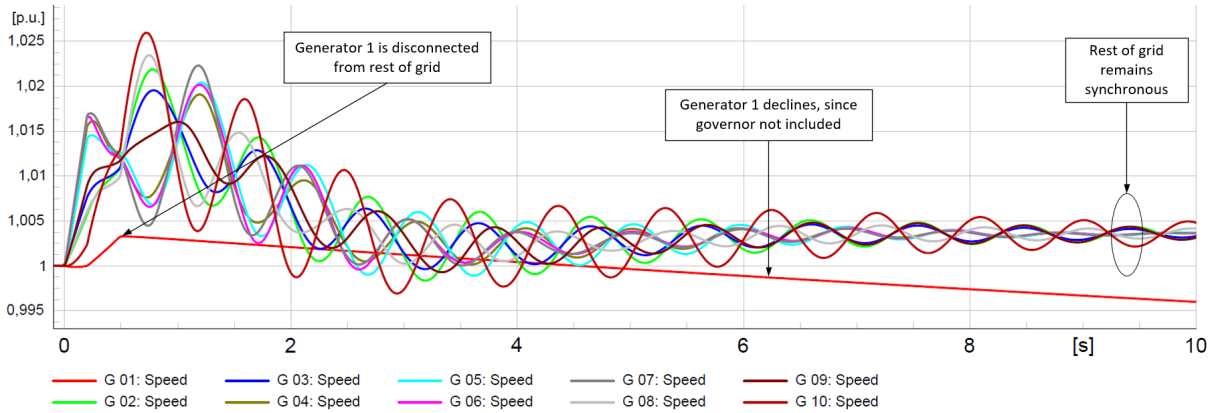

Figure 5.19: Plot of ω_{rot} for all generation units, where the corrective measure is the disconnection of lines to bus nr.39.

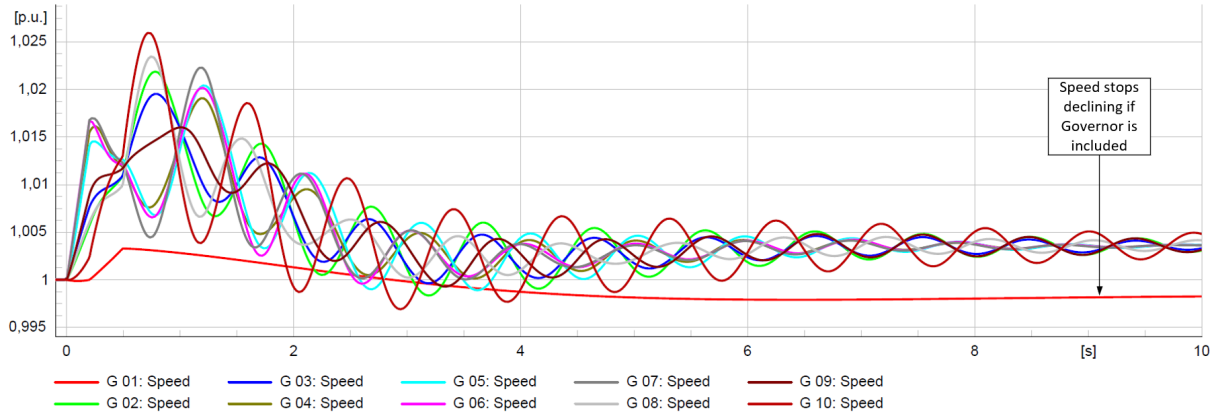

Figure 5.20: Plot of ω_{rot} if governor model is included for generation unit nr.1.

5.3 Comparison of results for 9 and 39 bus system

Figure 5.21 illustrates the P_a δ_u curves for both systems' unstable cases. Notably, the y-scale for the 10-generator system is tenfold greater and is displayed on the right, whereas the 3-generator system scale appears on the left. This comparison reveals distinct dynamic behaviors post-disturbance: the 10-generator system exhibits a relatively linear decrease in its trajectory towards δ_u, while the 3-generator system demonstrates a more pronounced parabolic trajectory.

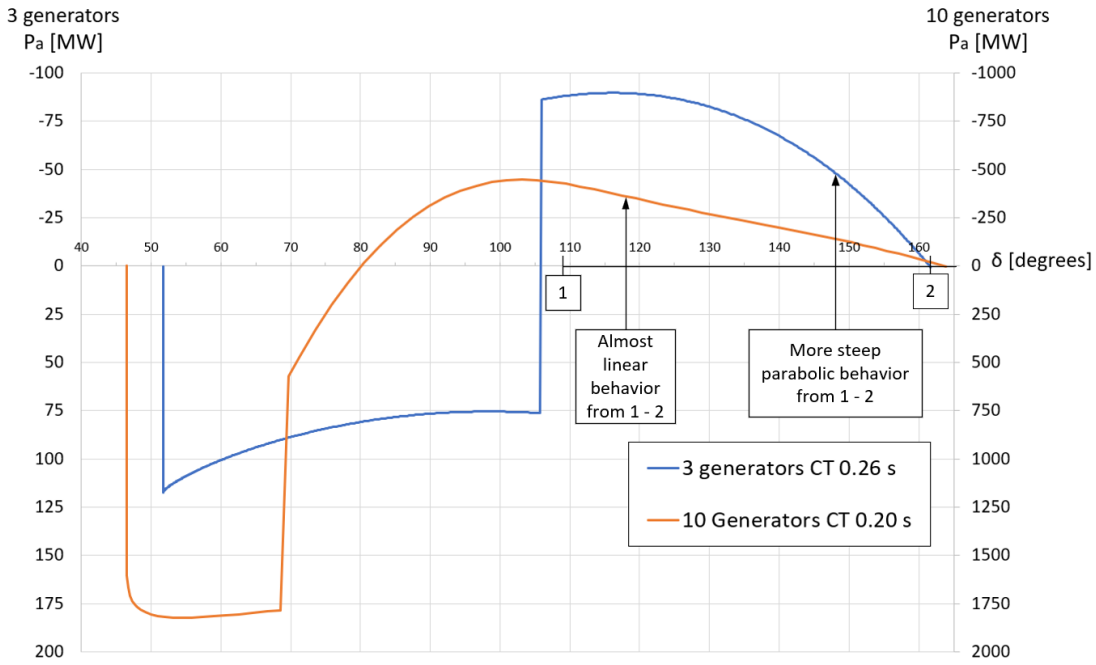

Figure 5.21: Comparison of unstable cases, where the first case is 39 bus system with 10 generators and CT 0.20 s and the second is 9 bus system with 3 generators and CT 0.26 s

An optimal set of weights was determined using the unstable case from the 9 bus system (CT = 0.26 s), where the same set of weights was used for the 39 bus system. The estimations of δ_u from in the 9 bus system initially overshoot before converging towards the TDS value as more measurements were incorporated. However, the opposite was the case in the 39 bus system, where it also converges with more measurements, but tends to undershoot the estimation of δ_u. This dynamic is depicted in Figure 5.22 that portrays the two last measurements and TDS result. In 3 generator case (a) it is shown that the 9 bus system results tend to overshoot. In the 10 generator case (b) the estimations of δ_u in the 39 bus system are shown to increase towards the TDS δ_u, indicating a tendency to undershoot. Despite this, in both cases, E-SIME was still able to distinguish between stable and unstable cases.

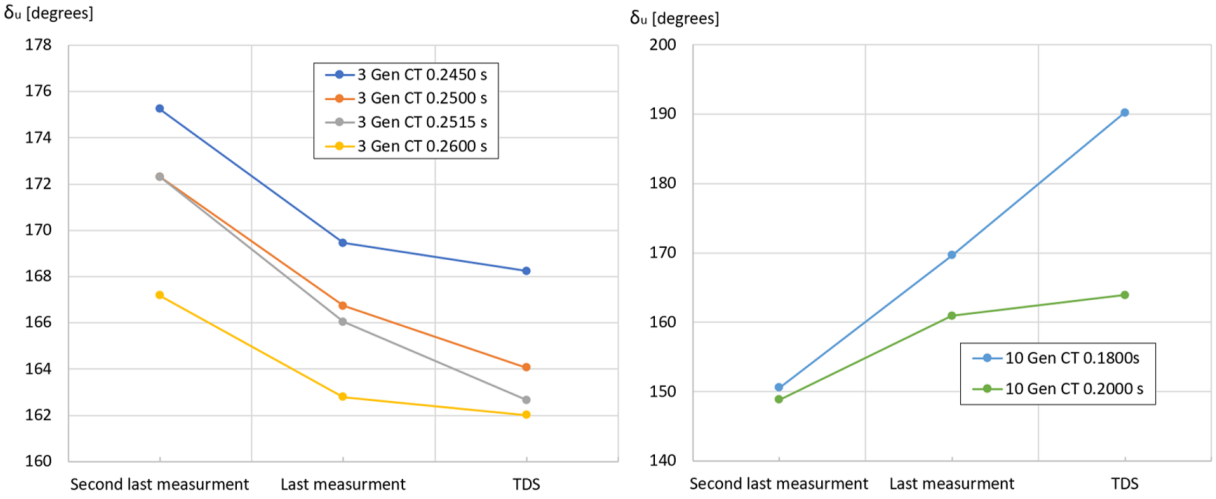

Figure 5.22: Comparison of δ_u values for 9 bus system with 3 generators (a) and 39 bus system with 10 generators (b), where it shows second last measurement, last measurement, and TDS.

Further analysis was conducted to determine whether similar dynamics would be observed under different contingency scenarios in the 39 bus system, particularly when the critical cluster consists of fewer generators. Consequently, an additional contingency was specifically implemented in the 39 bus system. This scenario involved a fault at bus nr.28, with a CT of 0.13 s, critically affecting only Generator nr.9. The details of this specific case are provided in Appendix C.7. The comparison of P_a δ curve for a fault at bus nr.16 and nr.28 is shown in Figure 5.23, where both these cases were unstable. It is shown that the resulting behavior of this added scenario of a fault at bus nr.28, leads to having a more pronounced parabolic behavior, and displays a shape closer to the unstable case for the 9 bus system.

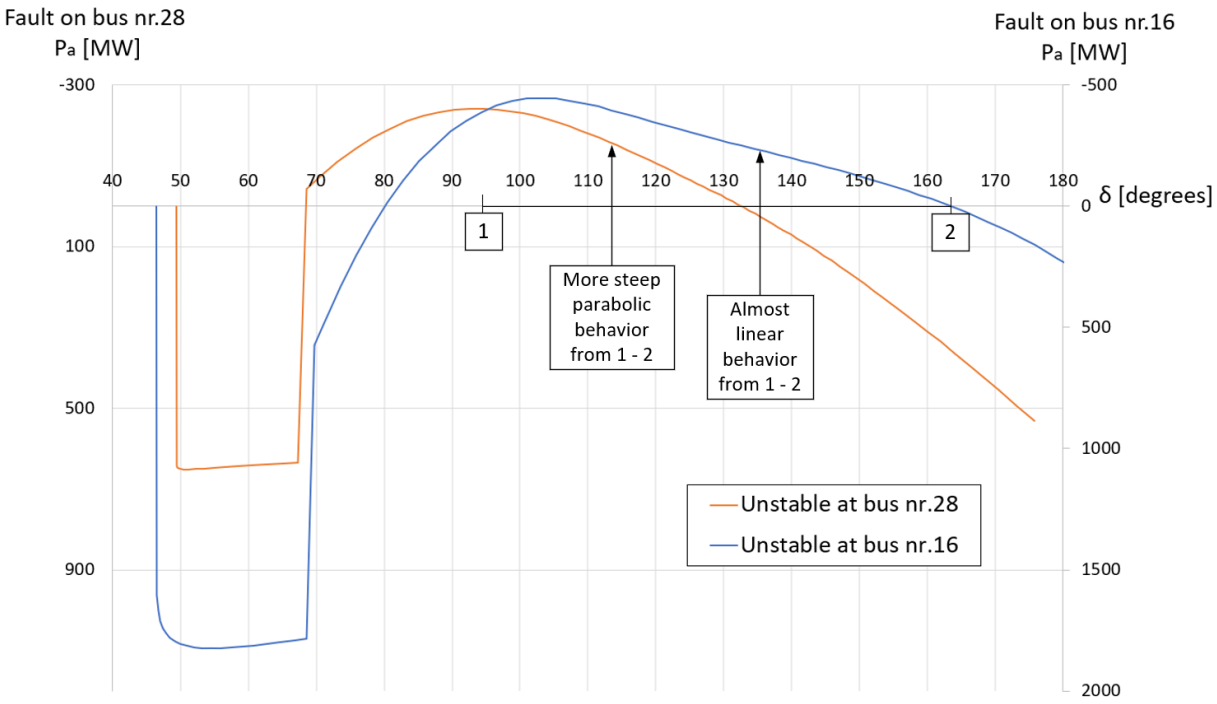

Figure 5.23: Comparison of 39 bus system unstable cases, where one case is fault on bus nr.16 with CT 0.2 s, and the second is on bus nr.28 with CT 0.13 s.

6 Discussion

Time-consuming methodology to perform Contingency Analysis
It was time-consuming to study one contingency on the 39 bus system, which is the reason that for this system only two different CTs were done. It also took time to run contingencies on the 9 bus system, but considerably less than in the 39 bus system case. The reason it took more time in the 39 bus system, is there were more variables and this resulted in more work in processing the data. The method for processing data was using Excel and Python, followed by running numerous Python scripts to calculate the results. This process tended to be prone to human error and therefore always needed to be done twice or more. If this rather was all integrated inside PowerFactory using DPL, then the time to run different contingencies would decrease. This would allow for a larger set of contingencies and would provide more insight into the overall performance of the E-SIME methodology.

Simplification of the system using OMIB
One strength that is shown is that the SIME methodology is able to reduce both the 39 and 9 bus system to an OMIB, where the 39 bus system contains dynamic models for AVR, PSS, and governors. Also, found literature shows this also works for bigger grid models [4], where this suggest it could also be employed on the Nordic power system. The results in Appendix C.6 shows that including governors in generators has minimal effect on the Pa δ curve, which was not a surprising result because the time the governor uses to start affecting the P_m is higher than the duration of the transient event.

However, the magnitude of the effects from AVR and PSS on the Pa δ curve is not directly measured. This could be done by removing the dynamic models and then comparing the results. One speculation is that possibly including AVR results in a more linear shape on the P_a δ curve because the AVR will eventually drive the voltage up. This in turn will make P_e increase, and this will increase the decelerating area but also make it more linearly shaped. Possibly this in turn could make the TDS and E-SIME results diverge more, due to it being estimated via a parabolic function. However, the actual extent of this is unknown and would have to be further investigated.

Finding critical machines using Taylor expansion
For the 9 bus system, CMs were identified using the Taylor expansion of each δ. This was achieved using the proposed method nr.1 or method nr.2, wherein both methods δ were represented using the variable firot. Here using firot has the possibility of giving erratic

results at the moment a discrete event occurs, such an event can example be clearing a fault. This is due to firot being referenced to the terminal voltage, which can have discrete changes. However, this is mostly just relevant at the first measurement after an event, and the issue quickly subsides. It was shown that method Nr.2 provided the lowest overall error in predicting δ compared to method nr.1, where it is worth noting this was only tested on one scenario. Further method nr.2 gave an error of 0.025 s in comparison to the TDS, where it was used to predict when generator unit 3 would reach 180 degrees. Also, method nr.2 would be easier to implement in real life applications due to it only using values δ_i and δ_{i-1}, while method nr.1 uses δ_i, ω_i and γ_i.

In contrast, the 39 bus system relied on the complete TDS to determine CMs and is something that needs to be looked more into. However, the emphasis was placed on demonstrating potential methods for estimation of δ trajectories, and then how these could be sorted in descending order. How this can be integrated into an automated algorithm that updates values given more measurements needs further investigation. A starting point could be to use method nr.2 and perform the test of running predictions until one generator reaches 180 degrees, and refreshing these estimations as more measurements come in.

Sensitivity analysis
Sensitivity analysis of CT was done using the measured η, and this was conducted both on the 9 and 39 bus system. Here the error is the difference between the CCT that is estimated using two measurements of η and the actual CCT, where the actual CCT was found using PowerFactory. In the 9 bus system, an error of 0.0011 seconds was observed, which could potentially be reduced by using CT values closer to the actual CCT value. Part of this error can also be due to the precision of the found CCT value, which was five decimal places.

In contrast, the 39 bus system showed an error of 0.0033 seconds. The CT for both the stable and unstable cases in the 39 bus system were further from the CCT compared to those in the 9 bus system, also the actual CCT was found in this case with a precision of four decimal places. This in turn can explain why it has a slightly higher error than in the result for the 9 bus system. However, the error in estimating the CCT in both the 9 and 39 bus system, seems reasonable. To reduce this further, it is possible in both cases to pick a stable and unstable CT that is closer to CCT, which would reduce the error.

Checking OMIB using integral of P_a against kinetic energy change
The OMIB was partly checked using the measurements for ω and the P_a δ curve, which was done by checking if the "Integral of P_a" was approximately equal to the change in kinetic energy. The integral of P_a was estimated using the trapezoidal method, and the kinetic energy change was calculated using measurements for ω. The formula for calculating the percentage error (4.11) was used to calculate the error between the estimated integral of P_a and kinetic energy change. First, this was done for the whole of A_{acc}, which in both the 9 and 39 bus system had a percentage error under 10%. Also, a single time step was taken

from the decelerating area, and the percentage error was calculated. In the 9 bus system the error was -0.001%, while in the 39 bus system it was -2.13%. A possible reason for this difference is where the sample was taken in the 39 bus system, which comparatively has more change in the P_a value than in the 9 bus system sample. However, an error of -2.13% is considered reasonable given the trapezoidal estimation method's inherent inaccuracies with estimating functions that are parabolic. This error seems reasonable, and it was an indication that the OMIB was formulated correctly.

Sampling Rate Considerations
The choice of a 0.01s sampling rate for measurements was done to secure a minimum of five measurements post-disturbance. This was contrasted against a referenced study employing a 0.02s interval [4], however later it is seen that even in the 9 bus system there would the adequate time to use 0.02 s instead, but possibly the early accuracy would decrease and the fault would be allowed more time. How the 39 bus system would respond to this is unknown, but due to its longer fault period, it could still be able to see the difference between the stable and unstable case. However, implementing 0.02 s or more sampling time is suggested as something to look more into, which can provide insight into how the sampling rate affects the accuracy.

Noiseless signals
The measurements taken from PowerFactory are noiseless, while in real-life application there would be some noise there. This was not tested and is thought to affect the results negatively, meaning a worsening of the accuracy of the estimations of δ_u and t_{ui}. If this was tested with different levels of noise on the signals, it could provide insight into how sensitive the estimations of δ_u and t_{ui} are to noise. Further, by only introducing noise into one variable at a time, it would provide insight into how much the estimations of δ_u and t_{ui} are affected by noise on specific variables.

Suggestion to rather use firel instead of firol for measuring δ
Here firel measures the distance between the rotor of the machine and the reference machine's rotor, while firot measures the distance between the rotor of a machine and the angle at the terminal voltage of the reference machine. firot was employed in this thesis consistently. Despite this, the better choice is to rather use firel to represent δ. The reason is that firot can have discrete changes in the value of δ, when an event like clearing a fault occurs. This will affect the δ prediction to have more erratic behavior. However, this is more relevant in the measurement that is just after an event has occurred, and the issue subsides after this.

Using firel will capture the angular distance between the rotors of the machines in the system, which is more in alignment with what δ is supposed to represent. However, the results gained in E-SIME for η, δ_u, and t_u, would be the same if either firot or firel is used. The reason for this is that both are measuring the machine‘s rotor to a common reference point, and the OMIB δ being the angular distance between δ_C and δ_N. This

subtraction makes it so using firot or firel will result in the same value for the OMIB δ, which in turn will make the estimations of η, δ_u and t_u be the same in both cases.

In analyzing the 39 bus system, generator number 2 served as the reference machine for consistency with technical reference for the model [7], which is done to aid anyone who would try and verify the results. Alternative reference choices, like generator number 1, could improve readability due to having lower values for δ and ω.

Weight Selection for δ_u Estimation
An important part of the E-SIME methodology involves the estimation of the critical angle δ_u, which is crucial for assessing system stability and accurately estimating margin η. The accuracy of δ_u is influenced by the weight sets used in the WLS method. Different weight sets can significantly affect the outcome of the stability analysis, potentially leading to either an overestimation or underestimation of system stability. In the 9 bus system, the estimation process initially overshoots but eventually converges towards the correct value of δ_u in a decreasing manner, demonstrating more accurate predictions over iterations. Here the P_a δ curve has a parabolic shape.

Conversely, in the 39 bus system, the tendency is to undershoot the value of δ_u, and gradually increase and converge towards the correct estimation as more measurements are included. However, there is an exception to this in the case of going from 3 to 5 measurements, where there is a substantial decrease in the value of δ_u as more measurements were included. In both the 9 and 39 bus systems, estimations tended to converge to a more accurate value as more measurements were included. This convergence underscores the importance of using t_u to assess whether there is sufficient time for additional measurements to get more accurate estimations or if corrective measures are needed.

The P_a δ curve for the contingency on bus nr.16 shows a more linear shape in its post-fault trajectory, compared to the other fault at bus nr.28 shows a more parabolic shape. This result suggests that the shape of the P_a δ curve can vary from linear to parabolic depending on the fault location. The fact that P_a δ curve shapes vary, means that it would be beneficial to develop a set of weights that can deal with this. One possible approach is to use different weight sets for the 39 and 9 bus system. Here for both cases should also include additional contingencies and averaging the cases, which could lead to a general fit that minimizes estimation errors.

9 bus system corrective measures
Reducing the CT time in the 9 bus system can help mitigate having to disconnect machines. This can be achieved by having an adequate line protection system. Specifically, if zone 1 is set to clear faults within about 0.1 seconds for 85% of the line length, then zone 2 would be for the remaining 15%. However, due to protection schemes and coordination the whole line could be zone 1, and would then have the ability to clear any fault on the line within 0.1 s. The unstable case in the 9 bus system that had a CT of 0.26 s, would never have become unstable if this was implemented. This shows that having an adequate

protection system helps to reduce the reliance on E-SIME, reserving its use for cases of protection system failure.

39 Bus System Corrective Measures
Results showed that if the corrective measure for the fault at bus nr.16 was disconnecting CMs, this resulted in disconnecting all generators from the New England grid. This would lead to a very compromised grid and an extreme solution to the issue. A suggested alternative is to disconnect the two grids to allow for system stabilization over time, effectively reducing oscillations in δ and achieving a more stable ω profile. For the New England grid this alternative is equivalent to cutting generator unit nr.1. Moreover, similarly as in the 9 bus system the reliance on E-SIME could be reduced if adequate protection schemes are in place for the system.

Initial Neural Network Challenges
The focus in the initial stage of this thesis was placed on developing a neural network for transient stability assessment. Despite a significant amount of time invested into this, it was stopped due to the neural network's "black box" nature. This in turn made it difficult to know if the neural network understood the underlying dynamics, where this was exacerbated by the network's tendency to overfit specific scenarios. Although improvements were made, suspicions remained about the neural network's knowledge of the underlying dynamics. This prompted the exploration of alternative approaches, such as physics-informed neural networks and even possibly mixing a neural network with the SIME methodology, where SIME could provide the output of CMs and η. This in turn could be used as training labels, and help the neural network to learn the underlying dynamics even for a multi-generator system. However, it was then decided to rather focus on implementing the real-time method E-SIME.

Overall on the E-SIME methodology
The E-SIME methodology, evaluated through this thesis on the 9 bus and 39 bus system, demonstrated the ability to assess transient stability by identifying CMs and estimating η. Despite this, there are challenges with inaccuracies in the estimation of δ_u that leads to errors in t_{ui}. This in turn could lead to unnecessary generator shedding or deeming an unstable case as stable. In the 39 bus system, results suggest that if the fault location is in the center of the grid, then there is a risk it could perform unnecessary generator shedding. This is due to it tending to undershoot the estimations of δ_u, and also undershooting η.

In contrast, the 9 bus system tended to overshoot these estimations instead and therefore will be less prone to perform unnecessary generator shedding. However, the CCT case η was given a positive value in the 9 bus system, and this would suggest that the method would struggle around stability threshold limits. This result suggests that it could falsely deem an unstable case as stable, and in real-life application this would be very harmful. This is because the system would eventually become unstable, but the E-SIME would believe it was stable and no corrective measures are needed. In the other case, it might unnecessarily cut generators. If this is not an extreme case where most generator units in

the system are cut, then the system would most likely remain stable. It is worth noting that the mentioned issue that comes with either overestimating or underestimating δ_u would amplify in real life applications, because then there would be both noise in the signals and possibly a higher value for the sampling rate of measurements. The issue with estimating δ_u is more critical if the case has a CT value close to the CCT.

However, overall the E-SIME method shows promising results, indicating that it could be used to increase the transmission capabilities of power systems like the New England grid. This is due to its ability to assess transient events in real-time based on measurements and initiate corrective measures only when necessary. Therefore, this method can allow the grid to operate closer to its transmission limits, which would decrease operating costs. This contrasts with preventive actions, where the system is placed in operating points further from its limits. Additionally, it is worth noting that preventive actions might be taken for faults that never or rarely occur, unnecessarily putting the system in a less optimal operating point. Another point is that E-SIME can also enhance grid security, where it would be coordinated with existing protective devices and serve as a backup if other protective devices fail. Furthermore, the literature [4] suggests that E-SIME is within reach of today's technology, given that necessary PMUs are installed at the main power stations and there needs to be a communication system to relay the information.

7 Conclusion

In both the 39 and 9 bus system E-SIME proved capable of identifying which contingencies would remain stable, and which needed corrective measures. Subsequently, corrective measures were performed on the unstable cases, and these corrections resulted in stability being maintained. Corrective measures can be in the form of grid splitting or generator disconnection, where appropriate action seems to be dependent on the fault location.

However, results suggest that near stability thresholds there is a potential for misclassification. In real-life applications, this issue is thought to become worse, due to noise in measurements and a higher sampling rate than 0.01 s. Results also indicate that E-SIME will tend to perform unnecessary corrective measures if the fault location is closer to the center of the power grid. Conversely, in cases where the fault occurs on the outer limits of the grid, and the CT is close enough to the CCT, it may falsely classify an unstable case as stable.

In conclusion, the E-SIME method has demonstrated its potential as a viable tool for assessing transient stability on different transmission systems of varying sizes. Moreover, the method seems to be within reach of today's technology if necessary PMUs are installed in the system. Further, it shows the potential to both increase transmission capabilities and enhance grid security. Therefore, the method could become a valuable resource for the Nordic power system. Suggested future work to achieve this potential is outlined in the next section.

7.1 Future Work

To enhance the accuracy and reliability of the methodology employed in this thesis that used E-SIME, several initiatives are recommended:

1. **Further optimize set of weights used for δ_u estimation:**
   An essential step is to further optimize the weight sets used for the second-order fitting of the OMIB P_a and δ curves. Two proposed options are either developing a more tailored set of weights for each system or creating a more general set.

2. **Streamline the process of performing a contingency:**
   The process of obtaining E-SIME results can be streamlined using built-in features in PowerFactory, as suggested by existing literature [25]. The DIgSILENT Programming Language (DPL) and virtual Python environments within PowerFactory could be particularly useful. Additionally, this would enable the incorporation of a built-in algorithm for identifying CMs and NMs. This would allow the time to perform a contingency to be significantly reduced.

3. **Development of an automated algorithm for corrective measures:**
   An automated algorithm needs to be designed to determine whether corrective measures should be taken based on real-time measurements. This algorithm should also decide the type of corrective action required. Furthermore, it is essential to evaluate the algorithm for its ability to prevent instability and reduce unnecessary interventions, such as unwarranted generator disconnections.

4. **Control accuracy and use a larger set of contingencies:**
   To ensure consistency in accuracy, it is recommended to run a large set of contingencies that are varied in fault location, particularly with CT values close to the CCT. Consider incorporating other renewable energy sources besides hydropower to evaluate its impact on accuracy. Another suggestion is to increase the sampling rate and introduce noise into the signals to observe its effect on accuracy.

References

[1] M. Pavella, D. Ernst and D. Ruiz-Vega, *Transient Stability of Power Systems: A Unified Approach to Assessment and Control* (Power Electronics and Power Systems). Springer US, 2012, pp. xiii, 7–9, 11, 13–14, 33–46, 48–49, 63–64, 117, 177, 179, 182, 207, 570, ISBN: 9781461543190. [Online]. Available: `https://books.google.no/books?id=3hPpBwAAQBAJ`.

[2] P. Bhui and N. Senroy, 'Real-time prediction and control of transient stability using transient energy function,' eng, *IEEE transactions on power systems*, vol. 32, no. 2, pp. 923–934, 2017, ISSN: 0885-8950.

[3] J. Mitra and M. Benidris, 'A Homotopy-Based Method for Robust Computation of Controlling Unstable Equilibrium Points,' eng, *IEEE Transactions on Power Systems*, vol. 35, no. 2, pp. 1422–1431, 2020, ISSN: 0885-8950.

[4] M. Glavic, D. Ernst, D. Ruiz-Vega, L. Wehenkel and M. Pavella, 'E-SIME - A method for transient stability closed-loop emergency control: achievements and prospects,' eng, in *2007 iREP Symposium - Bulk Power System Dynamics and Control - VII. Revitalizing Operational Reliability*, IEEE, 2007, pp. 1–10, ISBN: 1424415187.

[5] K. H. LaCommare and J. H. Eto, 'Understanding the cost of power interruptions to U.S. electricity consumers,' eng, 2004.

[6] A. Shrestha and F. Gonzalez-Longatt, 'Parametric sensitivity analysis of rotor angle stability indicators,' eng, *Energies (Basel)*, vol. 14, no. 16, p. 5, 2021, ISSN: 1996-1073.

[7] DIgSILENT GmbH, '39 Bus New England System,' DIgSILENT GmbH, Gomaringen, Germany, Tech. Rep., This paper describes the PowerFactory model of the 39 Bus New England System and its parameters as provided by DIgSILENT.

[8] DIgSILENT GmbH, 'Nine-bus system,' DIgSILENT GmbH, Gomaringen, Germany, Tech. Rep., Technical Documentation. Describes the Nine-bus System, introduced in "Power System Control and Stability" by P. M. Anderson and A. A. Fouad, adapted for PowerFactory.

[9] P. Kundur, *Power System Stability and Control*, eng. McGraw-Hill, 1994, pp. 17, 20–21, 26, 36, 49, 99, 128–131, 572, 827, 829–835, ISBN: 9780070359581 Place: New York Series: The EPRI power system engineering series.

[10] P. Kundur, J. Paserba, V. Ajjarapu *et al.*, 'Definition and classification of power system stability,' eng, *IEEE transactions on power systems*, vol. 19, no. 3, pp. 1387–1401, 2004, ISSN: 0885-8950.

[11] N. Hatziargyriou, J. Milanovic, C. Rahmann *et al.*, 'Definition and Classification of Power System Stability - Revisited Extended,' eng, *IEEE transactions on power systems*, vol. 36, no. 4, pp. 3271–3281, 2021, ISSN: 0885-8950.

[12] M. Eremia and M. Shahidehpour, *Handbook of Electrical Power System Dynamics: Modeling, Stability, and Control* (IEEE Press Series on Power Engineering), eng, 1. Aufl. New York: Wiley-IEEE Press, 2013, vol. 92, pp. 570–573, 578, ISBN: 9781118497173.

[13] P. Anderson, eng, in *Power system control and stability*, Edition: 2nd ed. ISBN: 0471238627 Place: Piscataway, N.J Series: IEEE Press series on power engineering, IEEE Press, 2003, pp. 9, 13–16, 31–35, 38–39, 84–85.

[14] J. K. Yong Sun Jinpeng Ma and M. Zhan, 'Equal-area criterion in power systems revisited,' eng, *Proceedings of the Royal Society. A, Mathematical, physical, and engineering sciences*, 2018, ISSN: 1471-2946. [Online]. Available: https://doi.org/10.1098/rspa.2017.0733.

[15] A. Bahmanyar, D. Ernst, Y. Vanaubel, Q. Gemine, C. Pache and P. Panciatici, 'Extended Equal Area Criterion Revisited: A Direct Method for Fast Transient Stability Analysis,' *Energies*, vol. 14, no. 21, 2021, ISSN: 1996-1073. DOI: 10.3390/en14217259. [Online]. Available: https://www.mdpi.com/1996-1073/14/21/7259.

[16] M. La Scala, R. Sbrizzai, F. Torelli and P. Scarpellini, 'A tracking time domain simulator for real-time transient stability analysis,' eng, *IEEE Transactions on Power Systems*, vol. 13, no. 3, pp. 992–998, 1998, ISSN: 0885-8950.

[17] L. Chen, F. Xu, Y. Min, M. Wang and W. Hu, 'Transient energy dissipation of resistances and its effect on power system damping,' eng, *International journal of electrical power energy systems*, vol. 91, pp. 201–208, 2017, ISSN: 0142-0615.

[18] G. Dudgeon, W. Leithead, A. Dysko, J. O'Reilly and J. McDonald, 'The Effective Role of AVR and PSS in Power Systems: Frequency Response Analysis,' eng, *IEEE transactions on power systems*, vol. 22, no. 4, pp. 1986–1994, 2007, ISSN: 0885-8950.

[19] A. K. Samy and A. Venkadesan, 'Chapter 8 - Stability control and enhancement,' eng, in *Power Systems Operation with 100% Renewable Energy Sources*, Elsevier Inc, 2024, p. 115, ISBN: 9780443155789.

[20] DIgSILENT GmbH. 'PowerFactory applications.' Accessed on: Apr. 11, 2024. (), [Online]. Available: https://www.digsilent.de/en/powerfactory.html.

[21] DIgSILENT GmbH, *PowerFactory 2022 User Manual*, Online Edition, Heinrich-Hertz-Straße 9, 72810 Gomaringen, Germany: DIgSILENT GmbH, Aug. 2022, pp. 18–19, 307–309, 613, 618.

[22] DIgSILENT GmbH, *PowerFactory 2022 Technical Reference: Synchronous Machine*, Revision 2, DIgSILENT GmbH, Heinrich-Hertz-Straße 9, 72810 Gomaringen, Germany, Mar. 2022, pp. 22, 36–38, 45–47.

[23] S. C. Savulescu, 'Appendix B: Sime: A Comprehensive Approach to Transient Stability,' eng, in *Real-Time Stability Assessment in Modern Power System Control Centers*, ser. IEEE Press Series on Power Engineering, vol. 42, Hoboken, NJ, USA: John Wiley Sons, 2009, pp. 354–356, ISBN: 9780470233306.

[24] D. Ernst and M. Pavella, 'Closed-loop transient stability emergency control,' eng, in *2000 IEEE Power Engineering Society Winter Meeting. Conference Proceedings (Cat. No.00CH37077)*, vol. 1, IEEE, 2000, 58–62 vol.1, ISBN: 9780780359352.

[25] F. Gonzalez-Longatt and J. L. Rueda Torres, 'Implementation of the Single Machine Equivalent (SIME) Method for Transient Stability Assessment in DIgSILENT PowerFactory,' eng, in *Advanced Smart Grid Functionalities Based on PowerFactory*, ser. Green Energy and Technology, Switzerland: Springer International Publishing AG, 2018, pp. 319–353, ISBN: 9783319505312.

[26] P. Sarajcev, A. Kunac, G. Petrovic and M. Despalatovic, 'Artificial Intelligence Techniques for Power System Transient Stability Assessment,' *Energies*, vol. 15, no. 2, 2022, ISSN: 1996-1073. DOI: 10.3390/en15020507. [Online]. Available: https://www.mdpi.com/1996-1073/15/2/507.

[27] H.-D. Chiang, *Direct Methods for Stability Analysis of Electric Power Systems: Theoretical Foundation, BCU Methodologies, and Applications*, eng, 1st edition. Hoboken, New Jersey: Wiley, 2010, ISBN: 1-282-84903-4.

[28] A. K. Toft, *Direct methods for transient stability analysis and contingency screening in power systems*, eng, 2023. [Online]. Available: https://hdl.handle.net/11250/3080293.

[29] P. Sun, L. Huo, S. Liang and X. Chen, 'Fast Transient Stability Prediction Using Grid-informed Temporal and Topological Embedding Deep Neural Network,' eng, *arXiv (Cornell University)*, 2022.

[30] S. Cheng, Z. Yu, Y. Liu and X. Zuo, 'Power system transient stability assessment based on the multiple paralleled convolutional neural network and gated recurrent unit,' eng, *Protection and control of modern power systems*, vol. 7, no. 1, pp. 39–16, 2022, ISSN: 2367-2617.

[31] T. Wang, X. Wang, G. Liu, Z. Wang and Q. Xing, 'Neural Networks Based Lyapunov Functions for Transient Stability Analysis and Assessment of Power Systems,' *IEEE Transactions on Industry Applications*, vol. 59, no. 2, pp. 2626–2638, 2023. DOI: 10.1109/TIA.2022.3232611.

[32] G. S. Misyris, A. Venzke and S. Chatzivasileiadis, 'Physics-Informed Neural Networks for Power Systems,' eng, 2020. [Online]. Available: https://doi.org/10.48550/arXiv.1911.03737.

[33] B. Moseley. 'So, what is a physics-informed neural network?' Accessed: 2024-01-16. (2021), [Online]. Available: https://benmoseley.blog/my-research/so-what-is-a-physics-informed-neural-network/.

[34] X. Li, S. Chen, J. Zhang, J. Gao and Y. Bai, 'A Physics-Informed Deep Learning Paradigm for Transient Power Angle Stability Assessment,' *IEEE Journal of Radio Frequency Identification*, vol. 6, pp. 948–952, 2022. DOI: 10.1109/JRFID.2022.3213882.

[35] I. de Cominges Guerra, W. Li and R. Wang, 'A Comprehensive Analysis of PINNs for Power System Transient Stability,' *Electronics*, vol. 13, no. 2, 2024, ISSN: 2079-9292. DOI: 10.3390/electronics13020391. [Online]. Available: https://www.mdpi.com/2079-9292/13/2/391.

[36] Y. Zhang, L. Wehenkel, P. Rousseaux and M. Pavella, 'SIME: A hybrid approach to fast transient stability assessment and contingency selection,' eng, *International journal of electrical power energy systems*, vol. 19, no. 3, pp. 195–208, 1997, ISSN: 0142-0615.

Appendix A

Developed code

In this appendix the developed Python code that was employed in this thesis is presented.

A.1 Weighted least squares method for finding δ_u

```
import matplotlib.pyplot as plt
import numpy as np
from numpy.polynomial import Polynomial

#46 measuremnts 10 Generators 0.18s clearing time included so code will run. This can be changed to other
    examples
delta_omib_array = np.array([ 65.3106328,  66.6821248,  68.758437 ,  70.8573804,  72.9706682,
        75.0909631,  77.2117323,  79.3271338,  81.4320388,  83.5219976,
        85.5931515,  87.6421959,  89.6669998,  91.664606 ,  93.6324696,
        95.5697279,  97.4752197,  99.3480901, 101.18777  , 102.99393  ,
       104.766437 , 106.505302 , 108.21063  , 109.882591 , 111.521378 ,
       113.127191 , 114.700211 , 116.240594 , 117.748456 , 119.223876 ,
       120.666885 , 122.077476 , 123.455591 , 124.801141 , 126.11399  ,
       127.393972 , 128.640884 , 129.854499 , 131.034555 , 132.180769 ,
       133.292837 , 134.370345 , 135.412957 , 136.420406 , 137.392318 ,
       138.328307 ])*(np.pi/180)
Pa_array =-np.array([ 595.7675505 ,  502.2085021 ,  365.2934514 ,  238.1285034 ,
        121.6594904 ,   16.14906291,  -78.47204746, -162.5155433 ,
       -236.3488125 , -300.5610567 , -355.7275721 , -402.5297859 ,
       -441.2549449 , -473.8815635 , -499.7870798 , -520.1489376 ,
       -535.3898043 , -545.9441767 , -552.4256797 , -555.7030609 ,
       -556.5945325 , -555.8004672 , -553.9542544 , -551.5750454 ,
       -549.0489934 , -546.666786  , -544.6242126 , -543.0571232 ,
       -542.0408784 , -541.6147983 , -541.7877075 , -542.5484332 ,
       -543.8707969 , -545.7223914 , -548.0709921 , -550.8761761 ,
       -554.1079376 , -557.7338143 , -561.7285552 , -566.0634409 ,
       -570.7103299 , -575.6743199 , -580.9087681 , -586.3875827 ,
       -592.0985438 , -598.0212602 ])




# Example weights array, one for each data point
weights = np.array([0.1, 0.1, 0.1, 0.1, 0.1, 0.1, 0.1, 0.1, 0.1, 0.1, 0.1, 0.1, 0.1, 0.1, 0.1, 0.1, 0.1,
    0.1, 0.1, 0.1, 0.1, 0.1, 0.1, 0.1, 0.1, 0.1, 0.1, 0.1, 0.1, 0.1, 0.1, 0.1 ,0.1, 0.1, 0.1, 0.1, 0.1,
    0.1, 0.1, 0.1, 0.1, 0.1 ,0.1, 1, 1, 1])
```

```
# Fit a weighted second order polynomial to the data
coefs = np.polyfit(delta_omib_array, Pa_array, 2, w=weights)


polynomial = Polynomial(coefs[::-1])  # Polynomial expects coefs in increasing order

# The coefficients are in the order of c, b, a for np.polyfit
a, b, c = coefs[::-1]

# Coefficients are returned in the order of highest degree to lowest, so:
a = coefs[0]  # Coefficient of delta^2
b = coefs[1]  # Coefficient of delta
c = coefs[2]  # Constant term

# Polynomial expects coefs in increasing order
polynomial = Polynomial(coefs[::-1])


last_delta_value = delta_omib_array[-1]

delta_i = last_delta_value

# Find the roots of the polynomial
roots = polynomial.roots()

# Filter out the complex roots and the roots smaller than the last data point
real_roots = roots[np.isreal(roots)].real
valid_roots = real_roots[real_roots > last_delta_value]

# If there is no valid root, it means the polynomial does not intersect with Pa = 0
if valid_roots.size == 0:
    raise ValueError("The polynomial does not intersect with Pa = 0 beyond the last data point.")
else:
    delta_u = valid_roots
    print("Delta_u is found to be : ", np.round(valid_roots*(180/np.pi),4))
```

A.2 Optimization of Weights for least squares method

```
import matplotlib.pyplot as plt
import numpy as np
from numpy.polynomial import Polynomial
from scipy.optimize import minimize
import pandas as pd

# Define the delta and Pa arrays, where this can be changed, but these was used in the thesis. That are
    taken from the 0.26 clearing time 3 generators
delta_omib_array = np.array([107.61276994, 110.0484313 , 113.60656519, 117.02086452,
       120.29092519, 123.41758054, 126.4028057 , 129.24961233,
       131.96193608, 134.54453667, 137.00289151, 139.34310163,
       141.57180863, 143.69612031])
Pa_array =-np.array([-87.20231179, -88.29910849, -89.35644339, -89.56833606,
       -88.99341491, -87.69744836, -85.74955453, -83.21949005,
       -80.17503655, -76.68062197, -72.79565775, -68.57400147,
       -64.06304501, -59.30330649])

# Function to optimize weights to minimize Pa at the target delta
def optimize_weights(weights, delta, Pa, n_points, target_delta):
```

```
    coefs = np.polyfit(delta[:n_points], Pa[:n_points], 2, w=weights)
    polynomial = Polynomial(coefs[::-1])
    return (polynomial(target_delta))**2

# Initialize weights and set bounds
initial_weights = np.ones_like(delta_omib_array)
bnds = [(0, 1) for _ in delta_omib_array]
target_delta = 163.48172  # Target delta for optimization

# Container for optimized weights
weights_list = {}

# Plotting setup
plt.figure(figsize=(14, 8))
plt.scatter(delta_omib_array, Pa_array, color='blue', label='Original Data')

# Optimize and plot fits for different numbers of data points
for n in range(3, len(delta_omib_array) + 1):
    res = minimize(optimize_weights, initial_weights[:n], args=(delta_omib_array, Pa_array, n, target_delta
    ),
                   bounds=bnds[:n], method='SLSQP')
    optimal_weights = res.x if res.success else np.ones(n)
    weights_list[n] = optimal_weights  # Store the weights
    coefs = np.polyfit(delta_omib_array[:n], Pa_array[:n], 2, w=optimal_weights)
    polynomial = Polynomial(coefs[::-1])
    extended_delta_range = np.linspace(delta_omib_array.min(), delta_omib_array.max(), 300)
    fitted_curve = polynomial(extended_delta_range)
    plt.plot(extended_delta_range, fitted_curve, label=f'Fitted with {n} measurements')

plt.title('Comparison of Fitted Curves with Different Number of measurements')
plt.xlabel('$\delta$')
plt.ylabel('$P_a$')
plt.legend()
plt.grid(True)
plt.show()

# Create DataFrame from weights list
weights_df = pd.DataFrame.from_dict(weights_list, orient='index')

# Add column names
weights_df.columns = [f'w_{i+1}' for i in range(weights_df.shape[1])]

weights_df['Nr. of Meas. Incl.'] = weights_df.index

weights_df = weights_df.round(3)
```

A.3 Integral of $P_a(\delta)$ and calculation of η_u

```
delta_i = # inital rotor position of OMIB in measurment
delta_u = # Found value for the delta_u
M = # Inertia constant from OMIB parameters
wi = #  Inital rotor speed  of OMIB in measurment
a = # coefficent for 2 order element
b = # coefficent for 1 order element
c = # coefficent for 0 order element
```

```
# Calculate the definite integral from the last data point to the collision delta
integral_value = (a/3)*(delta_u**3 - delta_i**3) + (b/2)*(delta_u**2 - delta_i**2) + c*(delta_u - delta_i)



RotorEnergy = (1/2)*M*(wi)**2

print("n_u is equal to : ", np.round(integral_value - RotorEnergy,4))
```

A.4 Estimation of time to instability t_u

```
import numpy as np

def g(delta, delta_i, M, wi, a, b, c):
    # Calculate the integral of P_a from delta_i to delta

    IntPa = - (a/3 * (delta**3 - delta_i**3) + b/2 * (delta**2 - delta_i**2) + c * (delta - delta_i))
    # Calculate the integrand at delta
    Int_t = 1 / (np.sqrt((2/M) * IntPa + wi**2))
    return Int_t

# Initial values for the integration
delta_i = # inital rotor position of OMIB in measurment
delta_u = # Found value for the delta_u
M = # Inertia constant from OMIB parameters
wi = #  Inital rotor speed  of OMIB in measurment
a = # coefficent for 2 order element
b = # coefficent for 1 order element
c = # coefficent for 0 order element
ti = #  # Initial time ti, you can set it to your specific problem's initial time
dt = 0.001  # Integration step size

# Calculate the number of steps needed
num_steps = int((delta_u - delta_i) / dt)

# Initialize the integral sum
Integral_sum = 0

# Main integration loop using the trapezoidal rule
for i in range(1, num_steps):
    delta = delta_i + i * dt
    Integral_sum =Integral_sum+ g(delta, delta_i, M, wi, a, b, c)

# Apply the trapezoidal rule
t_u = dt * (0.5 * g(delta_i, delta_i, M, wi, a, b, c) + Integral_sum + 0.5 * g(delta_u, delta_i, M, wi, a,
     b, c))

t_u_i = t_u
t_u =t_u + ti

print("Time at instability:", np.round(t_u,4))

print("Time to instability:", np.round(t_u_i,4))
```

A.5 Unwrapping angles for δ

```
import pandas as pd
import numpy as np
import matplotlib.pyplot as plt

# Columns that contain angle data
#angle_columns = ['G1.3', 'G2.3', 'G3.3'] in my case with the 3 generator case
#Change this to the correct and also filepath

def make_continuous(angles, threshold=340, window=1):
    corrected_angles = np.copy(angles)
    for i in range(window, len(angles)):
        if (angles[i] - angles[i-window]) < -threshold:
            corrected_angles[i:] += 360  # Adjust all subsequent angles
    return corrected_angles

# Path to the CSV file
file_path_new = r"!FilePathHere!"
# Load and prepare the data
data = pd.read_csv(file_path_new, delimiter=';')
data = data.drop(index=0).reset_index(drop=True)
data = data.apply(pd.to_numeric, errors='coerce')


data_unstable = data

angles = data_unstable['G2.3'].values
continuous_angles = make_continuous(angles)

data_unstable['G2.3'] = continuous_angles


angles = data_unstable['G3.3'].values
continuous_angles = make_continuous(angles)

data_unstable['G3.3'] = continuous_angles

# Check the result by printing the first few rows of the modified DataFrame
print(data_unstable.head(70))  # Adjust the number of rows as needed



# Plot of the continuously unwrapped angle G3
plt.figure(figsize=(10, 5))
plt.plot(data_unstable['All calculations'], data_unstable['G2.3'], marker='o')
plt.title('G2 Continuous Rotor Angle Over Time')
plt.xlabel('Time (s)')
plt.ylabel('Rotor Angle (degrees)')
plt.grid(True)
plt.show()


#  Plot of continuously unwrapped angle G2
plt.figure(figsize=(10, 5))
plt.plot(data_unstable['All calculations'], data_unstable['G3.3'], marker='o')
plt.title('G3 Continuous Rotor Angle Over Time')
plt.xlabel('Time (s)')
plt.ylabel('Rotor Angle (degrees)')
plt.grid(True)
plt.show()
```

```
# Define the path where the new CSV file will be saved
new_file_path = r"!NewFilePath!"

# Save the DataFrame to a new CSV file
data_unstable.to_csv(new_file_path, sep=';', index=False)

print(f"File saved successfully to {new_file_path}")
```

A.6 9 bus system δ prediction and identification of CMs

```
import pandas as pd
import numpy as np
import matplotlib.pyplot as plt

def predict_rotor_angles(angle_t0, angle_t1, speed, acceleration, t_forward, sampling_rate=0.01):

    predicted_angles = angle_t1 + (speed * t_forward) + (0.5 * acceleration * t_forward ** 2)
    predicted_angles = predicted_angles*180

    print("Predicted angles Method 1: ", predicted_angles)

    predicted_angles = angle_t1 + t_forward*((angle_t1 - angle_t0)/sampling_rate)
    predicted_angles = predicted_angles*180
    print("Predicted angles, Method 2: ", predicted_angles)

    return predicted_angles



def identify_critical_machines(predicted_angles, labels):
    # Ensure labels array matches predicted_angles in size and order
    assert len(predicted_angles) == len(labels), "Labels array must match the size of predicted_angles"

    # Combine angles and labels for sorting in ascending order
    angles_labels = sorted(zip(predicted_angles, labels))

    # Extract angles and labels from the sorted combined list
    sorted_angles, sorted_labels = zip(*angles_labels)

    # Calculate adjacent differences (gaps) between sorted angles in ascending order
    adjacent_gaps = np.diff(sorted_angles)

    # Find the index of the largest gap
    largest_gap_index = np.argmax(adjacent_gaps)

    # Critical machines are after the largest gap, non-critical before
    critical_machines = sorted_labels[largest_gap_index + 1:]
    non_critical_machines = sorted_labels[:largest_gap_index + 1]

    return list(critical_machines), list(non_critical_machines)


# Path to the CSV file
file_path_new = r"FILEpathHere" # Note that code here is set for clearing at 0.26s now.

# Load and prepare the data
data_new = pd.read_csv(file_path_new, delimiter=';')
data_new = data_new.drop(index=0).reset_index(drop=True)  # Dropping descriptive header row
```

```
data_new = data_new.apply(pd.to_numeric, errors='coerce')  # Convert all data to numeric
data = data_new

num_steps=30

# Indexes for the next three successive measurements after 0.15s
indexes_to_extract = [i for i in range(1, num_steps + 1)]

# Filter the DataFrame to find all values <= 0.26, then find the max of these values, reason 0.27 s is used
      is to delay a little between event and measurement.
closest_value_to_027 = data_new[data_new['All calculations'] <= 0.27]['All calculations'].max()

# Now, find the index of this closest value
time_index_closest = data_new[data_new['All calculations'] == closest_value_to_027].index[0]

# Indexes for the next three successive measurements after 0.15s
indexes_to_extract = [time_index_closest+i for i in range(1, num_steps + 1)]

# Initialize arrays to store the results
Angle_1 = np.zeros(len(indexes_to_extract))
Angle_2 = np.zeros(len(indexes_to_extract))
Angle_3 = np.zeros(len(indexes_to_extract))
time_array = np.zeros(len(indexes_to_extract))


for i, index in enumerate(indexes_to_extract):
    # Extract the values for the current index
    current_data = data.loc[index]


    angle1 = current_data['G1.3']
    Angle_1[i] = angle1
    angle2 = current_data['G2.3']
    Angle_2[i] = angle2
    angle3 = current_data['G3.3']
    Angle_3[i] = angle3

    time_array[i] = current_data['All calculations']


# Extracting necessary data for prediction
time_index_new = data_new[data_new['All calculations'] > 0.26].index[0]
angle_columns_new = ['G1.3', 'G2.3', 'G3.3']  # Angles in degrees
speed_columns_new = ['G1.2', 'G2.2', 'G3.2']   # Speed in p.u.
acceleration_columns_new = ['G1.4', 'G2.4', 'G3.4']  # Speed derivative in p.u./s

angle_t0_new = data_new.loc[time_index_new - 1, angle_columns_new].to_numpy()
angle_t1_new = data_new.loc[time_index_new, angle_columns_new].to_numpy()
speed_new = data_new.loc[time_index_new, speed_columns_new].to_numpy()
speed_new = speed_new - 1 # since operation around here is close to 1 p.u. just when fault occured
acceleration_new = data_new.loc[time_index_new, acceleration_columns_new].to_numpy()

angle_t0_new_pu = angle_t0_new /180
angle_t1_new_pu = angle_t1_new /180


#%%
InitialTime = time_array[0]

# Setting t_forward for the prediction. Actual time predict is t_forward_new + (intital time=0.15)
t_forward_new = 0.28

T_pred = InitialTime+ t_forward_new
```

```
# Performing prediction
predicted_angles_new = predict_rotor_angles(angle_t0_new_pu, angle_t1_new_pu, speed_new, acceleration_new,
    t_forward_new)



Gen_1_pred = predicted_angles_new[0]
Gen_2_pred = predicted_angles_new[1]
Gen_3_pred = predicted_angles_new[2]


# Example predicted angles
predicted_angles_example = np.array(predicted_angles_new)
labels = np.array(['G1', 'G2', 'G3'])

# Identify critical and non-critical machines
critical_machines, non_critical_machines = identify_critical_machines(predicted_angles_example,labels)

print("Critical Machines:", critical_machines)
print("Non-Critical Machines:", non_critical_machines)

plt.figure(figsize=(10, 6))
plt.style.use('seaborn-v0_8-darkgrid')

# Actual angles
plt.plot(time_array, Angle_1, 'b-', label='Generator 1 Actual', linewidth=2)
plt.plot(time_array, Angle_2, 'r-', label='Generator 2 Actual', linewidth=2)
plt.plot(time_array, Angle_3, 'g-', label='Generator 3 Actual', linewidth=2)

# Predicted angles with distinct markers and colors corresponding to the actual data
plt.plot(T_pred, Gen_1_pred, 'bx', markersize=8, label='Generator 1 Prediction')
plt.plot(T_pred, Gen_2_pred, 'rx', markersize=8, label='Generator 2 Prediction')
plt.plot(T_pred, Gen_3_pred, 'gx', markersize=8, label='Generator 3 Prediction')


plt.xlabel('Time (seconds)', fontsize=12)
plt.ylabel('Rotor Angle (degrees)', fontsize=12)
plt.title('Actual vs. Predicted Rotor Angles of Generators', fontsize=14)
plt.ylim(-7,190)

# Adjusting legend
plt.legend(loc='upper left', fontsize='small')

plt.show()
```

A.7 Calculating OMIB variables and plot for 9 bus system

```
import pandas as pd
import numpy as np
import matplotlib.pyplot as plt

fn = 60

#Polepairs = 1 on all generators, meaning ws = w_mech
wmech = 2*np.pi*fn
wb = wmech #Base speed

Sgn_1= 247.5
Sgn_2 = 192
```

```
Sgn_3 = 128

PowerFactor_1 = 1
PowerFactor_2 = 0.85
PowerFactor_3 = 0.85

Pn_1 = (Sgn_1*PowerFactor_1)
Pn_2 = (Sgn_2*PowerFactor_2)
Pn_3 = (Sgn_3*PowerFactor_3)

hs_1 = 9.551516
hs_2 = 3.333333
hs_3 = 2.351562

M1 = hs_1*2*Sgn_1/(wmech)
M2 = hs_2*2*Sgn_2/(wmech)
M3 = hs_3*2*Sgn_3/(wmech)

print("M1 is : ", round(M1,3))
print("M2 is : ", round(M2,3))
print("M3 is : ", round(M3,3))


MC = M2+M3
MN = M1

M = (MC*MN)/(MC+MN)


print('MC is equal to :', round(MC,3))
print('MN is equal to : ', round(MN,3))
print('M is equal to : ', round(M,3))


# Path to the CSV file
file_path_new = r"InsertFilePathHERE!" # This code is set for CT 0.2515


# Load and prepare the data, specifying the correct decimal separator and skipping the descriptive header
    row
data_new = pd.read_csv(file_path_new, delimiter=';', decimal=',', skiprows=[1])

data_new = data_new.apply(pd.to_numeric, errors='coerce')  # Convert all data to numeric

data = data_new


closest_value_to_02515 = data['All calculations'].loc[data['All calculations'] <= 0.2515].max()

# Find the index of this closest value
time_index_closest = data.index[data['All calculations'] == closest_value_to_02515].tolist()

print(f"Indexes of the value closest to 0.2515 without going over: {time_index_closest}")


time_index_closest = time_index_closest[0]


# Define the number of steps forward you want to plot
num_steps = 46 # # Or any other number of steps you want

print(num_steps)

# Indexes for the next three successive measurements after 0.2515s
```

```
indexes_to_extract = [time_index_closest + i for i in range(1, num_steps + 1)]


# Initialize arrays to store the results
Pm_array = np.zeros(len(indexes_to_extract))
Pe_array = np.zeros(len(indexes_to_extract))
Pa_array = np.zeros(len(indexes_to_extract))
delta_omib_array = np.zeros(len(indexes_to_extract))
speed_omib_array = np.zeros(len(indexes_to_extract))
time_array = np.zeros(len(indexes_to_extract))

# Perform calculations for each index
for i, index in enumerate(indexes_to_extract):
    # Extract the values for the current index
    current_data = data.loc[index]

    # Calculate COA for the current index
    angle2 = current_data['G2.3']
    angle3 = current_data['G3.3']
    delta_C = (M2 * angle2 + M3 * angle3) / MC

    # delta_N is the rotor angle of Generator 1
    delta_N = current_data['G1.3']

    # delta_omib is COA minus delta_N
    delta_omib_array[i] = delta_C - delta_N


    # Calculate COA for the current index
    speed2 = current_data['G2.2']
    speed3 = current_data['G3.2']
    speed_C = (M2 * speed2 + M3 * speed3) / MC

    speed_N = current_data['G1.2']

    # delta_omib is COA minus delta_N
    speed_omib_array[i] = speed_C - speed_N

    # Pm and Pe for critical machines (G2 and G3)
    Pm_C = current_data['G2']*(Pn_2) + current_data['G3']*(Pn_3)
    Pe_C = current_data['G2.1']*(Pn_2) + current_data['G3.1']*(Pn_3)

    # Pm and Pe for non-critical machine (G1)
    Pm_N = current_data['G1']*(Pn_1)
    Pe_N = current_data['G1.1']*(Pn_1)

    # Calculate the equivalent OMIB mechanical and electrical power (Pm and Pe)
    Pm_array[i] = M * ((1/MC) * Pm_C - (1/MN) * Pm_N)
    Pe_array[i] = M * ((1/MC) * Pe_C - (1/MN) * Pe_N)

    # Calculate the equivalent OMIB accelerating power (Pa)
    Pa_array[i] = Pm_array[i] - Pe_array[i]


    time_array[i] = current_data['All calculations']

speed_omib_array_rad = speed_omib_array*wb

plt.figure(figsize=(10, 5))
plt.plot(delta_omib_array, -Pa_array , marker='o')

# Add a horizontal line at y = 0
plt.axhline(y=0, color='r', linestyle='--')  # 'r' is for red color, '--' for dashed line
```

```
plt.title('Equivalent Rotor Angle vs. -Pa: Accelerating Power')
plt.xlabel('Equivalent Rotor Angle (degrees)')
plt.ylabel('- Pa: Accelerating Power (MW)')
plt.grid(True)
plt.show()

plt.figure(figsize=(10, 5))
plt.plot(time_array, delta_omib_array, marker='o', color='green', label='w_omib: OMIB Rotor Speed')
# Add a horizontal line at y = 0
plt.axhline(y=0, color='r', linestyle='--')  # 'r' is for red color, '--' for dashed line
plt.title('Time vs. OMIB Rotor angle')
plt.xlabel('Time (s)')
plt.ylabel('OMIB Rotor angle (degrees)')
plt.grid(True)
plt.legend()
plt.show()


plt.figure(figsize=(10, 5))
plt.plot(time_array, speed_omib_array_rad, marker='o', color='green', label='w_omib: OMIB Rotor Speed')
# Add a horizontal line at y = 0
plt.axhline(y=0, color='r', linestyle='--')  # 'r' is for red color, '--' for dashed line
plt.title('Time vs. OMIB Rotor Speed')
plt.xlabel('Time (s)')
plt.ylabel('OMIB Rotor Speed (rad/s)')
plt.grid(True)
plt.legend()
plt.show()


plt.figure(figsize=(10, 5))
plt.plot(delta_omib_array, speed_omib_array_rad, marker='o', color='green', label='w_omib: OMIB Rotor Speed
    ')
# Add a horizontal line at y = 0
plt.axhline(y=0, color='r', linestyle='--')  # 'r' is for red color, '--' for dashed line
plt.title('Delta vs. OMIB Rotor Speed')
plt.xlabel('Delta (Degrees)')
plt.ylabel('OMIB Rotor Speed (rad/s)')
plt.grid(True)
plt.legend()
plt.show()
```

A.8 9 bus system case check of kinetic energy change against integral of P_a and δ for a single time-step

```
import numpy as np

#%% 3 Gen case
#array([0.265, 0.271667]) sample times Unstable Case. Clearing time 0.26s

wb = 2*np.pi*60

delta1 = 107.6127699*(np.pi/180)
delta2 = 110.0484313*(np.pi/180)

omega1 = 0.0172365*wb
omega2 = 0.0168046*wb
```

```
Pa1 = -87.2023
Pa2 = -88.2991

M = 3.5708

Area_1 = 1/2*M*(omega2**2 - omega1**2)
Area_2 = (delta2-delta1)*(1/2)*(Pa2 + Pa1)
Area_2 = (delta2-delta1)*(Pa1 + (1/2)*(Pa2 - Pa1))

print("Area 1 Omega is : ", round(Area_1,4), ". Area Pa 2 is : ",round(Area_2,4))
```

A.9 39 bus system case check of kinetic energy change against integral of P_a and δ for a single time-step

```
import numpy as np


#%% 10 Gen case V3
#array([0.601667, 0.611667]) sample times Unstable Case. Clearing time 0.2s

wb = 2*np.pi*60

delta1 = 150.313824*(np.pi/180)
delta2 = 152.029339*(np.pi/180)

omega1 = 0.00796208*wb
omega2 = 0.00793128*wb

Pa1 = -122.1217412
Pa2 = -108.1420464

M = 101.253951

Area_1 = 1/2*M*(omega2**2 - omega1**2)
Area_2 = (delta2-delta1)*(1/2)*(Pa2 + Pa1)
Area_2 = (delta2-delta1)*(Pa1 + (1/2)*(Pa2 - Pa1))

print("Area 1 Omega is : ", round(Area_1,4), ". Area Pa 2 is : ",round(Area_2,4))
```

A.10 Calculating OMIB variables and plot for 39 bus system

```


import numpy as np
import pandas as pd
import matplotlib.pyplot as plt

#%% Unstable case with clearing time of 0.2s for 10 generator system

Time_array_u = np.array([-0.1     , -0.09, -0.08, -0.07, -0.06, -0.05,
       -0.04    , -0.03    , -0.02    , -0.01    ,  0.      ,  0.005   ,
        0.011667,  0.021667,  0.031667,  0.041667,  0.051667,  0.061667,
        0.071667,  0.081667,  0.091667,  0.101667,  0.111667,  0.121667,
        0.131667,  0.141667,  0.151667,  0.161667,  0.171667,  0.181667,
```

```
        0.191667,  0.2     ,  0.205   ,  0.211667,  0.221667,  0.231667,
        0.241667,  0.251667,  0.261667,  0.271667,  0.281667,  0.291667,
        0.301667,  0.311667,  0.321667,  0.331667,  0.341667,  0.351667,
        0.361667,  0.371667,  0.381667,  0.391667,  0.401667,  0.411667,
        0.421667,  0.431667,  0.441667,  0.451667,  0.461667,  0.471667,
        0.481667,  0.491667,  0.501667,  0.511667,  0.521667,  0.531667,
        0.541667,  0.551667,  0.561667,  0.571667,  0.581667,  0.591667,
        0.601667,  0.611667,  0.621667,  0.631667,  0.641667,  0.651667,
        0.661667,  0.671667,  0.681667,  0.691667,  0.701667,  0.711667,
        0.721667,  0.731667,  0.741667,  0.751667,  0.761667,  0.771667,
        0.781667,  0.791667,  0.801667,  0.811667,  0.821667,  0.831667,
        0.841667,  0.851667,  0.861667,  0.871667,  0.881667,  0.891667,
        0.901667,  0.911667,  0.921667,  0.931667,  0.941667,  0.951667,
        0.961667,  0.971667,  0.981667,  0.991667,  1 ])

Delta_Unstable = np.array([  46.4496057, 46.4496057, 46.4496057, 46.4496057,
         46.4496057,   46.4496057,   46.4496057,   46.4496057,
         46.4496057,   46.4496057,   46.4496057,   46.4735224,
         46.5385051,   46.7040147,   46.9745375,   47.3533378,
         47.8425496,   48.4437609,   49.1581786,   49.9864487,
         50.9293004,   51.9875368,   53.1614885,   54.4513451,
         55.8571692,   57.3789148,   59.016431 ,   60.7694844,
         62.6377598,   64.6208756,   66.7183931,   68.5612555,
         69.6950842,   71.2173433,   73.5184324,   75.8399332,
         78.1734824,   80.5118226,   82.8485491,   85.1780964,
         87.4957381,   89.7974675,   92.0799589,   94.3405148,
         96.5777054,   98.7893132,  100.973649 ,  103.130857 ,
        105.26086  ,  107.363943 ,  109.44067  ,  111.491812 ,
        113.518279 ,  115.521064 ,  117.501198 ,  119.459723 ,
        121.397667 ,  123.316032 ,  125.215779 ,  127.097838 ,
        128.963093 ,  130.812393 ,  132.646556 ,  134.466367 ,
        136.272588 ,  138.065578 ,  139.846053 ,  141.615097 ,
        143.373422 ,  145.12174  ,  146.860763 ,  148.591214 ,
        150.313824 ,  152.029339 ,  153.738526 ,  155.442166 ,
        157.141074 ,  158.836085 ,  160.528068 ,  162.217928 ,
        163.906605 ,  165.595086 ,  167.284401 ,  168.975635 ,
        170.66993  ,  172.368493 ,  174.0726   ,  175.783607 ,
        177.502954 ,  179.23218  ,  180.972926 ,  182.726948 ,
        184.496122 ,  186.282461 ,  188.088119 ,  189.9154   ,
        191.766775 ,  193.644886 ,  195.552554 ,  197.492792 ,
        199.468818 ,  201.484047 ,  203.542107 ,  205.646829 ,
        207.802256 ,  210.012643 , -147.71755  , -145.383295 ,
       -142.979752 , -140.502269 , -137.945647 , -135.304531 ,
       -133.028608 ])

Pa_Unstable = np.array([   0.        ,    0.   ,    0. , 0.,
          0.        ,    0.        ,    0.        ,    0.        ,
          0.        ,    0.        ,    0.        , 1544.740435  ,
       1605.376075  , 1669.51429   , 1711.051458  , 1741.016372  ,
       1764.132873  , 1781.863786  , 1795.634887  , 1806.15293   ,
       1813.88071   , 1819.147133  , 1822.209014  , 1823.291802  ,
       1822.592487  , 1820.297194  , 1816.576135  , 1811.595791  ,
       1805.515348  , 1798.492101  , 1790.681887  , 1783.700079  ,
        572.665128  ,  473.9479597 ,  331.7759932 ,  202.5264928 ,
         86.4031863 ,  -16.76415883, -107.2336754 , -185.5258323 ,
       -252.2170488 , -307.9718316 , -353.4561276 , -389.4360625 ,
       -416.0819613 , -434.7896238 , -444.7503992 , -447.5389912 ,
       -444.3725339 , -436.5837833 , -425.4162704 , -411.9248376 ,
       -396.9897867 , -381.2984462 , -365.3539316 , -349.4913573 ,
       -333.9397177 , -318.8101148 , -304.1504146 , -289.973676  ,
       -276.2450566 , -262.9101474 , -249.8991277 , -237.1407552 ,
       -224.5560097 , -212.1553567 , -199.7377935 , -187.2726883 ,
       -174.6984252 , -161.9494881 , -148.9717624 , -135.713092  ,
       -122.1217412 , -108.1420464 ,  -93.73510623,  -78.84428623,
```

```
        -63.42807112,  -47.43329487,  -30.81567063,  -13.51204711,
          4.54053052,   23.40647485,   43.16914297,   63.90838459,
         85.71910494,  108.7052736 ,  132.9804775 ,  158.6623502 ,
        185.8975716 ,  214.8221804 ,  245.5914729 ,  278.3470998 ,
        313.2465145 ,  350.4367008 ,  390.0745476 ,  432.3093648 ,
        477.289738  ,  525.1645427 ,  576.0847044 ,  630.1851331 ,
        687.5624456 ,  748.2092797 ,  812.1688823 ,  879.4838838 ,
        950.1524422 , 1024.128086  , 1101.291299  , 1183.35617   ,
       1266.567567  , 1352.461124  , 1440.823115  , 1531.24652   ,
       1608.135365  ])


Speed_Unstable = np.array([0.        , 0.        , 0.   , 0.  , 0.,
       0.        , 0.        , 0.        , 0.        , 0.        ,
       0.        , 0.00022099, 0.00052762, 0.00100503, 0.00149968,
       0.00200755, 0.00252326, 0.00304438, 0.00357127, 0.00410112,
       0.00463337, 0.00516908, 0.00570426, 0.00624055, 0.0067775 ,
       0.00731413, 0.00784946, 0.00838385, 0.00891588, 0.00944624,
       0.00997534, 0.01041333, 0.01049834, 0.0105957 , 0.01071058,
       0.01078462, 0.0108222 , 0.01082907, 0.01080744, 0.0107624 ,
       0.01069801, 0.010616  , 0.01051946, 0.01041211, 0.01029624,
       0.01017528, 0.0100503 , 0.00992456, 0.00979829, 0.0096746 ,
       0.00955474, 0.00943738, 0.0093257 , 0.00921878, 0.00911577,
       0.00901802, 0.00892513, 0.00883743, 0.00875321, 0.0086727 ,
       0.00859772, 0.00852581, 0.00845715, 0.00839226, 0.00833064,
       0.00827335, 0.00821889, 0.00816789, 0.00812052, 0.00807538,
       0.00803412, 0.0079966 , 0.00796208, 0.00793128, 0.00790387,
       0.00788007, 0.0078601 , 0.00784366, 0.00783149, 0.00782412,
       0.00782163, 0.00782223, 0.00782879, 0.00784104, 0.00785825,
       0.00788027, 0.00790909, 0.00794433, 0.00798682, 0.00803588,
       0.00809335, 0.00815923, 0.0082341 , 0.00831773, 0.00841322,
       0.00851814, 0.00863549, 0.00876602, 0.00890902, 0.00906738,
       0.00924024, 0.00943006, 0.00963647, 0.00986124, 0.01010574,
       0.01036908, 0.01065433, 0.01096167, 0.01129201, 0.01164636,
       0.01202517, 0.01242891, 0.01278601])


# Creating the DataFrame
df = pd.DataFrame({
    "Time": Time_array_u,
    "Delta_Unstable": Delta_Unstable,
    "Pa_Unstable": Pa_Unstable,
    "Speed_Unstable": Speed_Unstable
})




# Step 1: Find the maximum value in 'all_calculations' that is <= 0.2
closest_value_to_02 = Time_array_u[Time_array_u <= 0.2].max()


# Step 2: Find the index of this closest value
time_index_closest = np.where(Time_array_u == closest_value_to_02)[0][0]

#time_index_closest = 0

print(f"Index closest to 0.2 without going over: {time_index_closest}")

# Step 3: Define the number of steps forward you want to analyze
num_steps = 20 # Change this to the number of steps you're interested in

# Generate indexes for the next 'num_steps' measurements
#after the closest value to 0.2
```

```
indexes_to_extract = [time_index_closest + i for i in range(1, num_steps + 1)]


print(f"First 10 indexes to extract: {indexes_to_extract[:10]}")



# Initialize arrays to store the results
Pa_array_u = np.zeros(len(indexes_to_extract))
delta_omib_array_u = np.zeros(len(indexes_to_extract))
speed_omib_array_u = np.zeros(len(indexes_to_extract))
time_array_u = np.zeros(len(indexes_to_extract))
rotor_energy_u = np.zeros(len(indexes_to_extract))

M = 101.253951
wb = 2*np.pi*60



for i, index in enumerate(indexes_to_extract):
    if index < len(Time_array_u):  # Ensure index does not exceed array bounds
        Pa_array_u[i] = Pa_Unstable[index]
        delta_omib_array_u[i] = Delta_Unstable[index]
        time_array_u[i] = Time_array_u[index]
        speed_omib_array_u[i] = Speed_Unstable[index]*wb
        rotor_energy_u[i] = (1/2)*M*(Speed_Unstable[index]*wb)**2


# Output example
print(f"First 10 indexes to extract: {indexes_to_extract[:10]}")
print(f"Extracted time values from unstable case : {time_array_u[:10]}")


plt.figure(figsize=(10, 6))  # Set the figure size
plt.plot(delta_omib_array_u, -Pa_array_u, color='blue', linestyle='-',
         linewidth=2, marker='o', markersize=5, label='Delta vs. -Pa')
# Adding a horizontal line at Pa = 0
plt.axhline(y=0, color='r', linestyle='-', label='Pa = 0 Line')
# Adding labels and title
plt.xlabel('Delta Omib', fontsize=14)
plt.ylabel('-Pa Omib', fontsize=14)
plt.title('Unstable: Delta Omib vs. -Pa Plot', fontsize=16)

# Adding grid
plt.grid(True)

# Adding a legend
plt.legend(fontsize=12)

# Show the plot
plt.show()


plt.figure(figsize=(10, 6))  # Set the figure size
plt.plot(time_array_u, speed_omib_array_u, color='blue', linestyle='-',
         linewidth=2, marker='o', markersize=5,
         label='Unstable: Time vs. Speed')
# Adding a horizontal line at Pa = 0
# Adding labels and title
plt.xlabel('Time', fontsize=14)
plt.ylabel('Speed', fontsize=14)
plt.title('Unstable: Time vs. Speed', fontsize=16)

# Adding grid
```

```
plt.grid(True)

# Adding a legend
plt.legend(fontsize=12)

# Show the plot
plt.show()


plt.figure(figsize=(10, 6))  # Set the figure size
plt.plot(time_array_u, delta_omib_array_u, color='blue', linestyle='-',
         linewidth=2, marker='o', markersize=5,
         label='Unstable: Time vs. Rotor angle')
# Adding a horizontal line at Pa = 0
# Adding labels and title
plt.xlabel('Time', fontsize=14)
plt.ylabel('Rotor angle', fontsize=14)
plt.title('Unstable: Time vs. Rotor angle', fontsize=16)

# Adding grid
plt.grid(True)

# Adding a legend
plt.legend(fontsize=12)

# Show the plot
plt.show()

#%% Stable case in 10 generator case with 0.18 s CT


Time_array_s = np.array([-0.1     , -0.09    , -0.08    , -0.07    , -0.06    , -0.05    ,
       -0.04    , -0.03    , -0.02    , -0.01    ,  0.      ,  0.005   ,
        0.011667,  0.021667,  0.031667,  0.041667,  0.051667,  0.061667,
        0.071667,  0.081667,  0.091667,  0.101667,  0.111667,  0.121667,
        0.131667,  0.141667,  0.151667,  0.161667,  0.171667,  0.18    ,
        0.185   ,  0.191667,  0.201667,  0.211667,  0.221667,  0.231667,
        0.241667,  0.251667,  0.261667,  0.271667,  0.281667,  0.291667,
        0.301667,  0.311667,  0.321667,  0.331667,  0.341667,  0.351667,
        0.361667,  0.371667,  0.381667,  0.391667,  0.401667,  0.411667,
        0.421667,  0.431667,  0.441667,  0.451667,  0.461667,  0.471667,
        0.481667,  0.491667,  0.501667,  0.511667,  0.521667,  0.531667,
        0.541667,  0.551667,  0.561667,  0.571667,  0.581667,  0.591667,
        0.601667,  0.611667,  0.621667,  0.631667,  0.641667,  0.651667,
        0.661667,  0.671667,  0.681667,  0.691667,  0.701667,  0.711667,
        0.721667,  0.731667,  0.741667,  0.751667,  0.761667,  0.771667,
        0.781667,  0.791667,  0.801667,  0.811667,  0.821667,  0.831667,
        0.841667,  0.851667,  0.861667,  0.871667,  0.881667,  0.891667,
        0.901667,  0.911667,  0.921667,  0.931667,  0.941667,  0.951667,
        0.961667,  0.971667,  0.981667,  0.991667,  1.      ])


Delta_Stable = np.array([ 46.4496057,  46.4496057,  46.4496057,  46.4496057,  46.4496057,
        46.4496057,  46.4496057,  46.4496057,  46.4496057,  46.4496057,
        46.4496057,  46.4735224,  46.5385051,  46.7040147,  46.9745375,
        47.3533378,  47.8425496,  48.4437609,  49.1581786,  49.9864487,
        50.9293004,  51.9875368,  53.1614885,  54.4513451,  55.8571692,
        57.3789148,  59.016431 ,  60.7694844,  62.6377598,  64.2903569,
        65.3106328,  66.6821248,  68.758437 ,  70.8573804,  72.9706682,
        75.0909631,  77.2117323,  79.3271338,  81.4320388,  83.5219976,
        85.5931515,  87.6421959,  89.6669998,  91.664606 ,  93.6324696,
        95.5697279,  97.4752197,  99.3480901, 101.18777  , 102.99393  ,
       104.766437 , 106.505302 , 108.21063  , 109.882591 , 111.521378 ,
       113.127191 , 114.700211 , 116.240594 , 117.748456 , 119.223876 ,
```

```
       120.666885 , 122.077476 , 123.455591 , 124.801141 , 126.11399  ,
       127.393972 , 128.640884 , 129.854499 , 131.034555 , 132.180769 ,
       133.292837 , 134.370345 , 135.412957 , 136.420406 , 137.392318 ,
       138.328307 , 139.227979 , 140.090931 , 140.916752 , 141.705027 ,
       142.455338 , 143.167264 , 143.840384 , 144.474277 , 145.068524 ,
       145.612524 , 146.116133 , 146.579457 , 147.001533 , 147.382644 ,
       147.721705 , 148.019147 , 148.266204 , 148.471245 , 148.633853 ,
       148.753681 , 148.830425 , 148.863781 , 148.853449 , 148.799128 ,
       148.702947 , 148.563746 , 148.377934 , 148.14518  , 147.865116 ,
       147.53737  , 147.161558 , 146.73729  , 146.264157 , 145.741741 ,
       145.169603 , 144.547284 , 143.986467 ])

Pa_Stable = np.array([   0.        ,    0.        ,    0.        ,    0.        ,
          0.        ,    0.        ,    0.        ,    0.        ,
          0.        ,    0.        ,    0.        , 1544.740435  ,
       1605.376075  , 1669.51429   , 1711.051458  , 1741.016372  ,
       1764.132873  , 1781.863786  , 1795.634887  , 1806.15293   ,
       1813.88071   , 1819.147133  , 1822.209014  , 1823.291802  ,
       1822.592487  , 1820.297194  , 1816.576135  , 1811.595791  ,
       1805.515348  , 1799.716922  ,  595.7675505 ,  502.2085021 ,
        365.2934514 ,  238.1285034 ,  121.6594904 ,   16.14906291,
        -78.47204746, -162.5155433 , -236.3488125 , -300.5610567 ,
       -355.7275721 , -402.5297859 , -441.2549449 , -473.8815635 ,
       -499.7870798 , -520.1489376 , -535.3898043 , -545.9441767 ,
       -552.4256797 , -555.7030609 , -556.5945325 , -555.8004672 ,
       -553.9542544 , -551.5750454 , -549.0489934 , -546.666786  ,
       -544.6242126 , -543.0571232 , -542.0408784 , -541.6147983 ,
       -541.7877075 , -542.5484332 , -543.8707969 , -545.7223914 ,
       -548.0709921 , -550.8761761 , -554.1079376 , -557.7338143 ,
       -561.7285552 , -566.0634409 , -570.7103299 , -575.6743199 ,
       -580.9087681 , -586.3875827 , -592.0985438 , -598.0212602 ,
       -604.146494  , -610.4574667 , -616.9471999 , -623.6007934 ,
       -630.4101264 , -637.3688901 , -644.4619878 , -651.6912426 ,
       -659.0461163 , -666.0831911 , -674.2967246 , -681.604315  ,
       -690.0286054 , -697.590714  , -706.2006197 , -714.0145066 ,
       -722.5313339 , -731.1830404 , -739.9352809 , -748.8254826 ,
       -757.8546441 , -767.0227492 , -776.3295741 , -785.7726211 ,
       -795.6133092 , -805.3210453 , -815.1960445 , -825.2484222 ,
       -835.4931287 , -845.9493714 , -856.630748  , -867.5488591 ,
       -878.7192082 , -890.1588478 , -901.877882  , -913.8979493 ,
       -924.0609541 ])

Speed_Stable = np.array([ 0.000000e+00,  0.000000e+00,  0.000000e+00,  0.000000e+00,
        0.000000e+00,  0.000000e+00,  0.000000e+00,  0.000000e+00,
        0.000000e+00,  0.000000e+00,  0.000000e+00,  2.209890e-04,
        5.276220e-04,  1.005026e-03,  1.499684e-03,  2.007555e-03,
        2.523260e-03,  3.044383e-03,  3.571267e-03,  4.101120e-03,
        4.633370e-03,  5.169079e-03,  5.704259e-03,  6.240545e-03,
        6.777500e-03,  7.314125e-03,  7.849464e-03,  8.383848e-03,
        8.915882e-03,  9.357568e-03,  9.447082e-03,  9.549736e-03,
        9.675093e-03,  9.759619e-03,  9.808410e-03,  9.824726e-03,
        9.811980e-03,  9.774665e-03,  9.715135e-03,  9.636389e-03,
        9.541917e-03,  9.432117e-03,  9.310132e-03,  9.180446e-03,
        9.041489e-03,  8.896442e-03,  8.747562e-03,  8.593918e-03,
        8.439263e-03,  8.284507e-03,  8.128558e-03,  7.972028e-03,
        7.817522e-03,  7.663254e-03,  7.510692e-03,  7.358403e-03,
        7.206452e-03,  7.056207e-03,  6.905899e-03,  6.755562e-03,
        6.605126e-03,  6.455049e-03,  6.304553e-03,  6.154063e-03,
        6.002489e-03,  5.849519e-03,  5.696303e-03,  5.541194e-03,
        5.385319e-03,  5.227475e-03,  5.068312e-03,  4.908144e-03,
        4.746389e-03,  4.582872e-03,  4.417636e-03,  4.250484e-03,
        4.080598e-03,  3.909500e-03,  3.736524e-03,  3.562218e-03,
        3.385666e-03,  3.206868e-03,  3.025630e-03,  2.843093e-03,
        2.658174e-03,  2.472207e-03,  2.283355e-03,  2.093546e-03,
```

```
        1.901608e-03,  1.708047e-03,  1.511824e-03,  1.314227e-03,
        1.115219e-03,  9.144720e-04,  7.121220e-04,  5.075680e-04,
        3.013910e-04,  9.374410e-05, -1.155550e-04, -3.267910e-04,
       -5.403720e-04, -7.553040e-04, -9.714750e-04, -1.190392e-03,
       -1.410435e-03, -1.632241e-03, -1.855411e-03, -2.081169e-03,
       -2.308522e-03, -2.537370e-03, -2.768362e-03, -3.002111e-03,
       -3.198814e-03])


# Creating the DataFrame
df = pd.DataFrame({
    "Time": Time_array_s,
    "Delta_Stable": Delta_Stable,
    "Pa_Stable": Pa_Stable,
    "Speed_Stable": Speed_Stable
})



# Step 1: Find the maximum value in 'all_calculations' that is <= 0.18
closest_value_to_018 = Time_array_s[Time_array_s <= 0.18].max()


# Step 2: Find the index of this closest value
time_index_closest = np.where(Time_array_s == closest_value_to_018)[0][0]


print(f"Index closest to 0.18 without going over: {time_index_closest}")

# Step 3: Define the number of steps forward you want to analyze
num_steps = 46 # Change this to the number of steps you're interested in

# Generate indexes for the next 'num_steps' measurements
# after the closest value to 0.18
indexes_to_extract = [time_index_closest + i for i in range(1, num_steps + 1)]


print(f"First 10 indexes to extract: {indexes_to_extract[:10]}")

wb = 2*np.pi*60

# Initialize arrays to store the results
Pa_array_s = np.zeros(len(indexes_to_extract))
delta_omib_array_s = np.zeros(len(indexes_to_extract))
speed_omib_array_s = np.zeros(len(indexes_to_extract))
time_array_s = np.zeros(len(indexes_to_extract))


for i, index in enumerate(indexes_to_extract):
    if index < len(Time_array_s):  # Ensure index does not exceed array bounds
        Pa_array_s[i] = Pa_Stable[index]
        delta_omib_array_s[i] = Delta_Stable[index]
        time_array_s[i] = Time_array_s[index]
        speed_omib_array_s[i] = Speed_Stable[index]*wb


# Output example
print(f"First 10 indexes to extract: {indexes_to_extract[:10]}")
print(f"Extracted time values from stable case: {time_array_s[:10]}")


# Creating the plot with enhancements
plt.figure(figsize=(10, 6))  # Set the figure size
# Plotting for "_s" with green markers and black line
```

```
plt.plot(delta_omib_array_s, -Pa_array_s, color='black', linestyle='-',
         linewidth=2, marker='o', markersize=5, markerfacecolor='green',
         markeredgewidth=1, markeredgecolor='black',
         label='Delta vs. -Pa (stable)')
# Adding a horizontal line at Pa = 0
plt.axhline(y=0, color='r', linestyle='-', label='Pa = 0 Line')
# Adding labels and title
plt.xlabel('Delta Omib', fontsize=14)
plt.ylabel('-Pa ', fontsize=14)
plt.title('Stable: Delta Omib vs. -Pa Plot', fontsize=16)

# Adding grid
plt.grid(True)

# Adding a legend
plt.legend(fontsize=12)

# Show the plot
plt.show()


plt.figure(figsize=(10, 6))  # Set the figure size
plt.plot(time_array_s, speed_omib_array_s, color='blue', linestyle='-',
         linewidth=2, marker='o', markersize=5, label='Delta vs. -Pa')
# Adding a horizontal line at Pa = 0
# Adding labels and title
plt.xlabel('Time', fontsize=14)
plt.ylabel('Speed', fontsize=14)
plt.title('Stable: Time vs. Speed', fontsize=16)
plt.grid(True)
plt.legend(fontsize=12)
plt.show()



plt.figure(figsize=(10, 6))  # Set the figure size
plt.plot(time_array_s, delta_omib_array_s, color='blue', linestyle='-',
         linewidth=2, marker='o', markersize=5, label='Delta vs. -Pa')
# Adding a horizontal line at Pa = 0
# Adding labels and title
plt.xlabel('Time', fontsize=14)
plt.ylabel('Rotor angle', fontsize=14)
plt.title('Stable: Time vs. Rotor angle', fontsize=16)

# Adding grid
plt.grid(True)

# Adding a legend
plt.legend(fontsize=12)

# Show the plot
plt.show()
```

Appendix B

Extra 3D plot for the 9 bus system and calculation of inertia constant M

B.1 Data for calculation M and calculated values for M

The table for the generator data and the calculated values for M is presented in Table C.1. The formula used for the calculation of M was 2.3.

Table B.1: 9 bus system generator data and calculated M.

Generator Unit No.	Sr in MVA	Pr in MW	H in s	M
1	247.5	247.5	9.551	12.541
2	192.0	163,2	3.922	3.395
3	128.0	108.8	2.767	1.597

B.2 Extra 3D plot

An extra plot to show how the ω is related to δ and P_a a 3D plot is included in Figure B.1. Here only the case of CT is equal to 0.245s and 0.260s. Here it is seen that the difference in area between the A_{cc} is directly connected to how much the ω has increased.

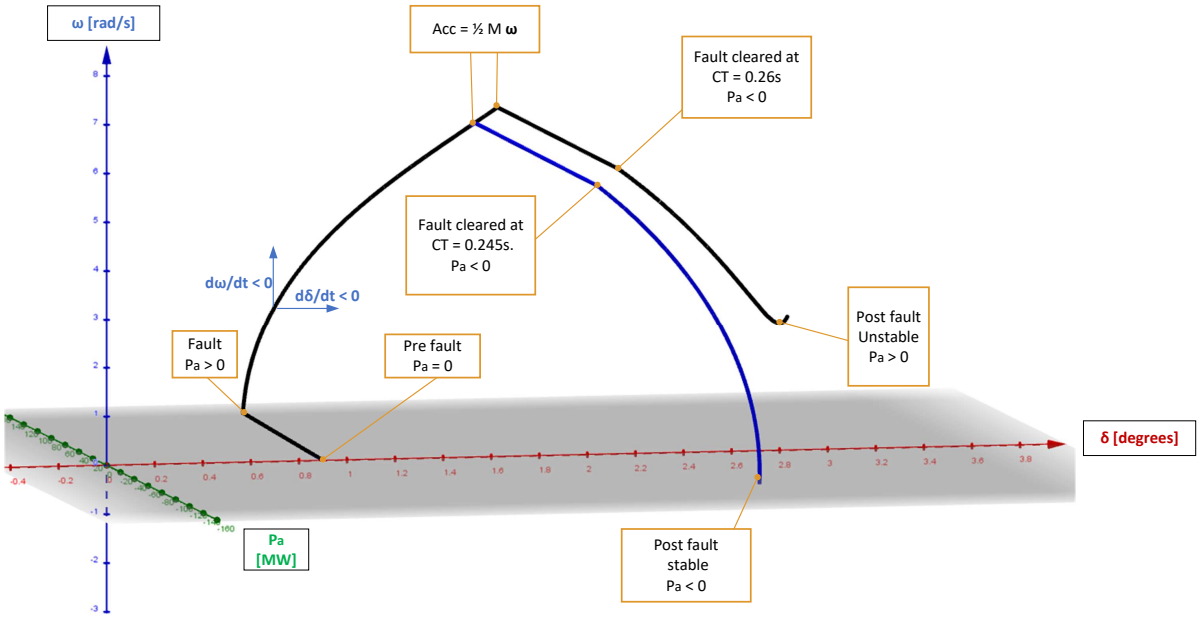

Figure B.1: Plot of δ, P_a and ω for CT equal to 0.245 s and 0.260 s.

Appendix C

Results for SIME Calculation of the 39 bus system

C.1 Data for calculation M and calculated values for M

The table for the generator data and the calculated values for M is presented in Table C.1. Where it is worth noting the multiplication of generator unit nr.5 S_r and H is because it is two parallel machines. The formula used for the calculation of M was 2.3.

Table C.1: 39 bus system generator data and calculated M.

Unit No.	**Sr in MVA**	**Pr in MW**	**H in s**	M
1	10000	8500	5.000	265.258
2	700	595	4.329	16.0762
3	800	680	4.475	18.992
4	800	680	3.575	15.173
5	300x2	255x2	4.333x2	27.585
6	800	680	4.350	18.462
7	700	595	3.771	14.004
8	700	595	3.471	12.890
9	1000	850	3.450	18.303
10	1000	850	4.200	22.282

C.2 Stable case numerical results

Numerical results for the stable case where the fault is on Bus 16, 50% with CT of 0.18 s is displayed in Figure C.1.

Time in s	SpeedC	SpeedN	Speed in p.u.	Speed in rad/s	DeltaC	DeltaN	Delta	Delta rad	PM_C	PM_N	PM	Pelec_C	Pelec_N	Pelec	Pa
-0,1	0	0	0	0	46,39546368	-0,054142	46,44960568	0,810698555	31,39106017	3,769909299	2796,750657	31,39106017	3,769909299	2796,750657	0
-0,09	0	0	0	0	46,39546368	-0,054142	46,44960568	0,810698555	31,39106017	3,769909299	2796,750657	31,39106017	3,769909299	2796,750657	0
-0,08	0	0	0	0	46,39546368	-0,054142	46,44960568	0,810698555	31,39106017	3,769909299	2796,750657	31,39106017	3,769909299	2796,750657	0
-0,07	0	0	0	0	46,39546368	-0,054142	46,44960568	0,810698555	31,39106017	3,769909299	2796,750657	31,39106017	3,769909299	2796,750657	0
-0,06	0	0	0	0	46,39546368	-0,054142	46,44960568	0,810698555	31,39106017	3,769909299	2796,750657	31,39106017	3,769909299	2796,750657	0
-0,05	0	0	0	0	46,39546368	-0,054142	46,44960568	0,810698555	31,39106017	3,769909299	2796,750657	31,39106017	3,769909299	2796,750657	0
-0,04	0	0	0	0	46,39546368	-0,054142	46,44960568	0,810698555	31,39106017	3,769909299	2796,750657	31,39106017	3,769909299	2796,750657	0
-0,03	0	0	0	0	46,39546368	-0,054142	46,44960568	0,810698555	31,39106017	3,769909299	2796,750657	31,39106017	3,769909299	2796,750657	0
-0,02	0	0	0	0	46,39546368	-0,054142	46,44960568	0,810698555	31,39106017	3,769909299	2796,750657	31,39106017	3,769909299	2796,750657	0
-0,01	0	0	0	0	46,39546368	-0,054142	46,44960568	0,810698555	31,39106017	3,769909299	2796,750657	31,39106017	3,769909299	2796,750657	0
0	0	0	0	0	46,39546368	-0,054142	46,44960568	0,810698555	31,39106017	3,769909299	2796,750657	31,39106017	3,769909299	2796,750657	0
0,005	0,000206989	-1,4E-05	0,000220989	0,083310923	46,4049934	-0,068529	46,4735224	0,811115981	31,39104979	3,769909299	2796,749606	17,22547921	4,860439047	1252,009171	1544,740435
0,011667	0,000495622	-3,2E-05	0,000527622	0,198908623	45,46868711	-1,069818	46,53850511	0,812250143	31,39103422	3,769909299	2796,74803	16,5043677	4,738190253	1191,371955	1605,376075
0,021667	0,000949026	-5,6E-05	0,001005026	0,378885704	43,96223273	-2,741782	46,70401473	0,815138831	31,39097142	3,769909299	2796,741671	15,7099716	4,577296098	1127,22738	1669,51429
0,031667	0,001426684	-7,5E-05	0,001499684	0,565367724	42,35403947	-4,620498	46,97453747	0,819860343	31,39083439	3,769909299	2796,727796	15,16425207	4,441941207	1085,676339	1711,051458
0,041667	0,001915555	-9,2E-05	0,002007555	0,75683056	41,53002684	-5,823311	47,35333784	0,826471657	31,39060446	3,769909299	2796,704515	14,74788595	4,321743244	1055,688143	1741,016372
0,051667	0,00241826	-0,000105	0,00252326	0,951246501	41,14440958	-6,69814	47,84254958	0,835010013	31,39028889	3,769909299	2796,672562	14,41134315	4,213818226	1032,53969	1764,132873
0,061667	0,002929383	-0,000115	0,003044383	1,147705535	41,03357995	-7,410181	48,44376095	0,845503131	31,38985342	3,769909299	2796,628469	14,1315865	4,109610341	1014,764683	1781,863786
0,071667	0,003448267	-0,000123	0,003571267	1,346336006	41,06738963	-8,090789	49,15817863	0,857972071	31,3893074	3,769909299	2796,573183	13,89531323	4,009888651	1000,938296	1795,634887
0,081667	0,00397312	-0,000128	0,00410112	1,546085842	41,21920565	-8,767243	49,98644865	0,87242811	31,38862903	3,769909299	2796,504495	13,69427177	3,913403429	990,3515644	1806,15293
0,091667	0,00450337	-0,00013	0,00463337	1,746739367	41,46280042	-9,4665	50,92930042	0,888883978	31,38782661	3,769909299	2796,423246	13,52303464	3,819289481	982,5425366	1813,88071
0,101667	0,005038079	-0,000131	0,005169079	1,948696802	41,78493581	-10,202601	51,98753681	0,907353687	31,38688301	3,769909299	2796,327703	13,37766341	3,726873878	977,1805701	1819,147133
0,111667	0,005576259	-0,000128	0,005704259	2,150454928	42,17963945	-10,981849	53,16148845	0,927843009	31,38578785	3,769909299	2796,216814	13,25516276	3,635708001	974,0078006	1822,209014
0,121667	0,006117545	-0,000123	0,006240545	2,352629859	42,6443001	-11,807045	54,4513451	0,950355254	31,38454893	3,769909299	2796,091368	13,15296141	3,545439363	972,7995665	1823,291802
0,131667	0,0066615	-0,000116	0,0067775	2,555057228	43,17779222	-12,679377	55,85716922	0,974891514	31,38314962	3,769909299	2795,949683	13,06880884	3,455779565	973,3571954	1822,592487
0,141667	0,007207125	-0,000107	0,007314125	2,75736016	43,79757078	-13,599344	57,37891478	1,001450984	31,38158318	3,769909299	2795,791075	13,00066786	3,366536342	975,4938808	1820,297194
0,151667	0,007754464	-9,5E-05	0,007849464	2,959178145	44,44924102	-14,56719	59,01643102	1,030031034	31,37986882	3,769909299	2795,617489	12,94665231	3,277485385	979,041354	1816,576135
0,161667	0,008302848	-8,1E-05	0,008383848	3,160636371	45,18635837	-15,583126	60,76948437	1,060627587	31,37797332	3,769909299	2795,425562	12,90498865	3,188530561	983,8297719	1811,595791
0,171667	0,008851882	-6,4E-05	0,008915882	3,36120849	45,99036684	-16,647393	62,63775984	1,093235145	31,37593353	3,769909299	2795,219025	12,87401341	3,099543693	989,7036775	1805,515348
0,18	0,009309568	-4,8E-05	0,009357568	3,527719885	46,71259594	-17,577761	64,29035694	1,122078406	31,37408319	3,769909299	2795,031671	12,8552468	3,025361265	995,3147488	1799,716922
0,185	0,009443082	-4E-06	0,009447082	3,561466036	47,15897375	-18,151659	65,31063275	1,139885578	31,37292056	3,769909299	2794,91395	22,1398258	0,420708893	2199,146399	595,7675505
0,191667	0,009606736	5,7E-05	0,009549736	3,600165646	44,43664582	-22,245479	66,68212482	1,16382263	31,3713671	3,769909299	2794,756656	22,97844852	0,336881148	2292,548154	502,2085021
0,201667	0,009824093	0,000149	0,009675093	3,647423992	46,10869498	-22,649742	68,75843698	1,200061114	31,36906779	3,769909299	2794,523842	24,21731055	0,225847839	2429,230391	365,2934514
0,211667	0,010003619	0,000244	0,009759619	3,67928987	47,87644435	-22,980936	70,85738035	1,236694586	31,36683284	3,769909299	2794,297545	25,3841368	0,13900793S	2556,169041	238,1285034
0,221667	0,01014941	0,000341	0,00980841	3,69768361	49,36905021	-23,601618	72,97066821	1,273578418	31,36474115	3,769909299	2794,085752	26,46091688	0,067613357	2672,426262	121,6594904
0,231667	0,010264726	0,00044	0,009824726	3,703834469	50,69656006	-24,394403	75,09096306	1,310584544	31,3628036	3,769909299	2793,889569	27,44019699	0,00679338	2777,74506	16,14906291
0,241667	0,01035298	0,000541	0,00981198	3,699029483	51,9179953	-25,293737	77,2117323	1,34759895	31,3610088	3,769909299	2793,707837	28,31995811	-0,046143713	2872,179884	-78,47204746
0,251667	0,010417665	0,000643	0,009774665	3,684961855	53,06547978	-26,261654	79,32713378	1,384519671	31,35939253	3,769909299	2793,544184	29,10148794	-0,093024443	2956,059727	-162,5155433
0,261667	0,010461135	0,000746	0,009715135	3,662519515	54,15636881	-27,27567	81,43203881	1,421257194	31,35790447	3,769909299	2793,393512	29,78746729	-0,134746051	3029,742324	-236,3488125
0,271667	0,010486389	0,00085	0,009636389	3,632832935	55,19993763	-28,32206	83,52199763	1,457733857	31,35654357	3,769909299	2793,255716	30,38265671	-0,172365994	3093,816772	-300,5610567
0,281667	0,010495917	0,000954	0,009541917	3,597217966	56,2011535	-29,391998	85,5931515	1,493882311	31,35526883	3,769909299	2793,126643	30,89205602	-0,206525159	3148,854215	-355,7275721
0,291667	0,010492117	0,00106	0,009432117	3,55582431	57,16190586	-30,48029	87,64219586	1,529644881	31,35405119	3,769909299	2793,003352	31,22166106	-0,23792852	3195,533137	-402,5297859
0,301667	0,010477132	0,001167	0,009310132	3,509836921	58,08321276	-31,583787	89,66699976	1,564984376	31,35286364	3,769909299	2792,883108	31,67498672	-0,265871101	3234,138053	-441,2549449
0,311667	0,010454446	0,001274	0,009180446	3,46094643	58,96235804	-32,702248	91,66460604	1,599849183	31,35167506	3,769909299	2792,76276	31,96679942	-0,295095453	3266,644323	-473,8815635
0,321667	0,010423489	0,001382	0,009041489	3,408561148	59,80732157	-33,825148	93,63246957	1,634194881	31,35030638	3,769909299	2792,624175	32,1945528	-0,321820353	3292,411255	-499,7870798
0,331667	0,010387442	0,001491	0,008896442	3,353879697	60,60886291	-34,960865	95,56972791	1,668006417	31,3485396	3,769909299	2792,445281	32,36751053	-0,348192767	3312,594219	-520,1489376
0,341667	0,010347562	0,0016	0,008747562	3,297753137	61,36906272	-36,106157	97,47521972	1,701263523	31,34631243	3,769909299	2792,219772	32,48850287	-0,375494464	3327,609577	-535,3898043
0,351667	0,010304918	0,001711	0,008593918	3,239830731	62,08433811	-37,263752	99,34809011	1,733951278	31,3436415	3,769909299	2791,94933	32,56081219	-0,404750859	3337,893506	-545,9441767
0,361667	0,010261263	0,001822	0,008439263	3,181527015	62,75142772	-38,436342	101,1877697	1,766059744	31,34055327	3,769909299	2791,636634	32,58869869	-0,437788476	3344,062314	-552,4256797
0,371667	0,010217507	0,001933	0,008284507	3,12318563E	63,3648555	-39,629075	102,9939305	1,797583197	31,33707213	3,769909299	2791,284155	32,57961305	-0,475760907	3346,987215	-555,7030609
0,381667	0,010174558	0,002046	0,008128558	3,064394066	63,92160149	-40,844836	104,7664375	1,8285192S	31,33321417	3,769909299	2790,893521	32,54165216	-0,518668151	3347,488054	-556,5945325
0,391667	0,010133028	0,002161	0,007972028	3,005383718	64,42245061	-42,082851	106,5053016	1,858866184	31,32901313	3,769909299	2790,46815	32,48173471	-0,566542253	3346,268617	-555,8004672
0,401667	0,010093522	0,002276	0,007817522	2,94713647	64,86844787	-43,342182	108,2106299	1,888631777	31,32447836	3,769909299	2790,008986	32,40663819	-0,618870505	3343,96324	-553,9542544
0,411667	0,010056254	0,002393	0,007663254	2,88897882	65,26192469	-44,620666	109,8825907	1,917812998	31,31963009	3,769909299	2789,51808	32,32205483	-0,675108155	3341,093125	-551,5750454
0,421667	0,010021692	0,002511	0,007510692	2,831464134	65,6055138	-45,915864	111,5213778	1,946415229	31,31449584	3,769909299	2788,998216	32,23253082	-0,73455023	3338,047209	-549,0489934
0,431667	0,009989403	0,002631	0,007358403	2,774052758	65,90197369	-47,225217	113,1271907	1,974441951	31,30907404	3,769909299	2788,449238	32,14157635	-0,796555844	3335,116024	-546,666786
0,441667	0,009959452	0,002753	0,007206452	2,716768514	66,15402906	-48,546182	114,7002111	2,001896336	31,30340622	3,769909299	2787,875349	32,05183953	-0,860452069	3332,499561	-544,6242126
0,451667	0,009932207	0,002876	0,007056207	2,660127456	66,36422065	-49,876373	116,2405937	2,028781084	31,29747525	3,769909299	2787,274815	31,96525374	-0,925630063	3330,331938	-543,0571232
0,461667	0,009906899	0,003001	0,006905899	2,603462666	66,5349272	-51,213529	117,7484562	2,05509825	31,29130917	3,769909299	2786,650474	31,88320014	-0,991480987	3328,691353	-542,0408784
0,471667	0,009883562	0,003128	0,006755562	2,546786861	66,66832174	-52,555554	119,2238757	2,080849179	31,28493443	3,769909299	2786,005007	31,80660622	-1,057492131	3327,619805	-541,6147983
0,481667	0,009862126	0,003257	0,006605126	2,490073899	66,76634524	-53,90054	120,6668852	2,106034445	31,27834481	3,769909299	2785,337782	31,73603358	-1,123182834	3327,125489	-541,7877075
0,491667	0,009842049	0,003387	0,006455049	2,433496228	66,83071551	-55,24676	122,0774755	2,13065389	31,27154914	3,769909299	2784,649693	31,67179727	-1,188136519	3327,198126	-542,5484332
0,501667	0,009823553	0,003519	0,006304553	2,376760503	66,86293993	-56,592651	123,4555909	2,154706542	31,26457232	3,769909299	2783,943263	31,61401615	-1,252000699	3327,81406	-543,8707969
0,511667	0,009806063	0,003652	0,006154063	2,320027085	66,86433471	-57,936806	124,8011407	2,178190816	31,25741904	3,769909299	2783,218965	31,56266322	-1,314486977	3328,941356	-545,7223914
0,521667	0,009789489	0,003787	0,006002489	2,262884905	66,83604985	-59,27794	126,1139899	2,201104356	31,25008773	3,769909299	2782,476641	31,517643	-1,375371043	3330,547633	-548,0709921
0,531667	0,009773519	0,003924	0,005849519	2,205216726	66,7790839	-60,614888	127,3939719	2,223444257	31,24258513	3,769909299	2781,716973	31,4787873	-1,434428586	3332,593149	-550,8761761
0,541667	0,009758303	0,004062	0,005696303	2,147455601	66,6943173	-61,946567	128,6408843	2,245206984	31,23485417	3,769909299	2780,934182	31,44587088	-1,491531431	3335,04212	-554,1079376
0,551667	0,009743194	0,004202	0,005541194	2,088980784	66,58252452	-63,271974	129,8544985	2,266388548	31,22684137	3,769909299	2780,122855	31,41867988	-1,546519355	3337,856669	-557,7338143
0,561667	0,009728319	0,004343	0,005385319	2,03021762	66,44439882	-64,590156	131,0345548	2,286984416	31,21848705	3,769909299	2779,276947	31,39696934	-1,599328271	3341,005502	-561,7285552
0,571667	0,009713475	0,004486	0,005227475	1,970711576	66,28056575	-65,900203	132,1807688	2,306989623	31,20978705	3,769909299	2778,396038	31,38051554	-1,64989409	3344,459479	-566,0634409
0,581667	0,009698312	0,00463	0,005068312	1,910708491	66,09159665	-67,20124	133,2928367	2,326398869	31,20069103	3,769909299	2777,47503	31,36905429	-1,698152723	3348,18536	-570,7103299
0,591667	0,009683144	0,004775	0,004908144	1,850326693	65,87799275	-68,492352	134,3703448	2,345204933	31,19120314	3,769909299	2776,514344	31,36264011	-1,74410417	3352,188664	-575,6743199
0,601667	0,009667389	0,004921	0,004746389	1,789346493	65,63896275	-69,773994	135,4129568	2,363401945	31,18129173	3,769909299	2775,510774	31,36071658	-1,787812521	3356,419542	-580,9087681
0,611667	0,009650872	0,005068	0,004582872	1,727701944	65,37806174	-71,042344	136,4204057	2,380985247	31,17097703	3,769909299	2774,46637	31,36311035	-1,829213685	3360,853952	-586,3875827
0,621667	0,009633636	0,005216	0,004417636	1,665409528	65,09395194	-72,298866	137,3923179	2,397483115	31,16025229	3,769909299	2773,380448	31,3696299	-1,868371753	3365,478991	-592,0985438
0,631667	0,009615484	0,005365	0,004250484	1,60239476	64,78711682	-73,54119	138,3283068	2,414284403	31,14912998	3,769909299	2772,254269	31,3800863	-1,905286723	3370,27553	-598,0212602
0,641667	0,009596598	0,005516	0,004080598	1,538349264	64,45809233	-74,769887	139,2279793	2,42998665	31,13762046	3,769909299	2771,088886	31,39430256	-1,940054729	3375,23538	-604,146494
0,651667	0,0095765	0,005667	0,0039095	1,473846663	64,1074108	-75,98352	140,0909308	2,445047995	31,12572272	3,769909299	2769,884192	31,41207989	-1,972707815	3380,341659	-610,4574667
0,661667	0,009555524	0,005819	0,003736524	1,408636348	63,73560726	-77,181145	140,9167523	2,459461298	31,11346632	3,769909299	2768,643183	31,43328282	-2,003342113	3385,590383	-616,9471999
0,671667	0,009533218	0,005971	0,003562218	1,342924726	63,34323597	-78,361791	141,705027	2,473219287	31,10087359	3,769909299	2767,36812	31,45772243	-2,032021712	3390,968913	-623,6007934
0,681667	0,009509666	0,006124	0,003385666	1,276365932	62,93086821	-79,52447	142,4553382	2,486314689	31,08794661	3,769909299	2766,059211	31,4852565	-2,058810701	3396,469338	-630,4101264
0,691667	0,009484868	0,006278	0,003206868	1,208960566	62,49910101	-80,668163	143,167264	2,498740138	31,07470509	3,769909299	2764,718455	31,51571428	-2,085837257	3402,087346	-637,3688901
0,701667	0,00945863	0,006433	0,00302563	1,140635742	62,04855807	-81,791826	143,8403841	2,510488299	31,061189	3,769909299	2763,349898	31,54895458	-2,107133423	3407,811886	-644,4619878
0,711667	0,009431093	0,006588	0,002843093	1,071820824	61,57989375	-82,894383	144,4742767	2,521551814	31,04739835	3,769909299	2761,95354	31,58483519	-2,128859421	3413,644783	-651,6912426
0,721667	0,009402174	0,006744	0,002658174	1,00210793	61,09379006	-83,974734	145,0685241	2,531923386	31,03336064	3,769909299	2760,532167	31,62321545	-2,14907934	3419,578283	-659,0461163
0,731667	0,009372207	0,0069	0,002472207	0,931999959	60,59088471	-85,021639	145,6125237	2,541417971	31,01919992	3,769909299	2759,098337	31,6601606	-2,167472736	3425,181529	-666,0831911
0,741667	0,009340355	0,007057	0,002283355	0,860804577	60,0667787	-86,049354	146,1161327	2,550207606	31,00461993	3,769909299	2757,621992	31,70827269	-2,185898177	3431,918717	-674,2967246
0,751667	0,009307546	0,007214	0,002093546	0,789248077	59,53799517	-87,041462	146,5794572	2,558294143	30,9900501	3,769909299	2756,146803	31,74988046	-2,201792123	3437,751118	-681,604315
0,761667	0,009272608	0,007371	0,001901608	0,716889436	58,98488822	-88,016645	147,0015332	2,565660076	30,97514924	3,769909299	2754,638032	31,80209688	-2,217944467	3444,666638	-690,0286054
0,771667	0,009237047	0,007529	0,001708047	0,643918718	58,42901432	-88,95363	147,3826443	2,572312404	30,96025876	3,769909299	2753,130313	31,84807991	-2,231785536	3450,721027	-697,590714
0,781667	0,009198824	0,007687	0,001511824	0,569944219	57,85002501	-89,87168	147,721705	2,578230129	30,94512122	3,769909299	2751,597577	31,90361934	-2,246141358	3457,798197	-706,2006197
0,791667	0,009160227	0,007846	0,001314227	0,495451918	57,27011544	-90,749032	148,0191474	2,583421479	30,9299868	3,769909299	2750,065157	31,95354337	-2,258254083	3464,079663	-714,0145066
0,801667	0,009120219	0,008005	0,001115219	0,42042749	56,66835652	-91,597847	148,2662035	2,587733421	30,91472054	3,769909299	2748,519388	32,00986134	-2,270783382	3471,050722	-722,5313339
0,811667	0,009078472	0,008164	0,000914472	0,344747849	56,06099934	-92,410246	148,4712453	2,591312076	30,89938421	3,769909299	2746,966524	32,06811426	-2,282639753	3478,149565	-731,1830404
0,821667	0,009035122	0,008323	0,000712122	0,268463527	55,44788831	-93,185955	148,6338553	2,594151012	30,88400948	3,769909299	2745,409772	32,12793051	-2,293887283	3485,345052	-739,9352809
0,831667	0,008990568	0,008483	0,000507568	0,191348497	54,82588087	-93,9278	148,7536809	2,596241506	30,86863944	3,769909299	2743,853492	32,18949848	-2,304750282	3492,678974	-748,8254826
0,841667	0,008944391	0,008643	0,000301391	0,113621835	54,19740305	-94,633022	148,830425	2,597580944	30,85322731	3,769909299	2742,292955	32,25278133	-2,31522875	3500,147599	-757,8546441
0,851667	0,008896744	0,008803	9,37441E-05	0,035340699	53,56301741	-95,300764	148,8637814	2,598163123	30,83784323	3,769909299	2740,735257	32,31768874	-2,325482909	3507,758006	-767,0227492
0,861667	0,008847445	0,008963	-0,000115555	-0,043563309	52,92382791	-95,929621	148,8534489	2,597982786	30,82247991	3,769909299	2739,17966	32,38417921	-2,335544802	3515,509234	-776,3295741
0,871667	0,008797209	0,009124	-0,000326791	-0,123197413	52,28078692	-96,518341	148,7991279	2,597034706	30,80716591	3,769909299	2737,629056	32,4521925	-2,345478518	3523,401677	-785,7726211
0,881667	0,008744628	0,009285	-0,000540372	-0,203715265	51,63524284	-97,067704	148,7029468	2,59535603	30,79194117	3,769909299	2736,087492	32,52377362	-2,355860853	3531,700801	-795,6133092
0,891667	0,008690696	0,009446	-0,000755304	-0,284742884	50,99344064	-97,570305	148,5637456	2,59292653	30,77676826	3,769909299	2734,550972	32,59460422	-2,365730481	3539,872017	-805,3210453
0,901667	0,008635525	0,009607	-0,000971475	-0,36623731	50,34499213	-98,032942	148,3779341	2,589683488	30,76167492	3,769909299	2733,022914	32,66701008	-2,375760329	3548,218958	-815,1960445
0,911667	0,008578608	0,009769	-0,001190392	-0,448767258	49,69673781	-98,448442	148,1451798	2,585621159	30,74668115	3,769909299	2731,504736	32,74104102	-2,386014488	3556,753158	-825,2484222
0,921667	0,008520565	0,009931	-0,001410435	-0,531721637	49,04974632	-98,81537	147,8651163	2,580733129	30,73180001	3,769909299	2729,997962	32,81679567	-2,396557044	3565,491091	-835,4931287
0,931667	0,008460759	0,010093	-0,001632241	-0,615340537	48,40527008	-99,1321	147,5373701	2,575012878	30,717045	3,769909299	2728,503959	32,89441311	-2,407452088	3574,45333	-845,9493714
0,941667	0,008399589	0,010255	-0,001855411	-0,699473377	47,76454932	-99,397009	147,1615583	2,568453725	30,70240729	3,769909299	2727,021833	32,97398679	-2,417831662	3583,652581	-856,630748
0,951667	0,008336831	0,010418	-0,002081169	-0,784582274	47,12876679	-99,608523	146,7372898	2,561048842	30,68791699	3,769909299	2725,554632	33,05562932	-2,430427811	3593,103491	-867,5488591
0,961667	0,008272478	0,010581	-0,002308522	-0,870292315	46,49910287	-99,765054	146,2641569	2,552791115	30,67358602	3,769909299	2724,103565	33,13950576	-2,442540536	3602,822773	-878,7192082
0,971667	0,00820663	0,010744	-0,00253737	-0,956566126	45,87677127	-99,86497	145,7417413	2,543673243	30,65941803	3,769909299	2722,669	33,22572407	-2,455133924	3612,827848	-890,1588478
0,981667	0,008138638	0,010907	-0,002768362	-1,043647827	45,26294666	-99,906656	145,1696027	2,53368754	30,64542496	3,769909299	2721,252146	33,31442802	-2,468175932	3623,130028	-901,877882
0,991667	0,008068889	0,011071	-0,003002111	-1,13176909	44,65882701	-99,888457	144,547284	2,522826031	30,63160524	3,769909299	2719,852845	33,40579771	-2,481698603	3633,750794	-913,8979493
1	0,008009186	0,011208	-0,003198814	-1,205924439	44,22949993	-99,756967	143,9864669	2,513037926	30,62025144	3,769909299	2718,703228	33,48321533	-2,49329862	3642,764182	-924,0609541

Figure C.1: Results from the stable case, that had CT 0.18 s.

C.3 Unstable case numerical results

Numerical results for the unstable case where the fault is on Bus 16, 50% with a CT of 0.2 s is displayed in Figure C.2.

Time in s	SpeedC	SpeedN	Speed in p.u.	Speed in rad/s	DeltaC	DeltaN	Delta deg	Delta rad	PM_C	PM_N	PM	Pelec_C	Pelec_N	Pelec	Pa
-0,1	0	0	0	0	46,39546368	-0,054142	46,44960568	0,810698555	31,39106017	3,769909299	2796,750657	31,39106017	3,769909299	2796,750657	0
-0,09	0	0	0	0	46,39546368	-0,054142	46,44960568	0,810698555	31,39106017	3,769909299	2796,750657	31,39106017	3,769909299	2796,750657	0
-0,08	0	0	0	0	46,39546368	-0,054142	46,44960568	0,810698555	31,39106017	3,769909299	2796,750657	31,39106017	3,769909299	2796,750657	0
-0,07	0	0	0	0	46,39546368	-0,054142	46,44960568	0,810698555	31,39106017	3,769909299	2796,750657	31,39106017	3,769909299	2796,750657	0
-0,06	0	0	0	0	46,39546368	-0,054142	46,44960568	0,810698555	31,39106017	3,769909299	2796,750657	31,39106017	3,769909299	2796,750657	0
-0,05	0	0	0	0	46,39546368	-0,054142	46,44960568	0,810698555	31,39106017	3,769909299	2796,750657	31,39106017	3,769909299	2796,750657	0
-0,04	0	0	0	0	46,39546368	-0,054142	46,44960568	0,810698555	31,39106017	3,769909299	2796,750657	31,39106017	3,769909299	2796,750657	0
-0,03	0	0	0	0	46,39546368	-0,054142	46,44960568	0,810698555	31,39106017	3,769909299	2796,750657	31,39106017	3,769909299	2796,750657	0
-0,02	0	0	0	0	46,39546368	-0,054142	46,44960568	0,810698555	31,39106017	3,769909299	2796,750657	31,39106017	3,769909299	2796,750657	0
-0,01	0	0	0	0	46,39546368	-0,054142	46,44960568	0,810698555	31,39106017	3,769909299	2796,750657	31,39106017	3,769909299	2796,750657	0
0	0	0	0	0	46,39546368	-0,054142	46,44960568	0,810698555	31,39106017	3,769909299	2796,750657	31,39106017	3,769909299	2796,750657	0
0,005	0,000206989	-1,4E-05	0,000220989	0,083310923	46,4049934	-0,068529	46,4735224	0,811115981	31,39104979	3,769909299	2796,749606	17,22547921	4,860439047	1252,009171	1544,740435
0,011667	0,000495622	-3,2E-05	0,000527622	0,198908623	45,46868711	-1,069818	46,53850511	0,812250143	31,39103422	3,769909299	2796,74803	16,5043677	4,738190253	1191,371955	1605,376075
0,021667	0,000949026	-5,6E-05	0,001005026	0,378885704	43,96223273	-2,741782	46,70401473	0,815138831	31,39097142	3,769909299	2796,741671	15,7099716	4,577296098	1127,22738	1669,51429
0,031667	0,001424684	-7,5E-05	0,001499684	0,565367724	42,35403947	-4,620498	46,97453747	0,819860343	31,39083439	3,769909299	2796,727796	15,16425207	4,441941207	1085,676339	1711,051458
0,041667	0,001915555	-9,2E-05	0,002007555	0,75683056	41,53002684	-5,823311	47,35333784	0,826471657	31,39060446	3,769909299	2796,704515	14,74788595	4,321743244	1055,688143	1741,016372
0,051667	0,00241826	-0,000105	0,00252326	0,951246501	41,14440958	-6,69814	47,84254958	0,835010013	31,39028889	3,769909299	2796,672562	14,41134315	4,213818226	1032,53969	1764,132873
0,061667	0,002929383	-0,000115	0,003044383	1,147705535	41,03357995	-7,410181	48,44376095	0,845503131	31,38985342	3,769909299	2796,628469	14,1315865	4,109610341	1014,764683	1781,863786
0,071667	0,003448267	-0,000123	0,003571267	1,346336006	41,06738963	-8,090789	49,15817863	0,857972071	31,3893074	3,769909299	2796,573183	13,89531323	4,009888651	1000,938296	1795,634887
0,081667	0,00397312	-0,000128	0,00410112	1,546085842	41,21920565	-8,767243	49,98644865	0,87242811	31,38862903	3,769909299	2796,504495	13,69427177	3,913403429	990,3515644	1806,15293
0,091667	0,00450337	-0,00013	0,00463337	1,746739367	41,46280042	-9,4665	50,92930042	0,888883978	31,38782661	3,769909299	2796,423246	13,52303464	3,819289481	982,5425366	1813,88071
0,101667	0,005038079	-0,000131	0,005169079	1,948696802	41,78493581	-10,202601	51,98753681	0,907353687	31,38688301	3,769909299	2796,327703	13,37766341	3,726873878	977,1805701	1819,147133
0,111667	0,005576259	-0,000128	0,005704259	2,150454928	42,17963945	-10,981849	53,16148845	0,927843009	31,38578785	3,769909299	2796,216814	13,25516276	3,635708001	974,0078006	1822,209014
0,121667	0,006117545	-0,000123	0,006240545	2,352629859	42,6443001	-11,807045	54,4513451	0,950355254	31,38454893	3,769909299	2796,091368	13,15296141	3,545439363	972,7995665	1823,291802
0,131667	0,0066615	-0,000116	0,0067775	2,555057228	43,17779222	-12,679377	55,85716922	0,974891514	31,38314962	3,769909299	2795,949683	13,06880884	3,455779565	973,3571954	1822,592487
0,141667	0,007207125	-0,000107	0,007314125	2,75736016	43,77957078	-13,599344	57,37891478	1,001450984	31,38158318	3,769909299	2795,791075	13,00066786	3,366536342	975,4938808	1820,297194
0,151667	0,007754464	-9,5E-05	0,007849464	2,959178145	44,44924102	-14,56719	59,01643102	1,030031034	31,37986882	3,769909299	2795,617489	12,94665231	3,277485385	979,041354	1816,576135
0,161667	0,008302848	-8,1E-05	0,008383848	3,160636371	45,18635837	-15,583126	60,76948437	1,060627587	31,37797332	3,769909299	2795,425562	12,90498865	3,188530561	983,8297719	1811,595791
0,171667	0,008851882	-6,4E-05	0,008915882	3,36120849	45,99036684	-16,647393	62,63775984	1,093235145	31,37593353	3,769909299	2795,219025	12,87401341	3,099543693	989,7036775	1805,515348
0,181667	0,00940124	-4,5E-05	0,00944624	3,561148514	46,86057163	-17,760304	64,62087563	1,127847045	31,37370326	3,769909299	2794,993201	12,85212691	3,01052478	996,5010998	1798,492101
0,191667	0,009951342	-2,4E-05	0,009975342	3,760615198	47,79614614	-18,922247	66,71839314	1,164455632	31,37132557	3,769909299	2794,752452	12,83780113	2,921441778	1004,070564	1790,681887
0,2	0,010409326	-4E-06	0,010413326	3,925731487	48,6304575	-19,930798	68,5612555	1,196619648	31,36918976	3,769909299	2794,536192	12,83037224	2,847195263	1010,836113	1783,700079
0,205	0,010542337	4,4E-05	0,010498337	3,957779981	49,14688215	-20,548202	69,69508415	1,216408691	31,36785741	3,769909299	2794,401286	22,09526024	0,153043314	2221,736158	572,665128
0,211667	0,010704697	0,000109	0,010595697	3,994483757	46,10671028	-25,110633	71,21734328	1,242977125	31,3660761	3,769909299	2794,220921	22,96511462	0,049732668	2320,272961	473,9479597
0,221667	0,010920581	0,00021	0,010710581	4,037794091	47,80620835	-25,712224	73,51843235	1,283138705	31,363428	3,769909299	2793,952791	24,23506972	-0,081776913	2462,176798	331,7759932
0,231667	0,011097624	0,000313	0,010784624	4,065707437	49,59750918	-26,242424	75,83993318	1,323656538	31,36087073	3,769909299	2793,693858	25,41235547	-0,178422357	2591,167365	202,5264928
0,241667	0,011241205	0,000419	0,010822205	4,079875086	51,14819438	-27,025288	78,17348238	1,364384655	31,35844945	3,769909299	2793,448694	26,48292431	-0,252284341	2707,045507	86,4031863
0,251667	0,011355065	0,000526	0,010829065	4,082461148	52,55313458	-27,958688	80,51182258	1,405196391	31,35620932	3,769909299	2793,221871	27,44202969	-0,309835806	2809,98603	-16,76415883
0,261667	0,011442443	0,000635	0,010807443	4,074309951	53,86442911	-28,98412	82,84854911	1,445979963	31,3541306	3,769909299	2793,011392	28,28874047	-0,354537527	2900,245068	-107,2336754
0,271667	0,011507398	0,000745	0,010762398	4,057328523	55,10984735	-30,068249	85,17809635	1,486638232	31,35220966	3,769909299	2792,81689	29,02543745	-0,389145312	2978,342722	-185,5258323
0,281667	0,01155301	0,000855	0,01069801	4,033054739	56,30486715	-31,190871	87,49573815	1,527088712	31,35044288	3,769909299	2792,637997	29,65611146	-0,415357505	3044,855045	-252,2170488
0,291667	0,011581999	0,000966	0,010615999	4,002137285	57,4576455	-32,339822	89,7974675	1,567261468	31,34879548	3,769909299	2792,47119	30,18597667	-0,434487919	3100,443022	-307,9718316
0,301667	0,011597457	0,001078	0,010519457	3,965742043	58,57246994	-33,507489	92,07995894	1,607098459	31,34723839	3,769909299	2792,313529	30,62068379	-0,447433794	3145,769656	-353,4561276
0,311667	0,011602108	0,00119	0,010412108	3,92527219	59,65083184	-34,689683	94,34051484	1,646552602	31,34572956	3,769909299	2792,160754	30,96676378	-0,455188501	3181,596817	-389,4360625
0,321667	0,011598244	0,001302	0,010296244	3,881592449	60,69354236	-35,884163	96,57770536	1,685598943	31,34406503	3,769909299	2791,992214	31,22556663	-0,457880218	3208,074175	-416,0819613
0,331667	0,011589277	0,001414	0,010175277	3,835988873	61,69555021	-37,093763	98,78931321	1,724198781	31,34195984	3,769909299	2791,779055	31,40463231	-0,461469173	3226,568679	-434,7896238
0,341667	0,011576299	0,001526	0,010050299	3,788873378	62,65885321	-38,314796	100,9736492	1,762322637	31,33933251	3,769909299	2791,513027	31,49711065	-0,464737686	3236,263426	-444,7503992
0,351667	0,011562556	0,001638	0,009924556	3,741469606	63,56524411	-39,565613	103,1308571	1,799973017	31,33621261	3,769909299	2791,197125	31,51387276	-0,472396261	3238,736116	-447,5389912
0,361667	0,011549294	0,001751	0,009798294	3,693869896	64,40756705	-40,853293	105,2608601	1,837148581	31,33262351	3,769909299	2790,833715	31,46545651	-0,485950976	3235,206249	-444,3725339
0,371667	0,011538598	0,001864	0,009674598	3,647237684	65,18182767	-42,182115	107,3639427	1,873854298	31,32860102	3,769909299	2790,426422	31,36441935	-0,506042718	3227,010205	-436,5837833
0,381667	0,011531742	0,001977	0,009554742	3,602053045	65,8873544	-43,553316	109,4406704	1,910100034	31,32414981	3,769909299	2789,975719	31,22304725	-0,532671486	3215,39199	-425,4162704
0,391667	0,011529384	0,002092	0,009437384	3,557809774	66,52533428	-44,966478	111,4918123	1,945899213	31,31930518	3,769909299	2789,485181	31,05211375	-0,565516837	3201,410018	-411,9248376
0,401667	0,011532699	0,002207	0,009325699	3,515705528	67,09797537	-46,420304	113,5182794	1,981267736	31,31407698	3,769909299	2788,955805	30,86086744	-0,60403402	3185,945592	-396,9897867
0,411667	0,011541782	0,002323	0,009218782	3,475398987	67,60826779	-47,912796	115,5210638	2,016222919	31,30849532	3,769909299	2788,39064	30,65692772	-0,647421927	3169,689086	-381,2984462
0,421667	0,011556774	0,002441	0,009115774	3,436565659	68,05969652	-49,441501	117,5011975	2,050782772	31,30256591	3,769909299	2787,790264	30,44616638	-0,694783322	3153,144195	-365,3539316
0,431667	0,011578015	0,00256	0,009018015	3,399711396	68,45577301	-51,00395	119,459723	2,08496549	31,29631159	3,769909299	2787,156989	30,23284517	-0,745188919	3136,648346	-349,4913573
0,441667	0,011605127	0,00268	0,008925127	3,364693554	68,79981325	-52,597854	121,3976672	2,118788998	31,28975052	3,769909299	2786,492655	30,02014109	-0,797741481	3120,432372	-333,9397177
0,451667	0,011638434	0,002801	0,008837434	3,331634141	69,09493877	-54,221093	123,3160318	2,152270775	31,28289723	3,769909299	2785,798732	29,81003113	-0,851575813	3104,608847	-318,8101148
0,461667	0,011677214	0,002924	0,008753214	3,29988396	69,3438442	-55,871935	125,2157792	2,185427622	31,27574602	3,769909299	2785,074644	29,60381545	-0,905858764	3089,225059	-304,1504146
0,471667	0,011721703	0,003049	0,008672703	3,269532045	69,54881503	-57,549023	127,097838	2,218275746	31,26833063	3,769909299	2784,323806	29,40232971	-0,959917405	3074,297482	-289,973676
0,481667	0,011771718	0,003174	0,008597718	3,241263137	69,71185367	-59,251239	128,9630927	2,250830581	31,26064326	3,769909299	2783,54543	29,20595902	-1,013014719	3059,790486	-276,2450566
0,491667	0,011826806	0,003301	0,008525806	3,214153133	69,83456808	-60,977825	130,8123931	2,283106962	31,25271039	3,769909299	2782,742196	29,01476929	-1,06457391	3045,652343	-262,9101474
0,501667	0,011887149	0,00343	0,008457149	3,188270078	69,91820605	-62,72835	132,646556	2,315119144	31,24452942	3,769909299	2781,91384	28,82861312	-1,114050224	3031,812968	-249,8991277
0,511667	0,011952261	0,00356	0,008392261	3,163808017	69,96368313	-64,502684	134,4663671	2,34688084	31,23611282	3,769909299	2781,061626	28,64721595	-1,161027087	3018,202381	-237,1407552
0,521667	0,012021642	0,003691	0,008330642	3,140578155	69,97161791	-66,30097	136,2725879	2,378405339	31,2274668	3,769909299	2780,186182	28,47022017	-1,205087924	3004,742192	-224,5560097
0,531667	0,012096349	0,003823	0,008273349	3,118979092	69,94234394	-68,123234	138,0655779	2,409698919	31,21859916	3,769909299	2779,288298	28,29812144	-1,245848204	2991,443655	-212,1553567
0,541667	0,012174887	0,003956	0,008218887	3,0984475	69,87424612	-69,971807	139,8460531	2,440774073	31,2095156	3,769909299	2778,368552	28,12910056	-1,283147705	2978,106345	-199,7377935
0,551667	0,012257888	0,00409	0,008167888	3,079221388	69,77147484	-71,843622	141,6150968	2,47164971	31,20022027	3,769909299	2777,427363	27,9632437	-1,316601897	2964,700052	-187,2726883
0,561667	0,012344523	0,004224	0,008120523	3,061365	69,63124303	-73,742179	143,373422	2,502338274	31,1907137	3,769909299	2776,464786	27,8001351	-1,346018514	2951,163211	-174,6984252
0,571667	0,012435376	0,00436	0,008075376	3,044345029	69,45313623	-75,668604	145,1217402	2,532852183	31,18099277	3,769909299	2775,480503	27,63941301	-1,371109158	2937,429991	-161,9494881
0,581667	0,012530125	0,004496	0,008034125	3,028793955	69,23666319	-77,6241	146,8607632	2,56320386	31,17109589	3,769909299	2774,478404	27,48074161	-1,391713607	2923,450167	-148,9717624
0,591667	0,012628598	0,004632	0,007996598	3,014646556	68,98118361	-79,61003	148,5912136	2,593405917	31,16099191	3,769909299	2773,455337	27,32376693	-1,407639597	2909,168429	-135,713092
0,601667	0,012731081	0,004769	0,007962081	3,001633933	68,68592826	-81,627896	150,3138243	2,623471145	31,15069745	3,769909299	2772,412982	27,16818688	-1,418694862	2894,534723	-122,1217412
0,611667	0,012837281	0,004906	0,007931281	2,990022676	68,35001821	-83,679321	152,0293392	2,653412529	31,14021925	3,769909299	2771,352023	27,01368278	-1,424655091	2879,49407	-108,1420464
0,621667	0,012946868	0,005043	0,007903868	2,979687867	67,97248162	-85,766044	153,7385256	2,683243459	31,12954746	3,769909299	2770,271462	26,85995671	-1,425424153	2864,006568	-93,73510623
0,631667	0,013060074	0,00518	0,007880074	2,970717787	67,55226436	-87,889902	155,4421664	2,712977599	31,11866493	3,769909299	2769,169564	26,7067206	-1,420713649	2848,01385	-78,84428623
0,641667	0,013177098	0,005317	0,007860098	2,963187191	67,08824012	-90,052834	157,1410741	2,742629134	31,10754729	3,769909299	2768,043858	26,55366823	-1,410395402	2831,471929	-63,42807112
0,651667	0,013297664	0,005454	0,007843664	2,956991537	66,57921967	-92,256865	158,8360847	2,772212648	31,09614626	3,769909299	2766,889458	26,40051465	-1,394181014	2814,322753	-47,43329487
0,661667	0,013421486	0,00559	0,007831486	2,95240048	66,02395502	-94,504113	160,528068	2,801743329	31,08440941	3,769909299	2765,701056	26,24693027	-1,371910264	2796,516727	-30,81567063
0,671667	0,013549124	0,005725	0,007824124	2,949625405	65,42115187	-96,796776	162,2179279	2,831236947	31,07235543	3,769909299	2764,480544	26,09259849	-1,343294753	2777,992591	-13,51204711
0,681667	0,013680628	0,005859	0,007821628	2,948684159	64,76947915	-99,137126	163,9066052	2,860709926	31,05995994	3,769909299	2763,225451	25,93712951	-1,308078128	2758,68492	4,540530518
0,691667	0,013815233	0,005993	0,007822233	2,948912387	64,06757603	-101,52751	165,595086	2,890179476	31,04721409	3,769909299	2761,934884	25,78016676	-1,26597199	2738,528409	23,40647485
0,701667	0,013953791	0,006125	0,007828791	2,951384648	63,3140622	-103,970339	167,2844012	2,919663588	31,03414697	3,769909299	2760,611786	25,62126855	-1,216623852	2717,442643	43,16914297
0,711667	0,014096045	0,006255	0,007841045	2,956004353	62,50755006	-106,468085	168,9756351	2,949181187	31,02075493	3,769909299	2759,255789	25,45996307	-1,159713273	2695,347404	63,90838459
0,721667	0,014242246	0,006384	0,007858246	2,962488776	61,64665659	-109,023273	170,6699296	2,978752205	31,00705252	3,769909299	2757,868365	25,29571209	-1,094855721	2672,14926	85,71910494
0,731667	0,014392271	0,006512	0,007880271	2,970792122	60,73001874	-111,638474	172,3684927	3,008397725	30,99306878	3,769909299	2756,452457	25,12796647	-1,021602577	2647,747183	108,7052736
0,741667	0,014546094	0,006637	0,007909094	2,981658257	59,75630991	-114,31629	174,0725999	3,038140006	30,97881671	3,769909299	2755,009379	24,95606601	-0,939505221	2622,028901	132,9804775
0,751667	0,014704329	0,00676	0,007944329	2,99494159	58,72426258	-117,059344	175,7836066	3,068002706	30,96432329	3,769909299	2753,541862	24,77932455	-0,848115034	2594,879512	158,6623502
0,761667	0,014866825	0,00688	0,007986825	3,01096197	57,63269045	-119,870264	177,5029545	3,098010987	30,9496233	3,769909299	2752,05343	24,59693707	-0,746823176	2566,155858	185,8975716
0,771667	0,015033884	0,006998	0,008035884	3,029457083	56,48052079	-122,751659	179,2321798	3,128191663	30,93472451	3,769909299	2750,544869	24,40811256	-0,635084893	2535,722689	214,8221804
0,781667	0,015205351	0,007112	0,008093351	3,051121306	55,26752073	-125,705405	180,9729257	3,158573411	30,91966483	3,769909299	2749,020017	24,21209222	-0,512163169	2503,428544	245,5914729
0,791667	0,015382231	0,007223	0,008159231	3,075957564	53,99438406	-128,732564	182,7269481	3,189186876	30,90447124	3,769909299	2747,481605	24,00795267	-0,377609384	2469,134505	278,3470998
0,801667	0,015564104	0,00733	0,008234104	3,104183977	52,6606721	-131,83545	184,4961221	3,220064788	30,88915775	3,769909299	2745,931054	23,79476174	-0,230814697	2432,684539	313,2465145
0,811667	0,015751735	0,007434	0,008317735	3,135712125	51,26635411	-135,016107	186,2824611	3,251242285	30,87377315	3,769909299	2744,373303	23,57162929	-0,071266401	2393,936602	350,4367008
0,821667	0,01594522	0,007532	0,00841322	3,171709374	49,81194362	-138,276175	188,0881186	3,282756954	30,85831433	3,769909299	2742,808036	23,33757954	0,101612301	2352,733489	390,0745476
0,831667	0,016145143	0,007627	0,008518143	3,211264189	48,2978782	-141,617522	189,9154002	3,314649034	30,84283631	3,769909299	2741,240825	23,09167357	0,288302073	2308,931461	432,3093648
0,841667	0,016351487	0,007716	0,008635487	3,255501804	46,72498645	-145,041789	191,7667754	3,346961627	30,82735362	3,769909299	2739,673142	22,83303525	0,489379711	2262,383404	477,289738
0,851667	0,016565024	0,007799	0,008766024	3,304713236	45,09456494	-148,550321	193,6448859	3,379740839	30,811873	3,769909299	2738,105668	22,56071372	0,705357922	2212,941125	525,1645427
0,861667	0,016786016	0,007877	0,008909016	3,358620045	43,40837464	-152,144179	195,5525536	3,413035922	30,79645466	3,769909299	2736,544501	22,27379132	0,936749416	2160,459796	576,0847044
0,871667	0,017015384	0,007948	0,009067384	3,418323152	41,6687333	-155,824059	197,4927923	3,446899475	30,78108512	3,769909299	2734,988273	21,97140285	1,184034855	2104,80314	630,1851331
0,881667	0,017253241	0,008013	0,009240241	3,483488661	39,87856964	-159,590248	199,4688176	3,481387623	30,76581108	3,769909299	2733,441716	21,65283306	1,447406505	2045,879271	687,5624456
0,891667	0,017500061	0,00807	0,009430061	3,555049352	38,04154516	-163,442502	201,4840472	3,516560013	30,75063409	3,769909299	2731,904987	21,31841259	1,727120721	1983,695707	748,2092797
0,901667	0,017756473	0,00812	0,009636473	3,632864891	36,16234474	-167,379762	203,5421067	3,552479929	30,73558686	3,769909299	2730,381395	20,96800336	2,023433855	1918,212513	812,1688823
0,911667	0,018023241	0,008162	0,009861241	3,717600345	34,24621188	-171,400617	205,6468289	3,58921426	30,72062009	3,769909299	2728,86595	20,60135937	2,336570218	1849,382066	879,4838838
0,921667	0,018300745	0,008195	0,010105745	3,809775949	32,29906539	-175,503191	207,8022564	3,626833567	30,70552563	3,769909299	2727,337577	20,21841885	2,666657986	1777,185134	950,1524422
0,931667	0,018589077	0,00822	0,010369077	3,909050119	30,32760525	-179,685038	210,0126432	3,665412095	30,69021733	3,769909299	2725,787551	19,81958663	3,013729204	1701,659465	1024,128086
0,941667	0,018889331	0,008235	0,010654331	4,016588266	28,3394088	176,056959	-147,7175502	-2,578157614	30,67468221	3,769909299	2724,214559	19,4058058	3,377559563	1622,92326	1101,291299
0,951667	0,019201668	0,00824	0,010961668	4,132451303	26,34301675	171,726312	-145,3832952	-2,537417179	30,65891665	3,769909299	2722,618233	18,96703363	3,765038574	1539,262063	1183,35617
0,961667	0,019527013	0,008235	0,011292013	4,256988631	24,33497572	167,314728	-142,9797523	-2,495467441	30,64292323	3,769909299	2720,998836	18,52600316	4,161810417	1454,431269	1266,567567
0,971667	0,019865364	0,008219	0,011646364	4,390575747	22,34779994	162,850069	-140,5022691	-2,452227202	30,62668898	3,769909299	2719,355054	18,07352754	4,573867364	1366,89393	1352,461124
0,981667	0,020217174	0,008192	0,012025174	4,533383742	20,38216116	158,327808	-137,9456468	-2,407605726	30,61022635	3,769909299	2717,688148	17,61108912	5,000568531	1276,865034	1440,823115
0,991667	0,020582905	0,008154	0,012428905	4,685586627	18,44684296	153,751374	-135,304531	-2,36150956	30,59351356	3,769909299	2715,995912	17,14143616	5,440664193	1184,749392	1531,24652
1	0,020899008	0,008113	0,012786008	4,82021143	16,84230986	149,870918	-133,0286081	-2,321787211	30,57938034	3,769909299	2714,564868	16,74496917	5,81769678	1106,429503	1608,135365

Figure C.2: Results from the unstable case, that had CT 0.20 s.

C.4 Unstable case plot with P_m and P_e

In Figure C.3, it is shown that P_m only changes slightly from its original value from δ_0 to δ_u.

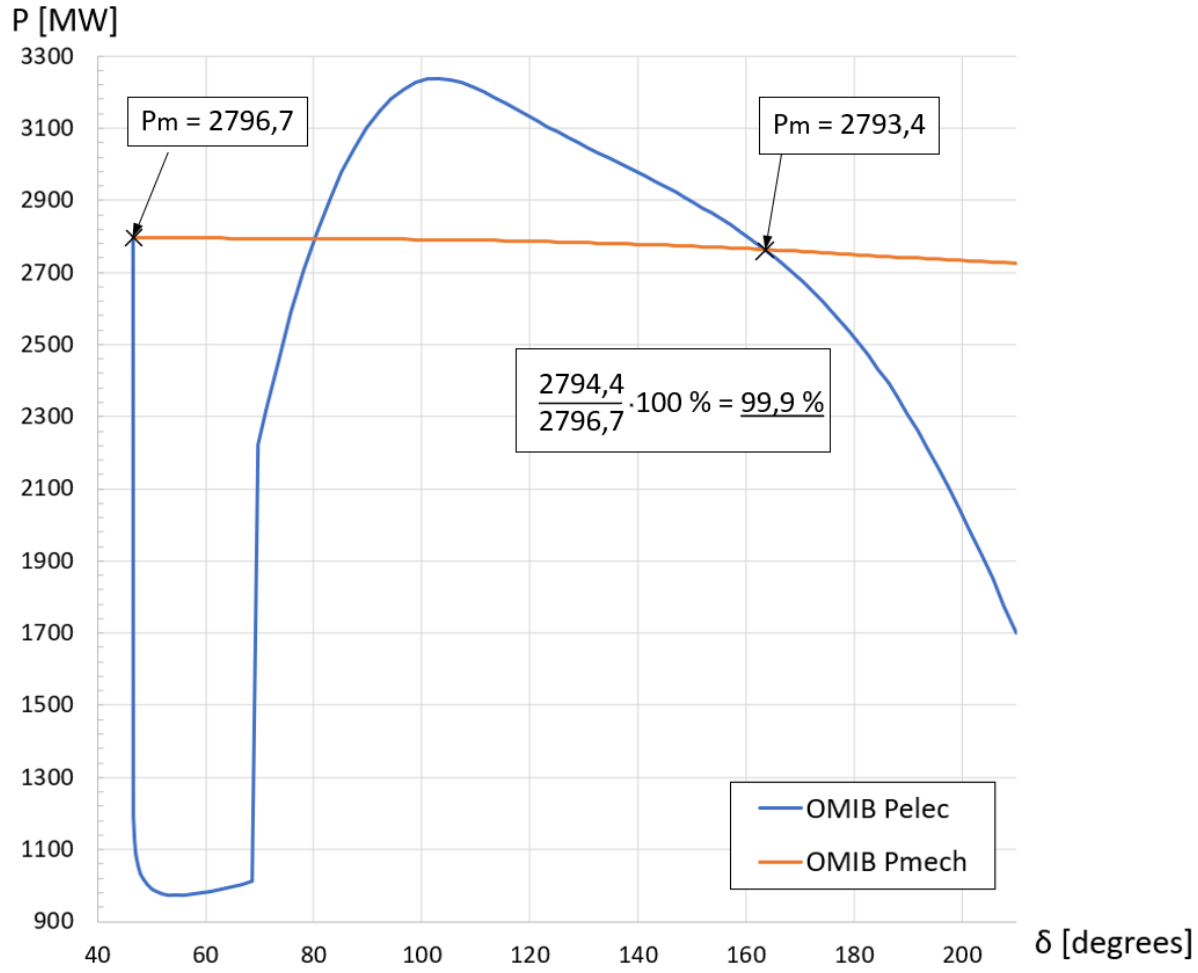

Figure C.3: Plot of P_e, P_m and δ in 10 generator case, for the unstable case with CT of 0.2 s.

C.5 Comparison of with and without corrective measures on unstable case

The correction that is compared here is the disconnection of generator unit nr. 1 from the rest of the grid, which is done by disconnecting the lines to bus nr.39. Figure C.4 shows a comparison of how the variable firot acts both without (a) any corrections and with corrections (b). Here PowerFactory gives a signal that Generator unit nr.1 is out of

step after 1.29 s, which means that there are more than 360 degrees between the rotor of generator 1 and the reference machine generator 2. At this point, it can be certain that the two groups have lost synchronism to each other. Rather in (b) it is shown that at the same point the system remains stable with corrective measures. Also to show this further a comparison of the speed ω_{rot} is included in Figure C.5, wherein (a) the uncorrected is shown (b) the corrected one is shown.

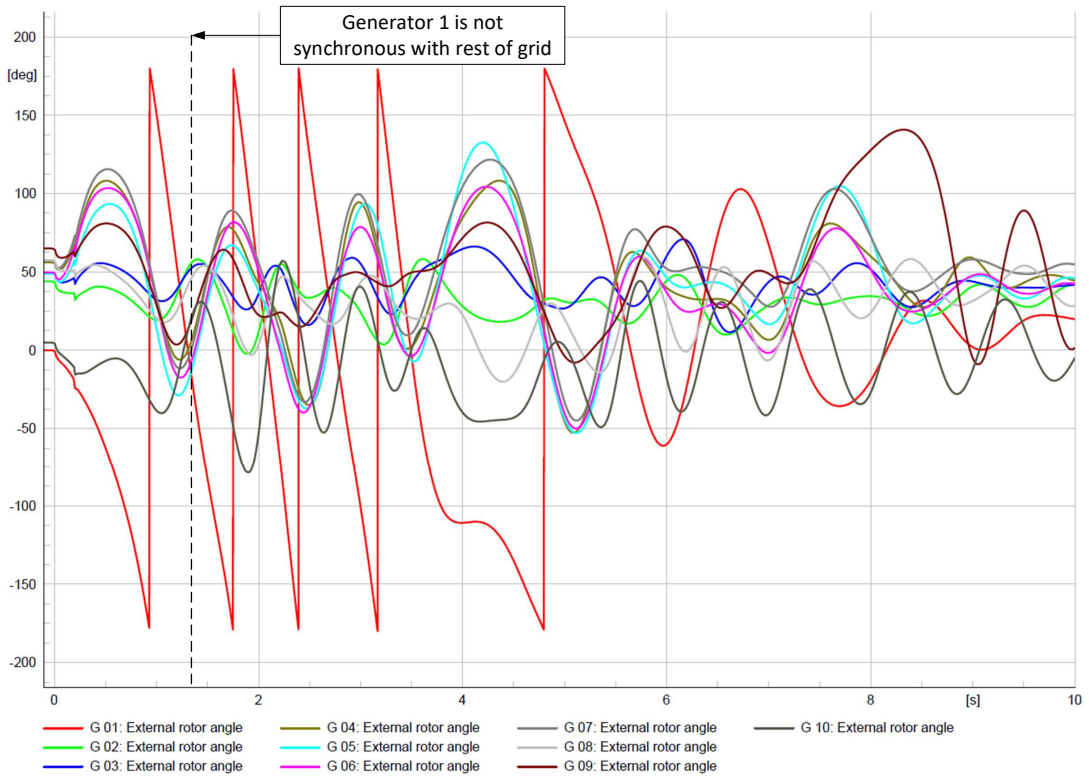

(a) Uncorrected Case

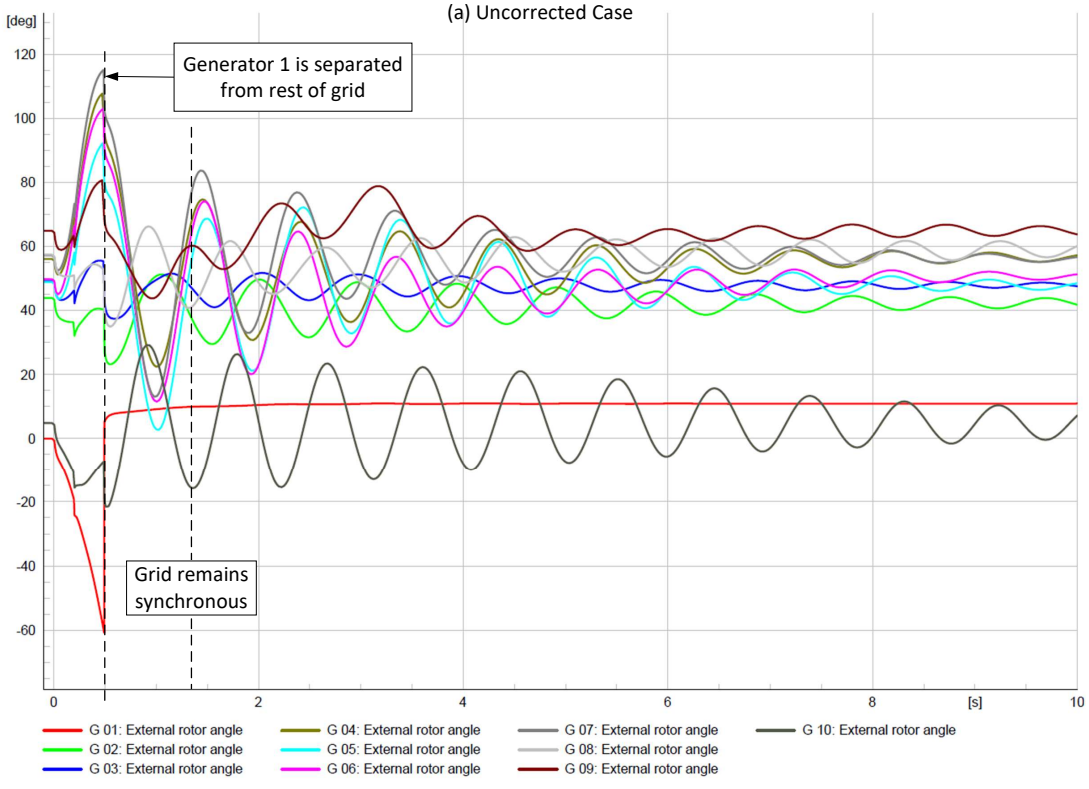

(b) Corrected Case

Figure C.4: Plot of firot, without corrective measures in (a), and with corrective measures in (b). Here the corrective measure is separating generator 1 from the rest of the grid.

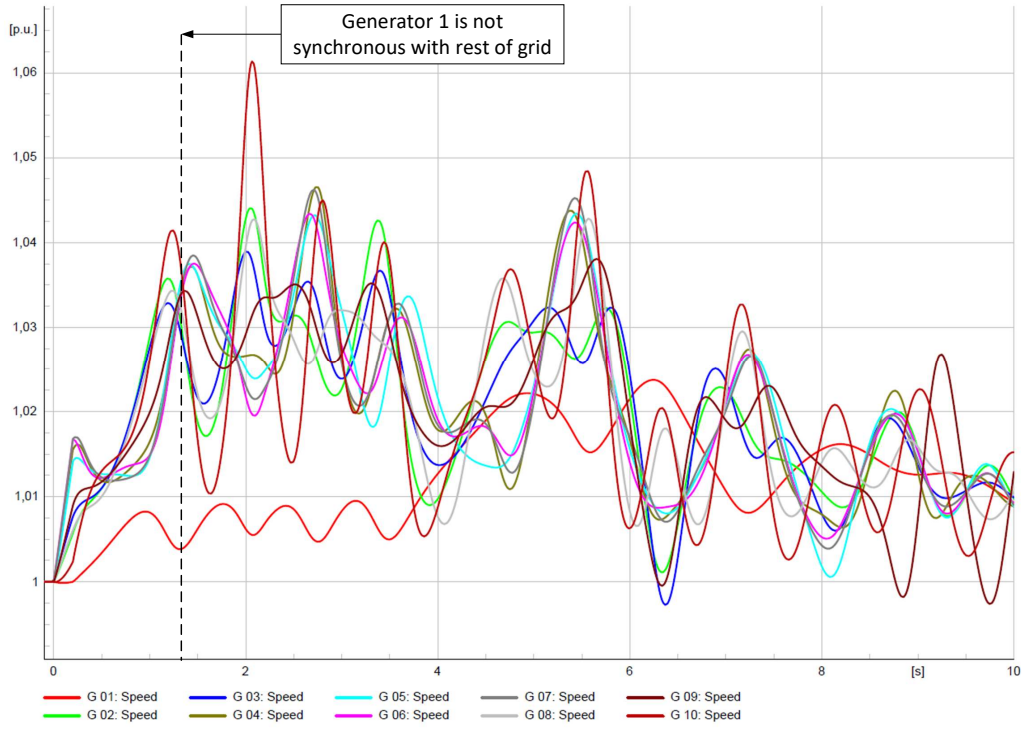

(a) Uncorrected Case

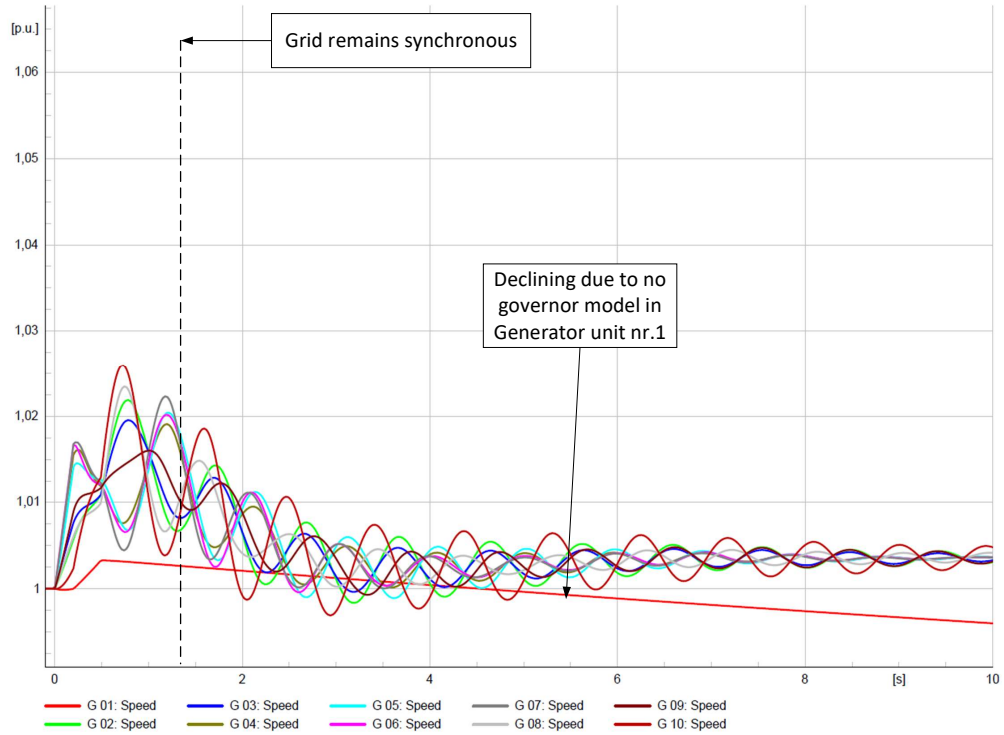

(b) Corrected Case

Figure C.5: Plot of ω_{rot}, without corrective measures in (a), and with corrective measures in (b). Here the corrective measure is separating generator 1 from the rest of the grid.

C.6 Inclusion Of governor on Generator 1

To show the effects of including a governor on the speed deviation, a dynamic model IEEE Type G1 (steam turbine) was installed on generation unit nr.1 with the setting shown in Table C.2.

Table C.2: Settings of the included governor for generator nr.1.

Name	Value	Unit	Type	Description
K	5	[p.u.]	d	Controller Gain
T1	0.2	[s]	d	Governor Time Constant
T2	1	[s]	d	Governor Derivative Time Constant
T3	0.6	[s]	d	Servo Time Constant
K1	0.3	[p.u.]	d	High Pressure Turbine Factor
K2	0	[p.u.]	d	High Pressure Turbine Factor
T5	0.5	[s]	d	Intermediate Pressure Turbine Time Constant
K3	0.25	[p.u.]	d	Intermediate Pressure Turbine Factor
K4	0	[p.u.]	d	Intermediate Pressure Turbine Factor
T6	0.8	[s]	d	Medium Pressure Turbine Time Constant
K5	0.3	[p.u.]	d	Medium Pressure Turbine Factor
K6	0	[p.u.]	d	Medium Pressure Turbine Factor
T4	0.6	[s]	d	High Pressure Turbine Time Constant
T7	1	[s]	d	Low Pressure Turbine Time Constant
K7	0.15	[p.u.]	d	Low Pressure Turbine Factor
K8	0	[p.u.]	d	Low Pressure Turbine Factor
PNhp	0	[MW]	d	HP Turbine Rated Power (=0->PNhp=PgnnHp)
PNlp	0	[MW]	d	LP Turbine Rated Power (=0->PNlp=Pgnnlp)
Uc	-0.3	[p.u./s]	d	Valve Closing Time
Pmin	0	[p.u.]	d	Minimum Gate Limit
Uo	0.3	[p.u./s]	d	Valve Opening Time
Pmax	1	[p.u.]	d	Maximum Gate Limit

C.7 M and OMIB formulation for the unstable case, where the fault is on bus nr.28

The fault is on bus nr.28 and the CT is 0.13 s, and it is unstable. This is shown in the plot of firot, which is shown in Figure C.6. Here it is seen that the generator unit nr. 9 is the CM, and the rest are the NMs, this is then summarized in (C.1).

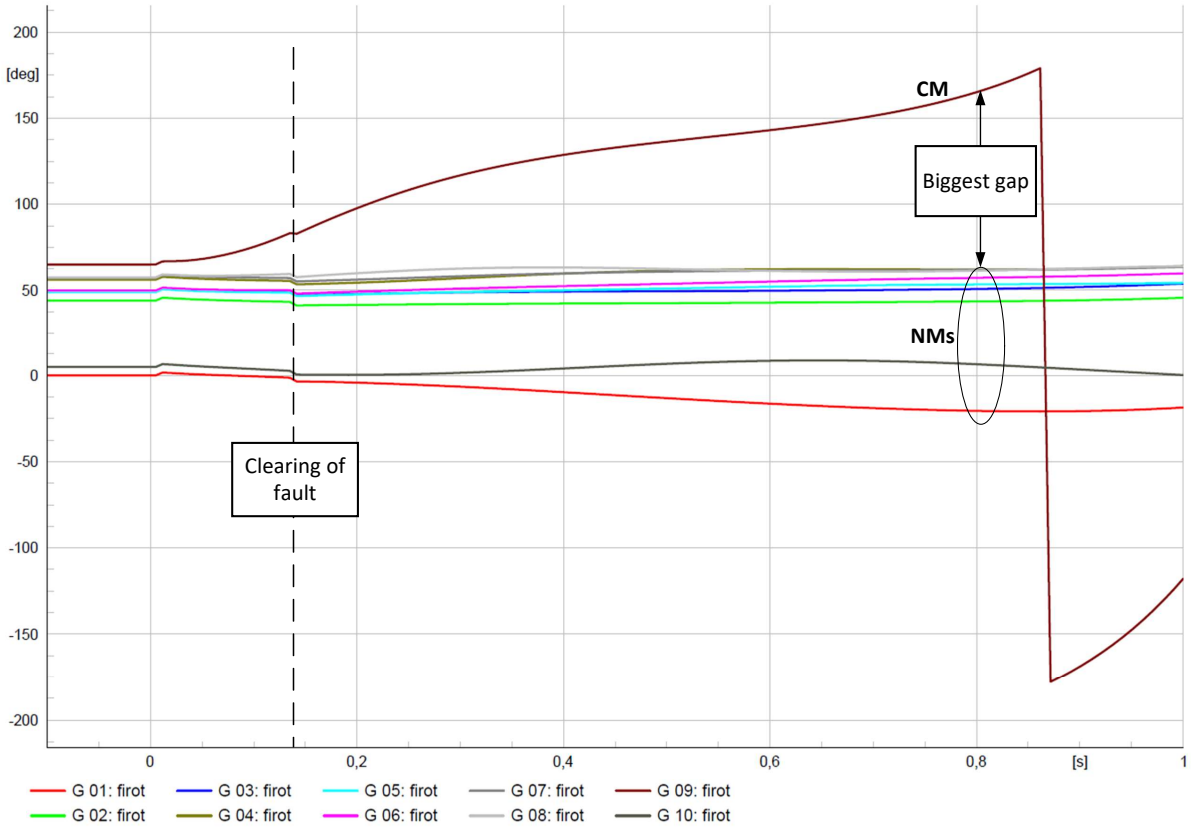

Figure C.6: Plot of δ for fault at bus nr.28 with CT 0.13 s.

$$\mathbf{CM} = [G9] \ ; \ \mathbf{NMs} = [G1,\ G2, ..., \ G8,\ G10] \tag{C.1}$$

The formulas from Chapter 3.2 are used to find the OMIB- parameters, where the calculated values for M are shown in Table C.3. The results from calculating the OMIB parameters are shown in Figure C.7

Table C.3: M used in OMIB formulation for the case of fault at bus nr.28.

Name	M	MC	MN
Value	17.522	18.302	410.722

Time in s	SpeedC	SpeedN	Speed in p.u.	Speed in rad/s	DeltaC	DeltaN	Delta deg	Delta rad	PM_C	PM_N	PM	Pelec_C	Pelec_N	Pelec	Pa
-0,1	0	0	0	0	64,913001	15,52447885	49,38852215	0,861992324	45,34822612	12,93042095	568,0245891	45,34822612	12,93042095	568,0245891	0
-0,09	0	0	0	0	64,913001	15,52447885	49,38852215	0,861992324	45,34822612	12,93042095	568,0245891	45,34822612	12,93042095	568,0245891	0
-0,08	0	0	0	0	64,913001	15,52447885	49,38852215	0,861992324	45,34822612	12,93042095	568,0245891	45,34822612	12,93042095	568,0245891	0
-0,07	0	0	0	0	64,913001	15,52447885	49,38852215	0,861992324	45,34822612	12,93042095	568,0245891	45,34822612	12,93042095	568,0245891	0
-0,06	0	0	0	0	64,913001	15,52447885	49,38852215	0,861992324	45,34822612	12,93042095	568,0245891	45,34822612	12,93042095	568,0245891	0
-0,05	0	0	0	0	64,913001	15,52447885	49,38852215	0,861992324	45,34822612	12,93042095	568,0245891	45,34822612	12,93042095	568,0245891	0
-0,04	0	0	0	0	64,913001	15,52447885	49,38852215	0,861992324	45,34822612	12,93042095	568,0245891	45,34822612	12,93042095	568,0245891	0
-0,03	0	0	0	0	64,913001	15,52447885	49,38852215	0,861992324	45,34822612	12,93042095	568,0245891	45,34822612	12,93042095	568,0245891	0
-0,02	0	0	0	0	64,913001	15,52447885	49,38852215	0,861992324	45,34822612	12,93042095	568,0245891	45,34822612	12,93042095	568,0245891	0
-0,01	0	0	0	0	64,913001	15,52447885	49,38852215	0,861992324	45,34822612	12,93042095	568,0245891	45,34822612	12,93042095	568,0245891	0
0	0	0	0	0	64,913001	15,52447885	49,38852215	0,861992324	45,34822612	12,93042095	568,0245891	45,34822612	12,93042095	568,0245891	0
0,005	0,000477	-1,00831E-05	0,000487083	0,183626011	64,965637	15,52449346	49,44114354	0,862910741	45,34817968	12,93041681	568,0238479	9,376889161	13,70551003	-75,84606914	643,8699171
0,011667	0,001116	-2,15725E-05	0,001137572	0,42885453	66,17299	17,18214458	49,59785442	0,865458862	45,34813324	12,93040646	568,0232155	9,068939322	13,56352526	-78,75410805	646,7733236
0,021667	0,002082	-3,4875E-05	0,002116875	0,798043071	66,852402	16,9056615	49,946787	0,871735884	45,34799392	12,93037107	568,0213944	8,701591527	13,36160289	-81,65269129	649,6740857
0,031667	0,003055	-4,23186E-05	0,003097319	1,167661612	67,063627	16,55700101	50,50662599	0,881506918	45,34766883	12,93029926	568,0169565	8,441986701	13,17666035	-82,96092348	650,97788
0,041667	0,004033	-4,51103E-05	0,00407811	1,53741136	67,562764	16,28379053	51,27897347	0,894986924	45,3470651	12,93018461	568,0083868	8,261517228	13,008589	-83,17816332	651,1865502
0,051667	0,005014	-4,24782E-05	0,005056478	1,906247372	68,319448	16,05608432	52,26336368	0,912167774	45,34608984	12,93002753	567,9940507	8,141328089	12,85667071	-82,62220536	650,616256
0,061667	0,005996	-3,68139E-05	0,006032814	2,274317243	69,314	15,85484702	53,45915298	0,933038235	45,34469661	12,9298301	567,9730979	8,068740908	12,71977821	-81,49544799	649,4685459
0,071667	0,006979	-2,65753E-05	0,007005575	2,641039654	70,535055	15,66944931	54,86560569	0,957585465	45,34283897	12,92959521	567,9446642	8,03456038	12,59659363	-79,9359195	647,8805837
0,081667	0,007961	-1,35215E-05	0,007974522	3,006323784	71,975944	15,49404088	56,48190312	0,985795177	45,34032405	12,92932969	567,9070023	8,031868805	12,48577861	-78,04141607	645,9484183
0,091667	0,008943	2,38407E-06	0,008940616	3,370532799	73,632156	15,32521271	58,30694329	1,017648137	45,33740538	12,92903478	567,8592767	8,054576423	12,38605334	-75,89611277	643,7553894
0,101667	0,009922	2,04679E-05	0,009901532	3,732789659	75,500077	15,16028999	60,33978701	1,053127953	45,33373655	12,92872725	567,80038	8,09813802	12,29622682	-73,55888701	641,359267
0,111667	0,010898	4,14081E-05	0,010856592	4,092838715	77,578143	14,99848393	62,57965907	1,092221096	45,32932466	12,92840275	567,7287608	8,157721739	12,21521214	-71,09532261	638,8240834
0,121667	0,011872	6,41944E-05	0,011807806	4,451437842	79,864162	14,83865304	65,02550896	1,134909229	45,3242626	12,928077	567,645771	8,228776369	12,14201778	-68,56779263	636,2135637
0,13	0,012681	8,45649E-05	0,012596435	4,748744146	81,921649	14,68735227	67,23429673	1,173459848	45,31947918	12,927809	567,566652	8,292632655	12,08681918	-66,48171374	634,0483657
0,135	0,012679	0,000116717	0,012562283	4,735868964	83,162202	14,57242933	68,58977267	1,197117366	45,31627476	12,92765172	567,51326	45,48058279	10,61707685	610,8781433	-43,36488331
0,141667	0,012655	0,000158758	0,012496242	4,710972219	82,846047	14,47521394	70,37083306	1,228202734	45,31181643	12,92746132	567,4384773	47,11469996	10,66131337	638,7360226	-71,29754532
0,151667	0,012578	0,000220413	0,012357587	4,65870053	85,550648	14,29589377	73,05475423	1,275045996	45,30466453	12,92721422	567,3174914	49,37772028	10,73166069	677,1560259	-109,8385345
0,161667	0,012445	0,000279461	0,012165539	4,586300062	88,216557	12,51369712	75,70285988	1,321264158	45,29681601	12,92704059	567,1830121	51,32638191	10,80618141	709,9947117	-142,8116996
0,171667	0,012266	0,000336809	0,011929191	4,497198989	90,794431	12,49022614	78,30420486	1,366666193	45,28827088	12,92695801	567,0347312	52,96686149	10,88155436	737,4185008	-170,3837696
0,181667	0,012047	0,000391821	0,011655179	4,393899021	93,294768	12,44466011	80,85010789	1,411100583	45,27912201	12,92697001	566,8742146	54,31155876	10,95583336	759,6787621	-192,8045476
0,191667	0,011796	0,000443732	0,011352268	4,279704317	95,719833	12,38640091	83,33343209	1,454442767	45,26936941	12,92708198	566,7013678	55,37965382	11,02764114	777,135702	-210,4343341
0,201667	0,01152	0,000494309	0,011025691	4,156587529	98,06869	12,32014429	85,74854571	1,496594451	45,25910597	12,92728914	566,5179019	56,19348476	11,09617866	790,194729	-223,676827
0,211667	0,011225	0,000542844	0,010682156	4,027077984	100,339059	12,24786956	88,09118944	1,537481298	45,24833167	12,92758777	566,3238821	56,77789749	11,16086127	799,3014369	-232,9775548
0,221667	0,010917	0,000589953	0,010327047	3,893205114	102,528579	12,17007227	90,35850673	1,57705345	45,23718585	12,92797353	566,1218258	57,15625178	11,22138785	804,8704122	-238,7485864
0,231667	0,010602	0,000634834	0,009967166	3,757532973	104,634075	12,08549148	92,54858352	1,6152775	45,22571494	12,92843917	565,9126736	57,35817697	11,27736149	807,4277744	-241,5151008
0,241667	0,010283	0,000678573	0,009604427	3,620783744	106,656972	11,99673853	94,66023347	1,652132745	45,2138725	12,92897249	565,6958257	57,40735792	11,32878526	807,3884755	-241,6926499
0,251667	0,009964	0,000720615	0,009243385	3,484674144	108,596762	11,90338319	96,69337881	1,687617825	45,2018443	12,92956251	565,4747292	57,32264965	11,37568072	805,082516	-239,6077868
0,261667	0,009648	0,000761269	0,008886731	3,350218674	110,451523	11,80264475	98,64887825	1,721747729	45,18958389	12,93020054	565,2487228	57,12471839	11,41807184	800,8715885	-235,6228657
0,271667	0,009338	0,000801153	0,008536847	3,218315403	112,222269	11,69429528	100,5279737	1,754544132	45,17718416	12,93088162	565,0195209	56,83474119	11,45567761	795,1316818	-230,1121609
0,281667	0,009036	0,000840581	0,008195419	3,089660028	113,912574	11,58025208	102,3323219	1,786035949	45,16464511	12,93158795	564,7874354	56,46714475	11,4884024	788,11673	-223,3292945
0,291667	0,008739	0,000879258	0,007859742	2,963052972	115,523134	11,46346518	104,0596688	1,816183839	45,15205961	12,9323036	564,554373	56,03618932	11,51948522	780,021424	-215,4670509
0,301667	0,008465	0,000916243	0,007548757	2,845814483	117,059643	11,34267582	105,7169672	1,845109153	45,13938124	12,93304159	564,3192915	55,55905515	11,53953851	771,3097083	-206,9904169
0,311667	0,008197	0,000953633	0,007243367	2,730684844	118,513249	11,20200041	107,3112486	1,872934612	45,1267493	12,93377151	564,0851651	55,04913369	11,55863816	762,0402035	-197,9550384
0,321667	0,007943	0,000990098	0,006952902	2,621182166	119,900851	11,05973965	108,8411114	1,899635755	45,11411737	12,93449026	563,8512346	54,51557379	11,57385063	752,4246174	-188,5733828
0,331667	0,007703	0,001026355	0,006676645	2,51703576	121,220453	10,91094715	110,3095059	1,925264073	45,10153188	12,93518914	563,6184659	53,9670599	11,58552999	742,6089146	-178,9904487
0,341667	0,007476	0,001062523	0,006413477	2,417823783	122,475548	10,75603637	111,7195116	1,949873317	45,08903926	12,93586318	563,3877598	53,41074394	11,59400553	732,7126414	-169,3248816
0,351667	0,007265	0,00109865	0,00616635	2,324659245	123,669644	10,59540291	113,0742411	1,973517806	45,07659309	12,93649521	563,1586036	52,85224526	11,59961456	722,8283493	-159,6697457
0,361667	0,007067	0,001134716	0,005932284	2,23641833	124,806286	10,42948132	114,3768047	1,99625183	45,06428625	12,93708813	562,932574	52,2959293	11,60271389	713,0262781	-150,0937042
0,371667	0,006884	0,001171378	0,005712622	2,15360785	125,889019	10,25872844	115,6302906	2,018129285	45,05211872	12,93762952	562,7098885	51,74513982	11,6035864	703,3600599	-140,6501714
0,381667	0,006714	0,001207569	0,005506431	2,0758757	126,921358	10,08361294	116,8377451	2,039203342	45,04009052	12,93811482	562,4906269	51,2021524	11,60254522	693,8640812	-131,3734543
0,391667	0,006559	0,00124376	0,00531524	2,003798129	127,906769	9,904606268	118,0021627	2,059526264	45,02824808	12,93853535	562,2757553	50,6685925	11,59982317	684,5627435	-122,2869882
0,401667	0,006417	0,001280169	0,005136831	1,936539636	128,848654	9,722173981	119,12648	2,079149303	45,01654497	12,93889131	562,0644563	50,14548181	11,59567398	675,4695032	-113,4050469
0,411667	0,006288	0,001316616	0,004971384	1,874167568	129,750341	9,536773786	120,2135672	2,098122553	45,00502761	12,93917049	561,8577575	49,6332383	11,59035902	666,5871041	-104,7293466
0,421667	0,006173	0,001353979	0,004819021	1,816727992	130,615081	9,348850693	121,2662303	2,11649499	44,99364958	12,93937827	561,654751	49,13190841	11,58400889	657,9140717	-96,29320464
0,431667	0,00607	0,001390808	0,004679192	1,764013859	131,446042	9,15883184	122,2872102	2,13431445	44,98250376	12,93950265	561,4572746	48,64130637	11,57683426	649,4434596	-87,98618496
0,441667	0,005973	0,001427995	0,004545005	1,713426547	132,246274	8,970286479	123,2759875	2,151571871	44,97145082	12,93958522	561,2621582	48,15130807	11,56944895	640,9871176	-79,7249594
0,451667	0,005902	0,001466354	0,004435646	1,672199111	133,019651	8,781207615	124,2384434	2,168369895	44,9607694	12,93949727	561,0765396	47,68973162	11,5604	633,0568645	-71,98032491
0,461667	0,00583	0,001504013	0,004325987	1,63085866	133,765081	8,587854548	125,1772265	2,18475475	44,95004155	12,93940559	560,8901726	47,21919207	11,55199478	624,9604184	-64,07024579
0,471667	0,005776	0,001542304	0,004233696	1,596065695	134,491698	8,39989434	126,0918031	2,200717123	44,93968522	12,93918042	560,7126544	46,7648604	11,54269868	617,1625079	-56,44985349
0,481667	0,005734	0,001580955	0,004153045	1,565661017	135,196386	8,208609941	126,9877761	2,216354802	44,92946821	12,93885758	560,539289	46,31665894	11,53330158	609,4737804	-48,93449138
0,491667	0,005704	0,001619696	0,004084304	1,539746293	135,885595	8,018000602	127,8675944	2,231710529	44,91943697	12,9384445	560,3707596	45,87338021	11,52380142	601,8731149	-41,50235535
0,501667	0,005685	0,001658887	0,004026113	1,517808778	136,561445	7,827769008	128,733676	2,246826504	44,90959149	12,93793353	560,2072003	45,43367744	11,51429878	594,3351508	-34,1279505
0,511667	0,005677	0,00169821	0,00397879	1,499968355	137,226597	7,638175162	129,5884218	2,261744634	44,89993178	12,93732592	560,0485894	44,99611095	11,50481415	586,8343031	-26,7857137
0,521667	0,00568	0,00173715	0,00394285	1,486419559	137,883727	7,449504519	130,4342225	2,27650664	44,89045783	12,93662332	559,8948979	44,55928752	11,49545182	579,3443322	-19,44943423
0,531667	0,005695	0,001777014	0,003917986	1,47704565	138,535512	7,26204238	131,2734696	2,291154265	44,88116964	12,93582448	559,7461476	44,12162815	11,48622691	571,8373061	-12,09115851
0,541667	0,005721	0,001817116	0,003903884	1,471729667	139,184616	7,076051721	132,1085643	2,305729417	44,87202078	12,93492527	559,6015972	43,68160029	11,47719985	564,2853128	-4,683715577
0,551667	0,005758	0,001857497	0,003900503	1,470454808	139,833717	6,891795239	132,9419218	2,320274249	44,86301123	12,93393707	559,4610473	43,23757851	11,46840022	556,6593528	2,801694515
0,561667	0,005807	0,00189752	0,00390948	1,473839361	140,485506	6,70951995	133,7759861	2,334831417	44,85141102	12,93284767	559,3247118	42,78793738	11,45984336	548,9306769	10,39403487
0,571667	0,005867	0,001938437	0,003928563	1,481033416	141,142683	6,529447182	134,6132358	2,349444182	44,84541012	12,93167239	559,1923224	42,33100502	11,45155739	541,0694975	18,12282488
0,581667	0,00594	0,001979015	0,003960985	1,493255983	141,808003	6,351807407	135,4561956	2,364156605	44,83681855	12,9304046	559,0639951	41,8649238	11,44359799	533,0422896	26,02170555
0,591667	0,006024	0,002019809	0,004004191	1,509544572	142,48428	6,176835205	136,3074448	2,379013707	44,82831986	12,92905382	558,9387495	41,38778964	11,43598193	524,8153962	34,1233533
0,601667	0,006121	0,002060963	0,004060037	1,530597801	143,174388	6,004759017	137,169629	2,394061659	44,81991405	12,92761115	558,8167413	40,89760557	11,42874211	516,35325	42,46349135
0,611667	0,006231	0,002101873	0,004129127	1,55664414	143,881278	5,835804959	138,045473	2,409348022	44,81160112	12,92609191	558,6977023	40,3923282	11,42190709	507,6195461	51,07815626
0,621667	0,006355	0,002142977	0,004212023	1,587895314	144,607986	5,670194962	138,937791	2,424921909	44,80338107	12,924493	558,5816869	39,86972836	11,41552798	498,5743295	60,00735749
0,631667	0,006492	0,0021839	0,0043081	1,624115546	145,357646	5,508149812	139,8494962	2,440834166	44,79525391	12,92281523	558,4686806	39,32753044	11,40962797	489,1773208	69,29135984
0,641667	0,006643	0,002225667	0,004417333	1,665295331	146,133506	5,349885656	140,7836203	2,457137708	44,78712675	12,92106773	558,3568963	38,76331952	11,40425362	479,3853898	78,97150653
0,651667	0,006809	0,002266511	0,004542489	1,712478005	146,938939	5,195617457	141,7433215	2,473887654	44,77904602	12,91925586	558,2470535	38,17463423	11,39942459	469,1550639	89,09198963
0,661667	0,006991	0,0023077	0,0046833	1,765562469	147,777458	5,045556821	142,7319012	2,491141623	44,77101174	12,91737569	558,1392211	37,55882744	11,39518061	458,4392638	99,69995731
0,671667	0,007189	0,002349174	0,004839826	1,824571416	148,652731	4,899914868	143,7528161	2,508959951	44,76297746	12,91543758	558,032404	36,91315912	11,39156577	447,1892066	110,8431974
0,681667	0,007405	0,002390564	0,005014436	1,890397708	149,568594	4,75889829	144,8096957	2,527405979	44,75494318	12,91344546	557,9265334	36,23474994	11,38860884	435,3539365	122,5725969
0,691667	0,007638	0,002431616	0,005206384	1,962760473	150,529073	4,622712772	145,9063602	2,546546386	44,74686246	12,91140097	557,8207665	35,52076701	11,3863903	422,8824049	134,9383616
0,701667	0,00789	0,002472407	0,005417593	2,042384576	151,538391	4,491560414	147,0468306	2,566451348	44,73873529	12,90931303	557,7149473	34,76809878	11,38489652	409,7203307	147,9946166
0,711667	0,008163	0,002513606	0,005649394	2,129771364	152,60099	4,365641091	148,2353489	2,587194906	44,73056169	12,90718369	557,6090396	33,97377303	11,38421006	395,8141878	161,7948518
0,721667	0,008456	0,002554534	0,005901466	2,224804027	153,721549	4,245148352	149,4764006	2,608855345	44,7222952	12,90501731	557,5021536	33,13458534	11,38436714	381,1071937	176,3949599
0,731667	0,008772	0,002594652	0,006177348	2,328805256	154,905005	4,130281982	150,774723	2,631515345	44,71393583	12,9028232	557,394126	32,24524143	11,38576324	365,4996527	191,8944733
0,741667	0,009124	0,002635336	0,006488664	2,446168525	156,115067	4,020581771	152,1363252	2,655270787	44,7053907	12,90290636	557,2835179	31,27606556	11,38907469	348,4597357	208,8207823
0,751667	0,009477	0,002675665	0,006801335	2,564042985	157,483066	3,917464033	153,565602	2,680225372	44,69684557	12,89835862	557,172899	30,29774083	11,3931175	331,2466973	225,9262017
0,761667	0,009882	0,002715755	0,007166245	2,70161062	158,889381	3,821263199	155,0681178	2,706449221	44,68792891	12,89609414	557,0563394	29,19862322	11,40011374	311,8653771	245,1909624
0,771667	0,01029	0,002755042	0,007534958	2,8406124	160,382539	3,732434722	156,6501043	2,734060093	44,67905869	12,89383194	556,9405538	28,0865486	11,40835853	292,2351471	264,7054067
0,781667	0,010756	0,002794716	0,007961284	3,001333468	161,969033	3,651136677	158,3178963	2,763168556	44,66972406	12,89155257	556,8169317	26,82484128	11,42096276	269,9066675	286,9102641
0,791667	0,011241	0,002833426	0,008407574	3,169580776	163,657929	3,578653798	160,0792752	2,793910416	44,66029655	12,88927774	556,6916023	25,50777636	11,43609182	246,5639727	310,1276296
0,801667	0,011762	0,00287118	0,00889082	3,351760043	165,455875	3,514865669	161,9410093	2,826403807	44,65054396	12,88700851	556,5604789	24,09351057	11,45488953	221,4538426	335,1066363
0,811667	0,01232	0,002908726	0,009411274	3,547966666	167,372018	3,460859802	163,9111581	2,86078939	44,64051272	12,88474772	556,4244477	22,57377742	11,47779214	194,4237879	362,0006598
0,821667	0,012919	0,002945833	0,009973167	3,759795233	169,415639	3,417262752	165,9983762	2,897218218	44,63010995	12,88248535	556,281689	20,94175009	11,50521936	165,3468352	390,9348538
0,831667	0,013562	0,002980962	0,010581038	3,988957497	171,596651	3,384682974	168,211968	2,935852683	44,61938209	12,88024633	556,1329476	19,18879056	11,53770326	134,0623062	422,0706415
0,841667	0,014252	0,003015743	0,011236257	4,235968333	173,92575	3,3638224	170,5619276	2,976867215	44,60823627	12,87802284	555,9766107	17,30672523	11,57576908	100,4177796	455,5588311
0,851667	0,014992	0,00304987	0,01194213	4,502077036	176,414372	3,355380435	173,0589916	3,020449203	44,59662603	12,87582252	555,8117302	15,28742694	11,61995117	64,26148863	491,5502416
0,861667	0,015786	0,003082009	0,012703991	4,789291913	179,074772	3,360092739	175,7146793	3,066799697	44,5845139	12,8736431	555,6383462	13,12295429	11,67088572	25,44313695	530,1952092
0,871667	0,016637	0,003112525	0,013524475	5,098606772	178,079914	3,378747408	181,4586614	3,167051098	44,57191945	12,87149839	555,4546678	10,80596961	11,72916294	-16,17618797	571,6308558
0,881667	0,01755	0,003141143	0,01440857	5,431902817	175,705705	3,412104922	-178,4478099	-3,114501826	44,55873023	12,86936808	555,2608148	8,329506757	11,79547364	-60,7306511	615,9914659
0,891667	0,018528	0,003167907	0,015360093	5,790618782	-171,777693	3,460949821	-175,2386428	-3,058491294	44,54489083	12,86727103	555,0550655	5,687667736	11,87045338	-108,3347333	663,3897987
0,901667	0,019576	0,003192359	0,016383641	6,176487045	-168,290038	3,526061197	-171,8160992	-2,998756639	44,5304477	12,86520585	554,8381791	2,875762011	11,95483746	-159,083506	713,921685
0,911667	0,020697	0,003214635	0,017482365	6,590696477	-164,555993	3,608162282	-168,1641553	-2,935018193	44,51530796	12,86316964	554,6085789	-0,109089756	12,04920514	-213,0375707	767,6461497
0,921667	0,021897	0,003234443	0,018662557	7,0356182	-160,55798	3,707839653	-164,2658197	-2,866979401	44,49956448	12,86116427	554,3678599	-3,265587218	12,15409387	-270,1835602	824,5514201
0,931667	0,023179	0,0032503	0,0199287	7,512942829	-156,277522	3,825627824	-160,1031498	-2,794327107	44,48312439	12,85919015	554,1143873	-6,582770314	12,26979836	-330,334596	884,4489833
0,941667	0,024546	0,003263201	0,021282799	8,023426039	-151,695444	3,961881827	-155,6573258	-2,716732841	44,46603412	12,85724211	553,8490654	-10,03779911	12,39636703	-393,0911677	946,9402331
0,951667	0,026002	0,003272949	0,022729051	8,568650396	-146,792096	4,116688958	-150,908785	-2,633855168	44,44829369	12,85532593	553,5717927	-13,59419046	12,5336219	-457,8113725	1011,383165
0,961667	0,027548	0,003277665	0,024270335	9,149700656	-141,547648	4,289792756	-145,8374408	-2,545343514	44,42985664	12,8534346	553,2818789	-17,19963244	12,68107353	-523,569552	1076,851431
0,971667	0,029184	0,003279192	0,025904808	9,76588243	-135,942483	4,480506071	-140,4229891	-2,450843505	44,41081585	12,8515685	552,980944	-20,78320074	12,8378223	-589,1073654	1142,088309
0,981667	0,030907	0,003275357	0,027631643	10,41688413	-129,957694	4,687622429	-134,6453164	-2,350004094	44,3911249	12,84973056	552,6681237	-24,25261722	13,00246093	-652,7832573	1205,451381
0,991667	0,032713	0,003267107	0,029445893	11,10084026	-123,575698	4,90932987	-128,4850279	-2,242486776	44,37078377	12,84790938	552,3436173	-27,49224395	13,17300226	-712,5362018	1264,879819
1	0,034282	0,003256269	0,031025731	11,69642507	-117,884353	5,133024287	-123,0173773	-2,147058271	44,35327553	12,84641104	552,063092	-29,96805663	13,31674323	-758,4360053	1310,499097

Figure C.7: Results from stable case 0.13 s CT.

Appendix D

Litterature found for different methods

Figure D.1 presents an overview of the methods selected to be considered for use in this thesis, where these are just some of the different approaches available [26]. The literature review highlights key studies that informed the selection of methods for further investigation, focusing on their outcomes and potential rather than theoretical background.

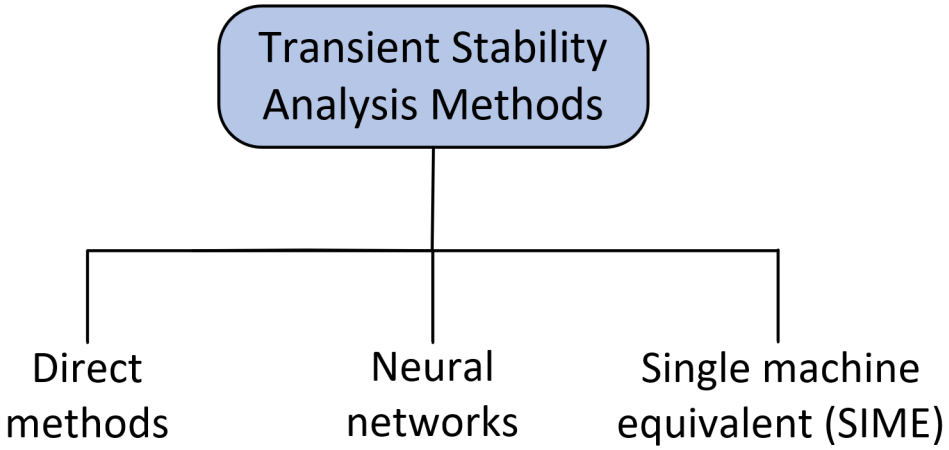

Figure D.1: Different real-time methods for transient stability assessment, that was considered for selection.

D.1 Direct methods

The book "Direct Methods for Stability Analysis of Electric Power Systems" explores the advancement and challenges of using direct methods for electric power system stability over six decades. It addresses the skepticism towards their practicality by providing a solid theoretical foundation and developing comprehensive BCU solution strategies. The book extends energy function theory, based on Lyapunov's, to craft numerical solutions for stability models, emphasizing that understanding theory and the specific problem's

features is crucial for creating effective solutions. This approach aims to make direct methods a practical tool for real-world stability analysis challenges [27]

Also, a recent master's thesis from the University of South-Eastern Norway, titled 'Direct Method for Transient Stability Analysis and Contingency Screening in Power Systems,' provides a modern perspective on the application of direct methods in power systems. This thesis emphasizes the role of contingency screening in enhancing the effectiveness of transient stability analysis. Here The thesis includes two test cases: a single-machine infinite bus test case and a multi-machine test case. Results obtained from these test cases align with expectations and existing literature, in computing critical clearing times (CCTs). [28].

A research paper that the thesis used in the mentioned master's thesis above is 'A Homotopy-Based Method for Robust Computation of Controlling Unstable Equilibrium Points,' published in the IEEE Transactions on Power Systems. It introduces a novel approach for the computation of controlling unstable equilibrium points, addressing key numerical challenges in transient stability analysis. This work underscores the importance of methodological innovation in improving the accuracy and reliability of direct methods in power system stability assessments. The proposed method is applied to several known systems including the NE 39 bus system and the reduced WECC system [3].

D.2 Neural network

Recent advancements in transient stability prediction in power systems have been significantly influenced by the integration of artificial intelligence (AI), particularly neural networks. The development of the Temporal and Topological Embedding Deep Neural Network (TTEDNN) leverages early transient dynamics for fast and efficient stability prediction, where a diagram of this network is shown in Figure D.2. This model has demonstrated robust performance in complex IEEE power systems environments [29].

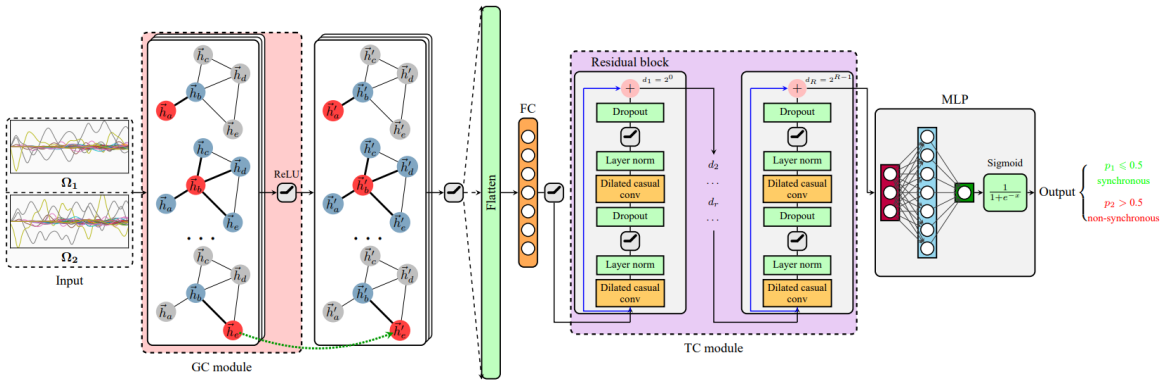

Figure D.2: Diagram of the TTEDNN structure [29].

Furthermore, Cheng et al. (2022) introduced an innovative transient stability assessment method using a multiple paralleled convolutional neural network (CNN) and gated recurrent unit (GRU). This approach effectively combines the capabilities of CNNs in extracting high-order features from short-term time sequences and GRUs in processing long-term time sequences. Their model demonstrates superior transient stability assessment performance, particularly in systems like the IEEE 39 and IEEE 145-bus systems, and offers a significant improvement over traditional methods. This study exemplifies the potential of combining different neural network architectures for enhancing the accuracy and efficiency of power system stability assessments [30].

AI has also been used in constructing Lyapunov functions for transient stability assessment. This method employs neural networks as Lyapunov function learners, using stochastic gradient descent and counterexamples to refine learning. It has shown promise in accurately estimating the stability region boundary in power systems, as validated using systems like the IEEE 9 bus 3-machine system [31].

The integration of renewable energy sources, leading to a reduction in system inertia, poses new challenges for transient stability. A comprehensive review of AI applications in this domain emphasizes the potential of deep learning models in managing these complexities [26].

Furthermore, the concept of physics-informed neural networks introduces an innovative framework that leverages the physical laws governing power systems for neural network training, where an illustration of this is shown in Figure D.3. This approach has been successfully applied to single-machine infinite bus systems, demonstrating substantial improvements in computational efficiency [32].

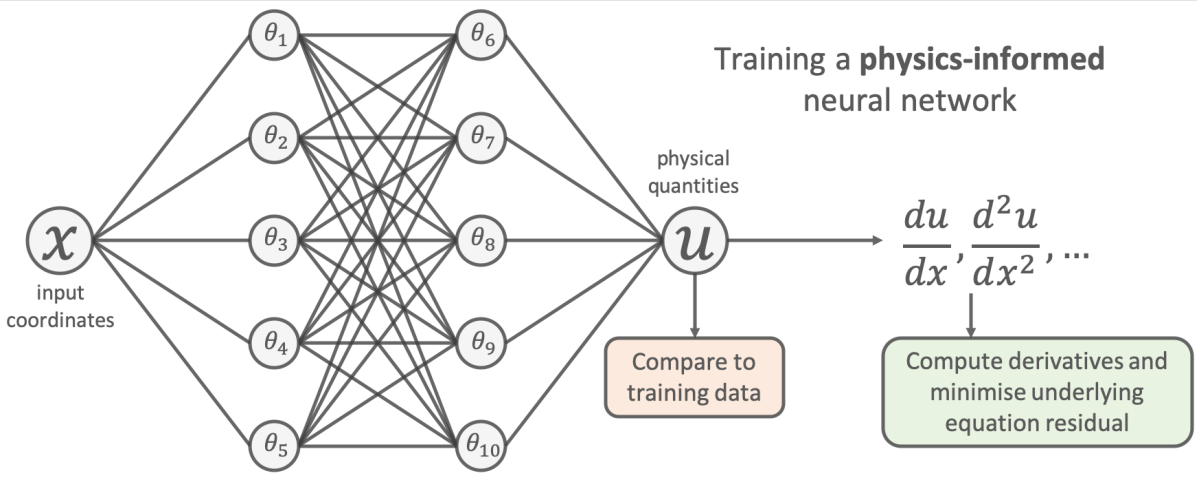

Figure D.3: Physics informed neural network picture taken from [33]

Lastly, the combination of physics models with data-driven algorithms for transient stability assessment, such as using recurrent neural networks guided by physical information of power systems, has been explored. This method was applied to the IEEE14 system and exemplifies the potential of physics-informed deep learning [34].

In addressing the computational challenges of transient stability in power systems, de Cominges Guerra et al. (2024) introduce physics-informed Neural Networks (PINNs). Their work evaluates the effectiveness of PINNs in complex multi-bus networks, highlighting their scalability and accuracy. The study's innovative method of adjusting loss weights enhances PINNs' adaptability, showing a significant efficiency advantage over conventional computational techniques like the ode45 method, particularly as the system size grows [35].

D.3 Single machine equivalent (SIME)

In 1997 the paper "SIME: A hybrid approach to fast transient stability assessment and contingency selection" proposed an integrated scheme for transient stability assessment which in a sequence screens contingencies and scrutinizes only the selected ones. This scheme is based on a hybrid method, called SIME for SIngle Machine Equivalent. SIME relies on a particular direct method coupled with time-domain programs so as to combine the strengths of both, namely: the flexibility with respect to power system modelling of time-domain methods; the speed and richer information of the direct method. This paper lays the foundations of SIME, devises appropriate techniques for transient stability assessment and contingency screening, and finally integrates these two techniques in a fully general function, i.e. able to comply with any power system modeling and stability scenario and to assess any type of stability limits (critical clearing times or power limits). Throughout, real-world examples illustrate the proposed techniques and highlight their performances [36].

The paper introduces a response-based technique for emergency control of transient stability in closed-loop power systems, utilizing E-SIME—a derivative of the SIME method. E-SIME leverages real-time data from phasor measurement units to predict and manage the stability of power systems by initiating countermeasures against potential instabilities. It continuously monitors the effectiveness of these measures, adjusting as necessary. The method's performance is evaluated for accuracy and speed through various real-world scenarios. Finally, it summarizes recent research findings and practical considerations for further improving the method [4].

Where an in-depth book that lays out the foundations for both how emergency SIME and Preventive SIME works is "TRANSIENT STABILITY OF POWER SYSTEMS A Unified Approach to Assessment and Control". This book delves into the transient stability challenge in power systems, starting with an overview of its problems, modeling, and the

evolution of analysis methods, including innovative approaches like SIME and automatic learning. It then focuses on the SIME (Single Machine Equivalent) methodology as a cornerstone for understanding transient stability solutions, detailing its preventive and emergency applications for assessing and controlling power system stability. Through real-world applications and potential integration into energy management systems, it showcases the practicality of these methodologies. The book culminates by contrasting the SIME approach with other transient stability methods, offering a comprehensive resource for tackling transient stability issues in modern power systems [1].

The chapter "Implementation of the Single Machine Equivalent (SIME) Method for Transient Stability Assessment in DIgSILENT PowerFactory" discusses the development of novel smart grid applications that enhance the real-time operational capabilities of transmission grids. It focuses on the integration of the Single Machine Equivalent (SIME) method with DIgSILENT PowerFactory using the DIgSILENT Programming Language (DPL). SIME, crucial for transient stability analysis, employs time-domain signals and the equal area criterion to assess and ensure power system stability by calculating stability margins. The application of SIME in PowerFactory, demonstrated through a benchmark power system example, showcases its potential to support both preventive and corrective control actions effectively. This integration aims to improve the system's self-healing capabilities and reduce blackout risks through real-time vulnerability assessments and adaptive responses [25].

D.4 Choice of method

After the methods have been explored through, the decision was made to proceed with the E-SIME approach due to its ability to handle systems with many generators and dynamic models. Each method has pros and cons, but the E-SIME methodology seemed promising to provide real-time transient stability assessment of a large generator system like the New England Grid. Also, this methodology was not directly tried before at USN and was wanted to be pursued to figure more out about its potential. Neural networks were pursued for a while, but issues were faced here with the black-box nature of the neural network. This means that there were issues with getting the neural network to understand the underlying dynamics of the system, and a tendency to overfit the data. This could possibly be resolved by either using Physics informed neural network or possibly getting training labels from the SIME methodology, but it was chosen to pursue the E-SIME method instead.